Interaction of the SecYEG translocon with the SRP receptor and the ribosome

Dissertation

for the award of the degree

"Doctor of Philosophy"
Division of Mathematics and Natural Sciences

of the Georg-August-Universität Göttingen

within the doctoral program *GGNB – Biomolecules*

of the Georg-August University School of Science (GAUSS)

submitted by

Albena Draycheva

from Sofia, Bulgaria

Göttingen, 2014

Members of the Examination Board /Thesis Committee

Prof. Dr. Wolfgang Wintermeyer (1st Referee)
Ribosome Dynamics group
Department of Physical Biochemistry
Max Planck Institute for Biophysical Chemistry,
Göttingen, Germany

Prof. Dr. Kai Tittmann (2nd Referee)
Department of Bioanalytics
Georg-August University,
Göttingen, Germany

Prof. Dr. Marina Bennati
Electron Spin Resonance Spectroscopy group
Max Planck Institute for Biophysical Chemistry,
Göttingen, Germany

Further Members of the Examination Board

Dr. Manfred Konrad
Enzyme Biochemistry group
Max Planck Institute for Biophysical Chemistry,
Göttingen, Germany

Prof. Dr. Peter Rehling
Institute for Cellular Biochemistry
Medical University Göttingen, Germany

Prof. Dr. Holger Stark
3D Cryo-Electron Microscopy group
Max Planck Institute for Biophysical Chemistry,
Göttingen, Germany

Date of oral examination: 16 May 2014

Affidavit

I hereby declare that my thesis entitled "Interaction of the SecYEG translocon with the SRP receptor and the ribosome" has been written independently and with no other sources and aids than quoted. This thesis (wholly or in part) has not been submitted elsewhere for any academic award or qualification.

Albena Draycheva

March, 2014

Göttingen, Germany

Contents

1. Abstract

Membrane targeting of ribosomes synthesizing membrane or secretory proteins is an essential process in all cells. One of the most conserved targeting pathways is the signal recognition particle (SRP) pathway. In bacteria, the SRP pathway targets ribosomes that are synthesizing polytopic membrane proteins to the SecYEG translocon for cotranslational insertion into the cytoplasmic membrane. The targeting cycle of SRP starts early during protein synthesis. SRP scans translating ribosomes and when it recognizes the N-terminal signal anchor sequence (SAS) of a membrane protein it forms a tight complex with the ribosome and the SAS. At this stage the complex is targeted to the SecYEG translocon in the membrane by the SRP receptor, FtsY. Then the translating ribosome is transferred to the SecYEG in a GTP-controlled manner, which initiates membrane insertion. Details of the processes at the membrane are poorly understood. This work aimed at studying the interaction between SecYEG and FtsY and before and after the translating ribosome has been transferred to the SecYEG translocon.

In this study we have used monomers of the SecYEG complex embedded into nanodiscs (SecYEG(ND)) in combination with fluorescence measurements, in particular fluorescence resonance energy transfer (FRET), to determine the affinity of FtsY binding to SecYEG (K_d 0.18 ± 0.02 μM). Using a rapid kinetics approach we verified that FtsY is primarily localized at the membrane and that it interacts with SecYEG(ND) via two interaction sites. The binding of FtsY to SecYEG(ND) is mediated via both the NG and the A domains. The A domain, especially the first 208 amino acids assure the stable binding of FtsY. Further, we have demonstrated that the A and NG domain of FtsY are strongly bound to one another keeping FtsY in a ‘closed’ conformation when bound to the membrane. The interaction of FtsY with SecYEG(ND) induces a rearrangement between the domains and FtsY adopts an ‘open’ conformation, which would facilitate the efficient binding of the FtsY-NG domain to the homologous domain of SRP. Due to the high affinity of the complex of translating ribosomes and SecYEG(ND), and the increased affinity of ribosome-bound SRP to FtsY the ribosome-SRP complex is localized properly at the site of the translocon. After the ribosome has been transferred to SecYEG and SRP and FtsY have been separated due to GTP hydrolysis, FtsY remains associated with the SecYEG complex to take part in another round of targeting. Our findings also show that the A domain of FtsY mainly takes part in the stabilization of FtsY on

the translocon before and after ribosomal transfer, but is not essential for GTPase activation. By contrast, the FtsY-NG domain is responsible for GTP-dependent complex formation with SRP.

2. Introduction

2.1 Membrane proteins and targeting mechanisms

Membrane proteins fulfill various and important functions in the cell, such as ion transport and nutrient uptake, cell signaling and cell-to-cell interactions. Membrane proteins account for 20-30 % of all open reading frames in the sequenced genomes (Holland, 2010; Pugsley, 1993). The study of protein translocation through or insertion into membranes started in the 1950's with the first description of the organelles in the cell (Siekevitz & Palade, 1958). Major insights into how this process works came from studies on the eukaryotic secretory pathway by Milstein and colleagues that noted in the early 1970's that immunoglobulins were made in precursor form with a hydrophobic N-terminal sequence that is cleaved in the mature protein (Milstein et al, 1972). It was not until few years later that Blobel and Dobberstein provided evidence for the signal sequence hypothesis (Blobel & Dobberstein, 1975). Their model, for which Blobel received the Nobel Prize in 1999, stated that proteins that are destined for translocation are recognized by way of a hydrophobic N-terminal signal sequence that was cleaved during the translocation process. At about the same time signal sequences were identified in *Escherichia coli*. Further studies using gene fusion techniques to study protein secretion in *E.coli* provided direct evidence for the presence of signal sequences (Bassford & Beckwith, 1979). Furthermore, proteins were identified that comprised the machinery required for protein secretion.

Over the years a remarkable array of protein translocation pathways was found in bacteria (Papanikou et al, 2007), but only three systems appear to be present in most bacterial species: (a) the Tat pathway, (b) the YidC insertase and (c) the Sec translocon (Figure 2-1). The twin arginine translocation (Tat) pathway transports folded proteins across the cytosolic bacterial membrane (Berks et al, 2000). Proteins transported by the Tat pathway usually bind to cofactors in the cytoplasm, such as redox cofactors, and fold or even oligomerize before translocation through the membrane. The Tat substrates have usually in their N terminus a 'twin arginine' (RR) motif. This pathway is present in most bacterial and archaeal species, as well as in chloroplast, but is absent in mitochondria (for a comprehensive review, see (Kudva et al, 2013)). In contrast the Sec translocon and YidC insertase transport proteins in unfolded state and insert them into the plasma membrane in a co-translational manner.

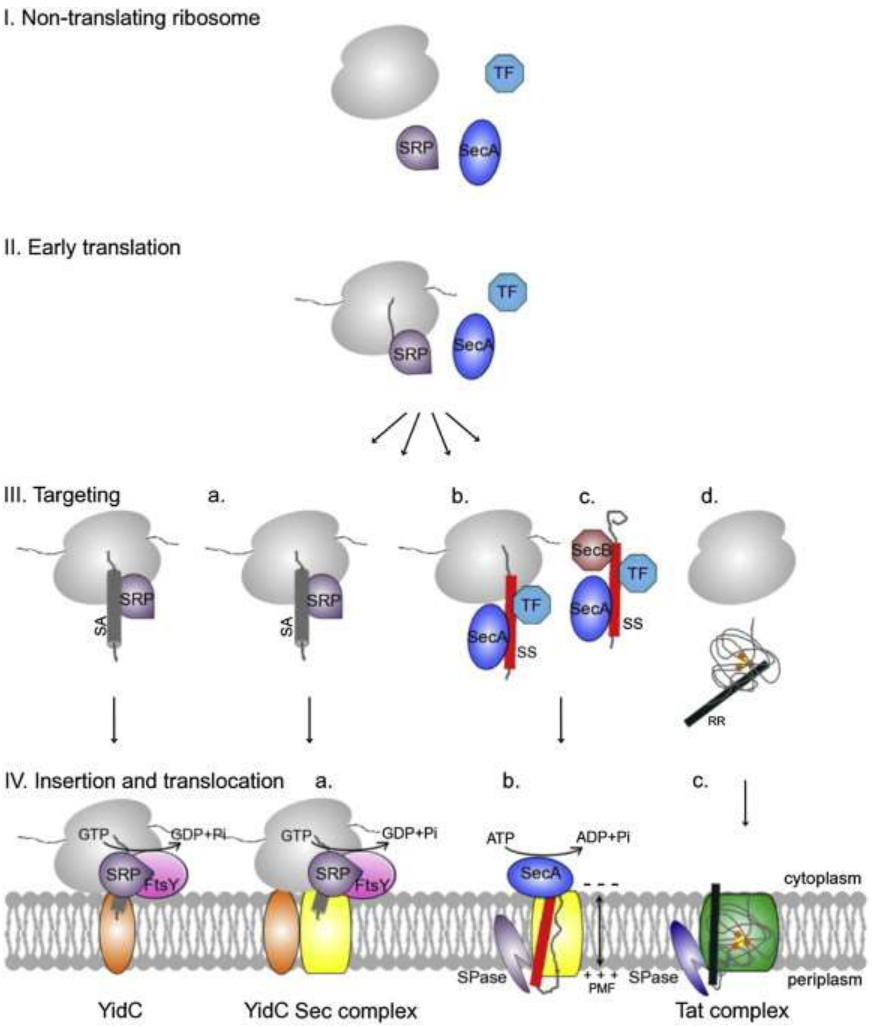

Figure 2-1 Overview of the major protein targeting pathways in Gram-negative bacteria

I. In the cell ribosomes associate with various protein factors that are responsible for the proper localization of extracytosolic proteins. II. In the early stages of translation the factors scan the ribosomes for specific substrates. III.(a) If a signal anchor (SA) sequence is exposed from the ribosome tunnel, SRP associates tighter with the ribosome nascent chain complex (RNC). III. (b) Cotranslational targeting of secretory proteins by SecA, has been also suggested as an alternative pathway. III (c) Secretory proteins are targeted post-transitionally by SecA/SecB to the SecYEG complex. IV. (a) The SRP-RNC complex is tethered to the membrane by the SRP receptor, FtsY. At the membrane the RNC is transferred in a GTP-dependent manner to the SecYEG complex or to YidC insertase for membrane insertion. IV. (b) SecA facilitates the translocation of secretory proteins through SecYEG by utilizing ATP. IV (c) Folded proteins have a double arginine (RR) motif and are translocated via the Tat complex. Signal sequenced (SS) of both of Sec and Tat translocated proteins are removed by the signal peptidases (SPase) at the periplasmic side of the membrane (figure adopted from (Kudva et al, 2013)).

The YidC insertase appears to be the simplest pathway for insertion of proteins into the cytosolic membrane (Dalbey et al, 2011). It is present in most bacteria and archaea, and related pathways have been described for organelles such as mitochondria (Oxa1) and chloroplasts (Alb3) (Funes et al, 2011). YidC can function on its own or in cooperation with the Sec translocon during membrane insertion of proteins (Beck et al, 2001; Nagamori et al, 2004).

The Sec translocon is arguably the best characterized protein transport machinery. It is present in all bacteria, archaea, the endoplasmic reticulum of eukaryotic cells, and chloroplasts, but not in mitochondria. It has a dual function, as it both transports fully synthesized, but unfolded proteins through the membrane in cooperation with the SecA translocase and inserts proteins into the membrane in a cotranslational manner. For co-translational membrane insertion, ribosomes synthesizing membrane proteins are targeted to the Sec translocon by the signal recognition particle (SRP) pathway.

2.2 SRP targeting pathway in bacteria

2.2.1 SecYEG - the protein-conducting channel

The core of the Sec translocon is the SecYEG heterotrimer. It is an evolutionary conserved complex which in Gram-negative bacteria is embedded in the plasma membrane and in eukaryotes in the membrane of the endoplasmic reticulum. The first high-resolution structure at 3.2 Å was obtained for the SecYEβ translocon of the archaeon *Methanococcus jannaschii* which gave major insights into the structure-function relationship of protein-conducting channels of the Sec type in general (Van den Berg et al, 2004). The SecY subunit (Sec61α in eukaryotes) comprises ten transmembrane (TM) α-helices. They are organized like a clamp-shell with one half formed by TM segments 1 – 5 and the second by TM segments 6 – 10. The two halves have pseudo-symmetry, in that the second half is essentially the inverted version of the first. Exposed to the cytosol are the cytosolic loops C4, C5 and C6, which have an important role in docking targeting factors and the ribosome (Figure 2-2, panel A.) (Cheng et al, 2005; Chiba et al, 2002; Kuhn et al, 2011).

The translocation channel of SecY is shaped like an hour-glass with a central constriction (pore-ring) that is formed by six hydrophobic amino acids with the side-chains pointing

towards the center of the channel. They are suggested to play a role maintaining the permeability barrier during translocation by forming a seal around the peptide passing through the channel (Park & Rapoport, 2012). On the periplasmic site the channel is 'closed' by helix TM2a, which forms the so-called plug domain. It was suggested that during translocation the plug is displaced towards the SecE subunit (Tam et al, 2005), although crosslinking data (Lycklama & Driessen, 2012) and molecular dynamics simulations (Zhang & Miller, 2012) indicate that the plug remains in its original position. However, deletion of the TM2a does not result in translocation defects (Maillard et al, 2007), but in fluctuations of the channel between 'opened' and 'closed' state (Saparov et al, 2007). In the plane of the membrane SecY can open laterally for the insertion of membrane proteins into the lipid bilayer (Bonardi et al, 2010; Higy et al, 2005; Martoglio et al, 1995). For lateral opening of the channel and lateral movement of hydrophobic TM segments into the phospholipid bilayer TM2b and TM7 move apart, hence the designation as lateral gate. Recent structural data have revealed a TM segment entering the lipid phase through the opened lateral gate (Frauenfeld et al, 2011; Gogala et al, 2014) (Figure 2-2, panel B.).

The two halves of SecY are clamped together on the 'back' side by the SecE subunit (Sec61ɣ in eukaryotes). In *E.coli* SecE consists of three TM segments and is essential for protein translocation. In other bacteria it is represented by only one TM helix and, in fact, much of the N-terminal part of *E.coli* SecE can be deleted without compromising protein translocation (de Gier & Luirink, 2001; Murphy & Beckwith, 1994) (Murphy and Beckwith 1994, de Gier and Luirink 2001). In the absence of SecE, SecY is unstable and is degraded (Kihara et al, 1995). The third subunit of the SecYEG trimer is SecG in bacteria, and its homolog in eukaryotes and archea is called Sec61β. Unlike the other two subunits, SecG is not evolutionary conserved. SecG in *E.coli* comprises two TM helices and occupies a position close to the lateral gate of SecY (Satoh et al, 2003; van der Sluis & Driessen, 2006). SecG is not essential for cell viability or protein translocation in *E.coli*; it was shown *in vitro* to stimulate protein translocation at low temperatures or when the proton-motive force (PMF) was compromised (Hanada et al, 1996; Nishiyama et al, 1996). Its main function was proposed to be connected with the SecA dependent protein secretion (Nishiyama et al, 1996).

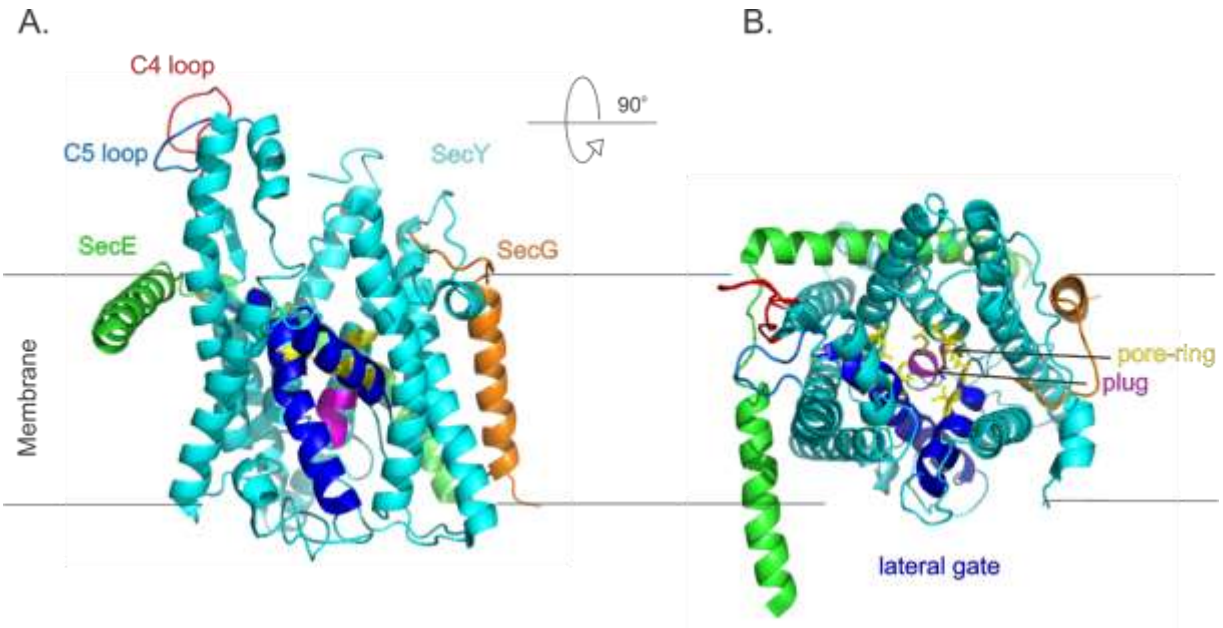

Figure 2-2 Structure of SecYEG

A. Side view of the SecYEG from *Methanococcus jannaschii* ((Van den Berg et al, 2004) PDB ID 1RHZ) illustrating the main structural elements of the complex according to the *E.coli* nomenclature. **B.** Top view from the cytosolic side of the SecYEG channel.

It has been a long lasting debate in the field of protein translocation whether the SecYEG complex functions as a monomer or as a dimer. Finally it has been shown that a single copy is sufficient *in vivo* and *in vitro* for protein translocation and for membrane protein insertion (Becker et al, 2009; Cannon et al, 2005; Frauenfeld et al, 2011; Kedrov et al, 2011; Park & Rapoport, 2012). Nevertheless, different oligomeric states of the SecYEG have been observed by native electrophoresis (Bessonneau et al, 2002; Boy & Koch, 2009; Deville et al, 2011; Scheuring et al, 2005; Veenendaal et al, 2001), crosslinking experiments (Deville et al, 2011; Veenendaal et al, 2001) and electron microscopy (Breyton et al, 2002; Hanein et al, 1996; Mitra et al, 2005). The significance of these oligomeric states is yet to be elucidated.

In the course of studying protein translocation and membrane insertion it was found that SecYEG interacts with several other partners: on the cytoplasmic site – SecA, FtsY, the ribosome and Syd, and in the membrane – SecDFYajC and YidC. The exact interaction site of SecDFYajC with SecYEG is not known, but due to its low abundance it is supposed to interact

only with a small fraction of SecYEG complexes (Pogliano & Beckwith, 1994). Based on the crystal structure of SecDF it was proposed that it transports protons from the periplasm to the cytosol (Scotti et al, 2000; Tsukazaki et al, 2011). YidC was first identified as a protein that copurified with the complex of SecYEG and SecDFYajC (Scotti et al, 2000). YidC is believed to facilitate the lateral exit of TM regions from SecY and has been found to crosslink to the lateral gate (Sachelaru et al, 2013).

The motor protein SecA, which takes part in post-translational protein translocation through the SecYEG translocon, has been found to crosslink to the cytosolic loops of SecY (Mori & Ito, 2006), and these contacts were confirmed by crystal structure data (Zimmer et al, 2008). The cytosolic loops of SecY are also binding platform for the ribosome and for FtsY. The cryo-electron microscopy (cryo-EM) structure of the translating ribosome and SecYE in nanodiscs and biochemical studies show that the ribosome contacts the C4 and C5 loops of SecY via 23S rRNA helices 24, 50, 53 and 59 and proteins L23, L24 and L29 (Cheng et al, 2005; Frauenfeld et al, 2011; Kuhn et al, 2011; Raden et al, 2000). Also it interacts with the SecE subunit via the proteins L23 and L29 (Figure 2-3). On the other hand, FtsY also interacts with the C4 and C5 loops of SecY and, thereby may occupy the binding site for the ribosome and SecA (Kuhn et al, 2011).

The main function of the SecYEG complex is to facilitate the membrane insertion of protein or their transport across the cytoplasmic membrane. How exactly the channel distinguishes between the substrates is not entirely clear. Biochemical data and molecular dynamics simulations have converged to a model where during cotranslational membrane insertion the ribosome is docked on SecY and in this way a continuous channel is formed from the peptidyl transferase center to the periplasm. The cytoplasmic part of SecY is mostly polar and functions as an extension of the ribosomal exit tunnel. This allows any secondary structure formed in the ribosome to be retained in the channel. The hydrophobic pore-ring stimulates helix formation.

Thus, even sequences with low helix-forming tendency may enter the lipid phase in α-helical conformation (Gumbart et al, 2011b). This is energetically more favorable than embedding an extended peptide backbone (White & von Heijne, 2008). The pore ring helps to define energetic threshold separating membrane insertion from transport into the periplasm (Gumbart et al,

2011a; Junne et al, 2010). Molecular dynamics simulations of different nascent helices in SecY indicate that even when the lateral gate is closed, lipids can contact the helix with a probability that is proportional to the hydrophobicity of the helix. For hydrophobic TM sequences, the interaction with lipids appears to draw them into the membrane, whereas hydrophilic ones remain in the channel, thereby minimizing the contact with lipids (Gumbart et al, 2013).

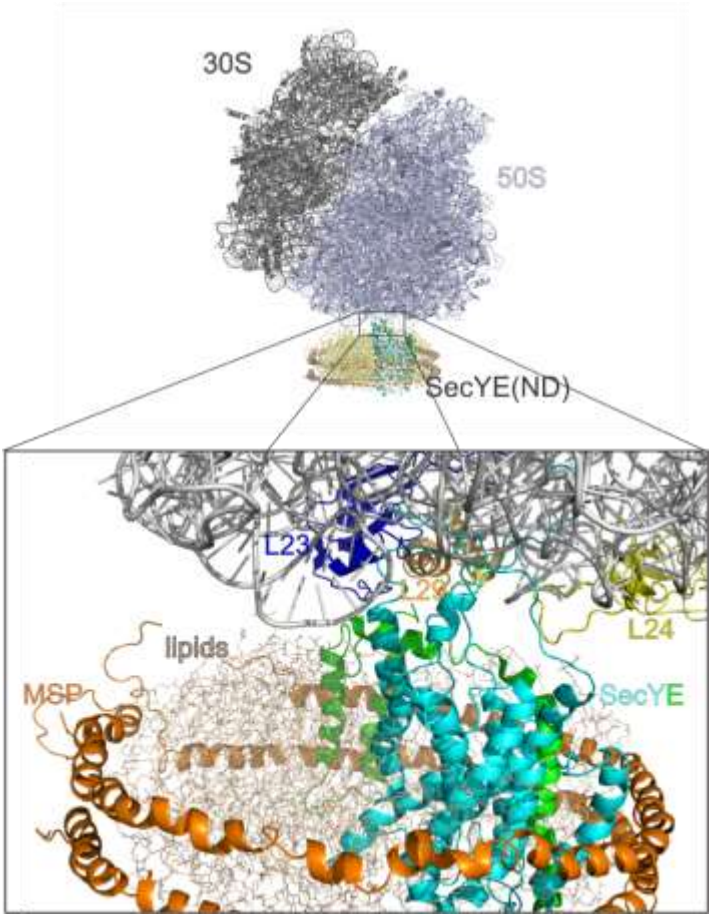

Figure 2-3 Structure and connections of the nanodiscs embedded SecYE to the ribosome

Cryo-EM reconstitution of the *E.coli* RNC-SecYE embedded in nanodiscs ((Frauenfeld et al, 2011) PDB ID 3J00 and 3J01). Illustrated are the main connections of the ribosome and SecY, the 23S rRNA and the ribosomal proteins L23, L24 and L29.

Overall the insertion and translocation of proteins by the SecYEG translocon is a complex process governed by kinetic and thermodynamic phenomena. These depend on the rate of

protein synthesis, protein folding, and on protein-protein and protein-lipid interaction and recognition. Thus, it is important to deliver correct substrates to SecYEG. This is achieved by the signal recognition particle (SRP) and its receptor, SR, or FtsY in bacteria.

2.2.2 SRP and membrane targeting of the ribosome

SRP is evolutionary conserved and present in all three domains of life. In eukaryotes, SRP targets ribosomes synthesizing secretory or membrane proteins to the Sec translocon at the ER membrane, or to the thylakoids in chloroplasts. It is generally accepted that *E.coli* SRP is mainly responsible for the co-translational targeting of inner-membrane proteins to the SecYEG translocon (Beckwith, 2013). SRP differs in size and composition among species, the bacteria SRP contains the core of the ribonucleoprotein. It can functionally substitute its more complex eukaryotic SRP homologue (Bernstein et al, 1993; Powers & Walter, 1997). Bacterial SRP is comprised of a protein part, the Ffh protein (homologue of SRP54, the only evolutionary conserved protein in the eukaryotic SRP particle), which binds to 4.5S RNA (7S RNA in eukaryotes) (Bernstein et al, 1993; Powers & Walter, 1997). The 114 nucleotide SRP RNA adopts a hairpin structure. In *E.coli* it is required for cell viability (Brown & Fournier, 1984; Hsu et al, 1984) (Figure 2-4, panel A.). Nevertheless, truncated RNA containing only 44 nucleotides from the apical hairpin, i.e. part of helix 8, is sufficient to sustain cell growth (nomenclature according to (Batey et al, 2001; Zwieb et al, 2005)). Helix 8 includes two evolutionary conserved regions that are important for the *in vivo* activity of SRP. The first one comprises two internal loops near the hairpin tip where the SRP M domain binds (Batey et al, 2000). The second is the GGAA tetraloop (GNRA in bacteria (Rosendal et al, 2003)), which is located at the tip of the hairpin and is essential for SRP-FtsY complex formation (Jagath et al, 2001; Shen et al, 2012; Zhang et al, 2008).

Ffh comprises two functional domains connected with a flexible linker. The C-terminal M domain binds 4.5S RNA and the signal sequence (Batey et al, 2000; Hainzl et al, 2011; Janda et al, 2010; Keenan et al, 1998). It is preceded by the NG domain that is composed of a helical N domain and the G domain, which binds and hydrolyzes GTP. The NG domain of Ffh interacts with the homologous NG domain of FtsY, and the N domain binds to ribosomal proteins L23 and L29 (Figure 2-4, panel B.), forming a major interaction site. Additional contacts are

established between the M domain, the ribosomal RNA, and the ribosomal protein L22. These interactions have been characterized via crosslinking analysis (Gu et al, 2003; Pool et al, 2002) and cryo-EM reconstitutions (Halic et al, 2006a) (Figure 2-4, panel C.). Ribosomes synthesizing proteins destined for membrane insertion are targeted by SRP in an early stage of translation. SRP binds with high affinity to ribosomes synthesizing any protein already when the first 30 – 35 amino acids are in the ribosomal tunnel. Later, when the peptide emerges from the tunnel SRP recognizes whether the peptide encodes a signal-anchor sequence (SAS), or not. When it encodes one then SRP also binds to its substrate, and translation continues. Since the interaction of SRP with the isolated peptide is weak with a K_d in the micromolar range (Bradshaw 2009), primarily it is the multiple interactions with the ribosome that allow the SRP to bind to the ribosome in a wide range of affinities, from K_d = 100 nM to vacant ribosomes to K_d = 1 nM to ribosomes that have the exit tunnel filled or expose a SAS (Bornemann et al, 2008; Flanagan et al, 2003; Holtkamp et al, 2012a).

N-terminal SAS are similar in eukaryotes and prokaryotes. They share a common architecture with a short positively charged N-terminal region, a central hydrophobic region and a C terminal slightly polar region (von Heijne & Abrahmsen, 1989). The SAS does not have a conserved amino acid sequence, but is typically 8 – 12 amino acids long and adopts an α-helical structure (Hegde & Bernstein, 2006). The first proof that the M domain of SRP functions as a signal sequence binding site was from crosslinking studies (Krieg et al, 1986; Zopf et al, 1990). The M domain is methionine-rich and can provide a hydrophobic environment to accommodate hydrophobic signal peptides in a sequence-independent manner. The crystal structures of Ffh (Keenan et al, 1998) and SRP54, fused to an SAS (Hainzl et al, 2011; Janda et al, 2010), showed that the SAS binds in a hydrophobic groove of the M domain. Another important region of the M domain is the flexible fingerloop, which lines the signal peptide binding groove. It mediates the information of the binding of the SAS to M domain to the NG domain of SRP (Ariosa et al, 2013).

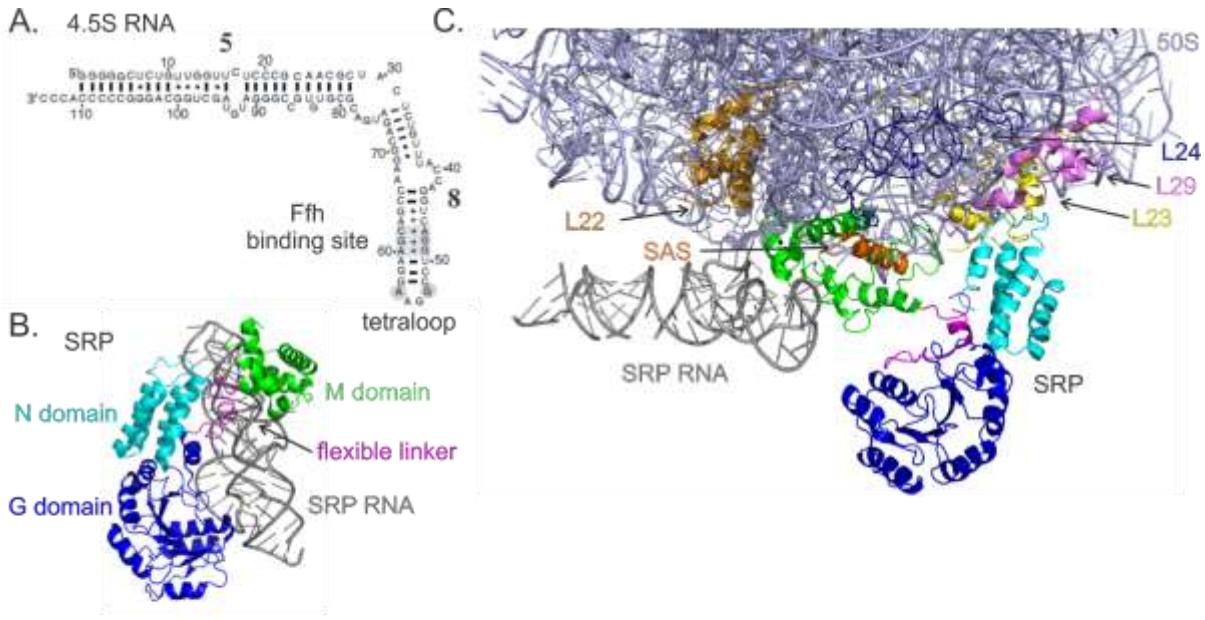

Figure 2-4 Structure of SRP and its contacts with the ribosome and the SAS

A. Representative secondary structure of *E.coli* 4.5S RNA. It comprises helix 8 (numbering according to (Zwieb et al, 2005)), previously assigned as domain IV, and helix 5 (domain II). The conserved motives are highlighted in grey. Canonical Watson-Crick base pairs are represented by lines, non-canonical Watson-Crick base pairs by plus signs and G-U pairs by filled circles (figure taken from SRPDB (Zwieb, 2011)). **B.** X-ray structure of the *Methanococcus jannaschii* SRP ((Hainzl et al, 2007) PDB ID 2V3C). **C.** Cryo-EM reconstruction of the *E.coli* RNC-SRP complex ((Halic et al, 2006a) PDB ID 2J28).

2.2.3 Interaction of SRP with FtsY

In the cell SRP rapidly scans the translating ribosomes until it recognizes a ribosome that has the exit tunnel filled or exposes an SAS which stabilizes the complex about 100-fold. After several discrete conformational changes it adopts a more opened conformation and switches to targeting mode. In this mode the recruitment of its receptor, FtsY is accelerated (Holtkamp et al, 2012a).

The complex formation of SRP and FtsY is mediated first by the 4.5S RNA of SRP and second by the interaction between the NG domains of both proteins. The initial interaction between

the proteins is facilitated by the tetraloop of 4.5S RNA (Jagath et al, 2001; Spanggord et al, 2005; Zhang et al, 2008), followed by the interaction of the NG domains of SRP and FtsY with one another. This second step requires that both proteins have GTP bound. At the final stage of assembly the complex travels 100 Å to the 3'-distal end of the RNA. There mutual activation of the GTP hydrolysis is triggered by the alignment of the GTP-binding pockets and the insertion of the catalytic G83 nucleotide from the SRP RNA (Figure 2-5). This movement on the 4.5S RNA does not occur when the complex is assembled on RNCs, but at a later stage the presence of SecYEG releases the complex (Shen et al, 2013; Voigts-Hoffmann et al, 2013). Additionally the targeting complex of the RNC-SRP-FtsY could be influenced by the interaction of FtsY with the membrane and SecYEG (Braig et al, 2009; Mircheva et al, 2009) by triggering conformational changes in the A domain (Stjepanovic et al, 2011b).

As mentioned above, both it is the protein component of SRP, Ffh, and FtsY are GTPases which form the regulatory center of the SRP-targeting pathway. In contrast to the canonical Ras-like GTPases, the SRP-related GTPases do not require GTPase-activating factors (GAPs), or nucleotide exchange factors (GEFs) for their function. They bind GTP and GDP with similar affinities (around 1 – 2 μM) and readily exchange GDP for GTP (Jagath et al, 1998; Leipe et al, 2002). Thus, both Ffh and FtsY belong to the SIMIBI class of GTPases, which is part of the superfamily of P-loop proteins (Leipe et al, 2002). In contrast to the Ras-like G proteins, which have a central six-stranded β-sheet and one antiparallel strand, the SIMIBI proteins have an exclusive parallel seven-stranded β-sheet architecture. This structure results in a particular orientation of the switch-1 region. The switch-1 and switch-2 regions are responsible for transferring the conformational change brought about by GTP hydrolysis to other parts of the protein.

SRP and FtsY share the conserved NG domain organization. The G domain has a unique α-β-α insertion box (IBD) that is located between the switch-1 and switch-2 regions. In complex with GTP SRP and FtsY form a quasi-symmetric heterodimer via their NG domains. The GTP-binding pockets align and form a composite active site. The IBD loops of each protein close the catalytic sites from the top and contribute to the formation of the active site. Ffh Arg141 and Gln147 and FtsY Arg333 and Gln339 position the GTP for hydrolysis and provide electrostatic balance where the phosphates are aligned. In this manner SRP and FtsY serve as GAPs for one

another, although full GTPase stimulation requires the environment of the membrane and, most likely, the translocon (Egea et al, 2004; Focia et al, 2004).

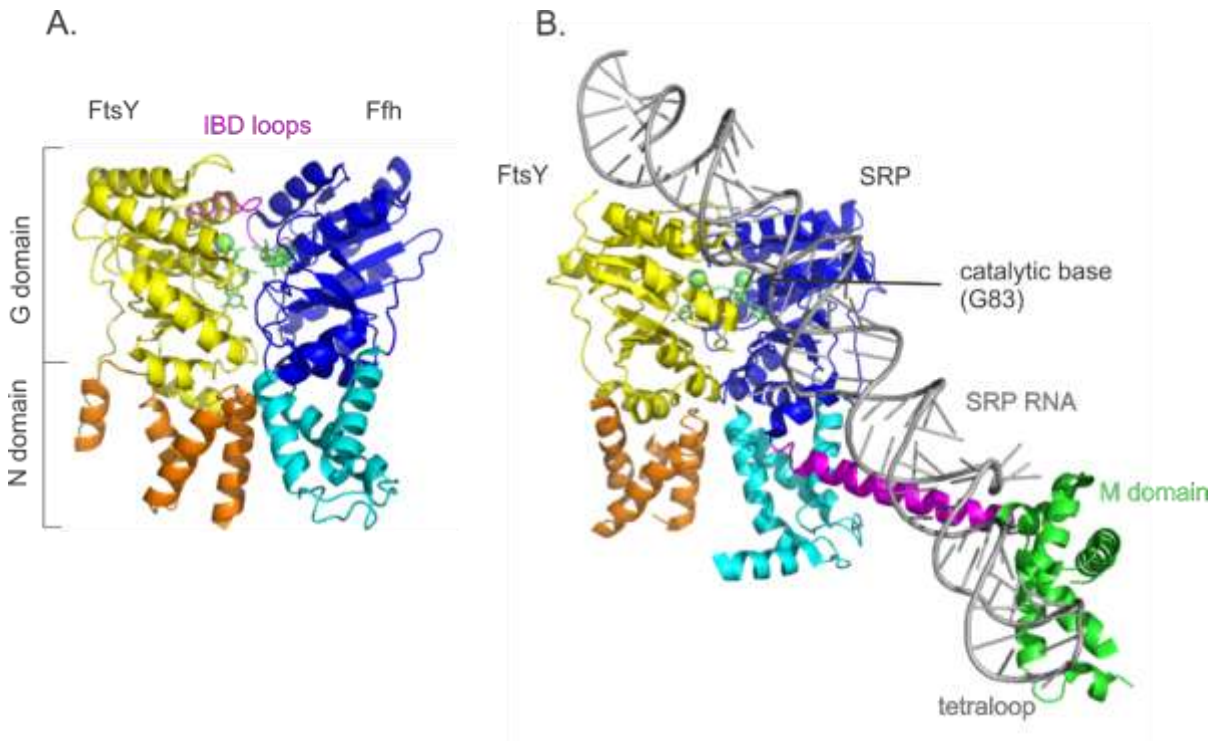

Figure 2-5 The complex of SRP and FtsY

A. Structure of the NG domains Ffh-FtsY heterodimer in complex with GDPCP (green) forming a composite active site ((Egea et al, 2004) PDB ID 1RJ9). **B.** Structure of the SRP-FtsY heterodimer forming a protein-RNA composite active site ((Ataide et al, 2011) PDB ID 2XXA).

According to a recent model based on single-molecule and crystallographic data, the active site is completed by a catalytic guanine residue (G83) from the 3'-distal end of the 4.5S RNA. The exact mechanism of catalysis is yet unknown, given that this nucleotide is not conserved (Voigts-Hoffmann et al, 2013). Though, the truncation of the distal end compromises the GTPase activation of SRP and FtsY (Ataide et al, 2011).

2.2.4 FtsY – structure and function

It is generally thought that the main function of the SR is to tether the complex of the ribosome and the SRP to the cytoplasmic membrane and to SecYEG. In eukaryotes, SR consists of two subunits: SRβ is an integral membrane protein which associates with SRα which, in turn, binds to the ribosome-SRP complex. In contrast, the bacterial SR is a single protein, called FtsY, which is homologous to SRα (Luirink et al, 1994); so far no homolog of SRβ has been identified in bacteria. The functional NG domain of FtsY comprises the N domain (amino acids 198 – 284) and the G domain (amino acids 292 – 497) and is preceded by an acidic A domain (amino acids 1-197) (Figure 2-6) (Bernstein et al, 1989; Romisch et al, 1989). Among the various prokaryotes, the A domain is highly divergent in size and charge. Based on sequencing data it has been classified into four categories: (a) highly negative with high homology to *E.coli* FtsY; (b) moderately charged with low homology to *E.coli* FtsY; (c) very short (less that 30 amino acids) and positively charged; (d) no similarity to the A domain of *E.coli* FtsY with a single, putative TM helix. In contrast, the NG domain is highly conserved. There is no structural information on the A domain, and *in silico* analysis predicts it to be rather unstructured, except for amino acid 1-14 which are predicted to form an α-helix (Pollastri et al, 2002). Deuterium exchange experiments have also confirmed that the A domain is rather unstructured (Stjepanovic et al, 2011b).

Although in cell extracts FtsY seems to be about equally distributed between cytosol and membrane (Luirink et al, 1994), *in vivo* data suggest that FtsY is primarily located at the membrane (Mircheva et al, 2009). There FtsY is involved in protein-lipid and protein-protein interactions (Angelini et al, 2006; Millman et al, 2001). Furthermore, it has been shown that FtsY interacts physically and functionally with SecYEG (Angelini et al, 2005; Kuhn et al, 2011). In addition ample data has been gathered on the interaction of FtsY with lipids. It preferentially binds to anionic phospholipids (e.g. phosphatidyl glycerol) in a salt-sensitive manner with an optimum around 100 mM. Binding to phospholipids and lipid vesicles leads to changes in the structure of FtsY (de Leeuw et al, 2000; Reinau et al, 2010) and can activate its GTPase function, at least to some extent (de Leeuw et al, 2000; Lam et al, 2010). Two conserved sites at the A domain were proposed to be the main lipid interaction sites. The first is located at the N terminus of the A domain (amino acids 1 – 14) and the second at the interface between the A and N domains (amino acids 195 – 207). Using site-directed crosslinking data

suggest that these regions bind preferentially to anionic phospholipids and the region connecting them does not contribute to the lipid interaction. However, the two lipid-binding regions apparently provide stable binding to the membrane which is comparable to the binding of integral membrane proteins (Braig et al, 2009; Stjepanovic et al, 2011b; Weiche et al, 2008).

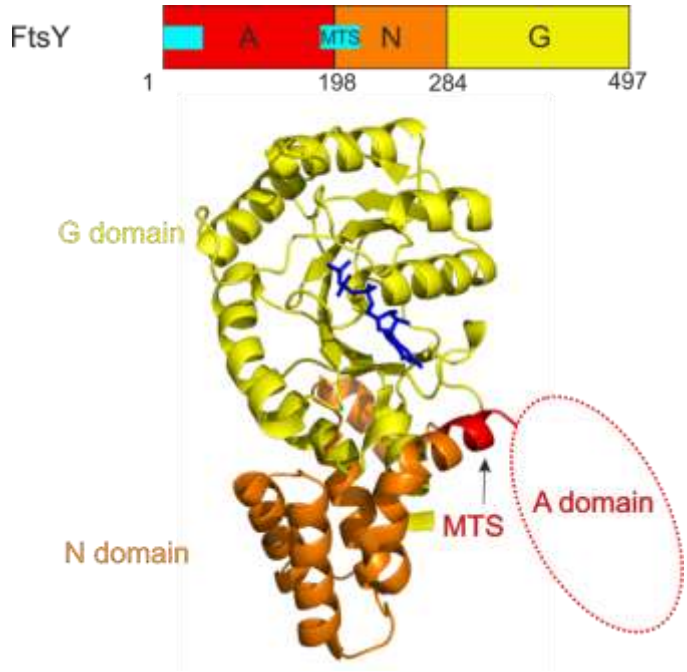

Figure 2-6 Structure of FtsY

Schematic representation of the domain organization of FtsY (top panel) crystal structure of the *E.coli* FstY-NG+1 in complex with GMPPNP (bottom panel). The MTS in the structure forms an α-helix, which is shared between the N and the A domain. A hypothetical localization of the A domain is designated in red dashed line. ((Reyes et al, 2007) PDB ID 2Q9B).

Regarding the second amphiphilic region between the A and N domain, it has been shown that an FtsY construct which encompasses the NG domain and Phe196 of the A domain (FtsY-NG+1) can rescue the otherwise severe ΔFtsY phenotype. In comparison, the NG domain construct lacking this single amino acid could not rescue the ΔFtsY phenotype and was not capable of releasing SRP from the ribosome *in vitro* (Bahari et al, 2007; Eitan & Bibi, 2004). The

crystal structure of these constructs revealed that the FtsY-NG+1 variant forms a helix at its N terminus due to the presence of Phe196, but in the case of FtsY-NG the N terminus remains unstructured. Thus, this second amphiphilic region belonging to both A domain and N domain was designated as the membrane targeting sequence (MTS) (Parlitz et al, 2007).

2.2.5 Membrane localization of FtsY and interaction with SecYEG

In the past most of the studies on FtsY addressed the localization of FtsY in the cells and the potential of FtsY to bind to lipids. The main reason was that *E.coli* FtsY does not have an additional integral membrane binding partner as in eukaryotes. Nevertheless, FtsY exists as a peripheral membrane protein that interacts with the membrane phospholipids via two conserved sequence in the A domain (Braig et al, 2009; Weiche et al, 2008). In addition it has been shown that FtsY also has a protein binding partner at the membrane (Millman et al, 2001). Furthermore, the study of the separate domains of FtsY has indicated that both seem to have affinity to the membrane. *In* vivo the A domain competes with full-length FtsY for membrane association, whereas the NG domain does not (de Leeuw et al, 1997). The protein binding partner of FtsY at the membrane was identified as SecYEG. This finding suggested how FtsY guides the RNC-SRP complex to an available SecYEG channel (Angelini et al, 2005). Later crosslinking studies have pinpointed the A domain of FtsY as the main site of interaction with the SecY subunit (Kuhn et al, 2011).

Currently, there are two models regarding the cellular localization of FtsY. The first one assumes that FtsY exists in a cytosolic and membrane-bound form. This model is based on cell fractionation and liposome binding experiments which show that FtsY is bound weakly to the membrane (Lam et al, 2010; Luirink et al, 1994; Parlitz et al, 2007). The second model is based on *in vivo* localization studies which indicate that FtsY is mostly associated with the membrane and on the observation that membrane targeting of RNC-SRP complexes via contact with FtsY requires that FtsY is initially in contact with the membrane (Mircheva et al, 2009).

2.3 Aim of this study

According to the current model of cotranslational membrane targeting of proteins, membrane proteins are early recognized during their synthesis by the SRP. After binding to the ribosome and the SAS, SRP recruits its receptor FtsY. The receptor tethers the RNC-SRP complex to the membrane, where the RNC is transferred to the SecYEG channel in a GTP-controlled manner. This process has been extensively studied in the past 30 years. However, there are still open questions concerning the localization of FtsY when it binds the RNC-SRP complex; the interaction of FtsY and SecYEG; the exact mechanism and timing of the GTP hydrolysis; the transfer of the RNC on SecYEG.

In this project we set out to investigate one of the least understood aspects of the SRP pathway – the interaction between FtsY and SecYEG and how this interaction changes after the RNC is transferred on SecYEG. The first part of the project aim at establishing an efficient expression and purification protocol for SecYEG that yield high amounts of pure complex suitable for biochemical studies. Furthermore, the incorporation of SecYEG into nanodiscs (SecYEG(ND), adopting a protocol from the literature. Here the main aim was to isolate the monomeric translocon in a biochemically defined form that would allow quantitative biochemical and biophysical experiments. For monitoring the interaction between FtsY and SecYEG, fluorescence labels were to be introduced into both partners to allow fluorescence resonance energy transfer (FRET) measurements. At the beginning of the project little was known about the interaction site of FtsY and SecYEG, which presented a challenge. Major aims were to characterize the interaction of FtsY and SecYEG(ND) by measuring the affinity and kinetic stability of the complex. Following up the finding that FtsY interacts with the lipid-embedded translocon via two interaction sites, the contribution of the NG and A domains of FtsY to the binding to SecYEG(ND) was to be determined. This aim included the characterization of conformational rearrangements between the domains of FtsY upon binding to SecYEG. In the second part of the project the main question was whether FtsY remains associated with the translocon after the RNC is transferred on the SecYEG translocon,. Finally, the GTPase activation of the SRP-FtsY complex in the context of SecYEG(ND) was to be characterized.

3. Results

3.1 SecYEG incorporation into nanodiscs

In this project, the main focus is on the SecYEG translocon and its interaction with the SRP receptor, FtsY and the ribosome. In order to monitor these interactions, we needed to handle SecYEG in an environment that mimicked the cytoplasmic membrane as closely as possible and should also provide SecYEG in a biochemically defined manner, allowing for quantitative measurements. The *in vitro* work with membrane proteins requires an adequate hydrophobic environment. Some of the commonly used methods include the addition of small amounts of detergents or embedding the proteins into lipid vesicles (e.g. proteoliposomes or inverted vesicles). The use of detergents avoids problems of aggregation and precipitation of the membrane proteins, but could potentially influence the interaction between binding partners. The use of proteoliposomes and inverted vesicles has the advantage that the proteins are in their native lipid environment which very much resembles the membrane of the cell. However, these methods have little control over the actual concentration and orientation of the proteins in the lipid bilayer. This is especially important when the membrane proteins have transport functions, such as membrane transporters. Another obstacle is that different oligomeric states cannot be controlled. In conclusion, the current methods for handling membrane proteins predominantly allow for qualitative measurements.

In this work, we have applied the recently developed method for embedding membrane proteins into nanodiscs (Alami et al, 2007; Dalal & Duong, 2010; Denisov et al, 2004). This technique allows the insertion of membrane proteins into a small lipid disc which is held together by two amphipathic α-helical proteins (membrane scaffold proteins – MSP) derived from apolipoprotein A-I which wraps around lipids in HDL. The discs can vary in size depending on the length of the scaffold proteins. The advantage of this method is that monomeric proteins are inserted into a membrane-like lipid environment. Since the discs engulf no lumen, the directionality of protein insertion is not an issue anymore, as proteins incorporated into nanodiscs are accessible from both sides. Thus, nanodiscs allow for the quantitative study of proteins in a biochemically defined system.

First, we established an expression and purification system for SecYEG, based on a plasmid encoding SecY, SecE, and SecG (a gift from Christiane Schaffitzel). The expression of the three

genes coding for SecYEG were under the control of a single *trc* promoter. For purification of SecYEG, SecE carried a C-terminal His_6-tag. The conventional *E.coli* strains for the expression of membrane proteins (CD41(DE3) and CD43(DE3)) did not yield sufficient amounts of protein. Therefore, we used the Lemo21(DE3) strain which is optimized for the overexpression of membrane proteins (Wagner et al, 2008). The growth and expression of SecYEG was performed at 37°C and the induction time was cut down from 16 to 4 hours.

SecYEG was purified according to an original protocol from the laboratory of Hans-Georg Koch (personal communication) with several modifications. We followed the centrifugation steps for separation of crude membranes, but added a cation exchange column as a third purification step. The cell debris was removed for 20 min at 20 000 x g and the membrane fraction was pelleted for 2 h at 150 000 x g. Afterwards, the membranes were solubilized in buffer containing 1 % DDM and 1 M NaCl. SecYEG was next purified on a Ni-affinity column, followed by a cation exchange chromatography on a HiTrapSP-HP column. This last step of purification removed some higher molecular weight contaminations (Figure 3-1).

In most of the experiments SecY was labeled at a specific cysteine via thio-maleimide coupling reaction. After completing the labeling and removing the unreacted dye, SecYEG was used for the formation of nanodiscs.

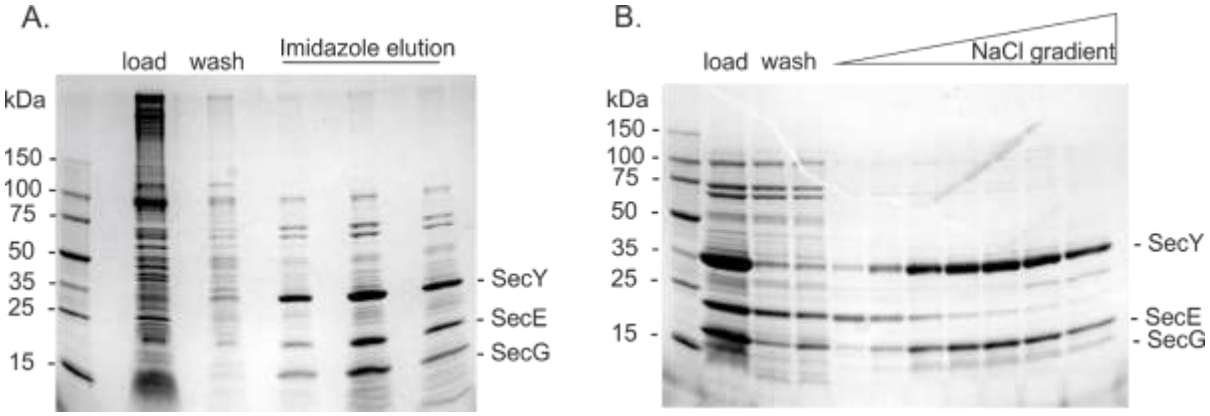

Figure 3-1: SecYEG purification.

The bacterial membranes containing SecYEG were pelleted and later solubilized by 1 % DDM. **A.** Afterwards the solubilized membranes we loaded on HisTrap column and SecYEG was eluted with 200 mM imidazole. **B.** The eluted fractions were rebuffered into low salt buffer and applied on SP cation exchange column. SecYEG was eluted in a 0 – 600 mM NaCl gradient.

The assembly of the nanodiscs was initially performed according to Alami *et al*, 2007. In order to increase the homogeneity of the nanodiscs we amended the ratio between SecYEG, MSP and the lipids, from 1:4:60 to 1:2:30 (SecYEG:MSP:lipids). To purify the complex of SecYEG in nanodiscs from excess of lipids we applied the sample on a 170 ml size exclusion column (Superdex 200). The routine quality control included clear native PAGE (CNP) and SDS-PAGE of the chromatographic peaks (Figure 3-2). The discs containing SecYEG (SecYEG(ND)) eluted in the peak at 0.55 column volume (CV). During the formation of nanodiscs containing SecYEG a small amount of empty discs was also formed. It eluted in a later peak at 0.65 CV.

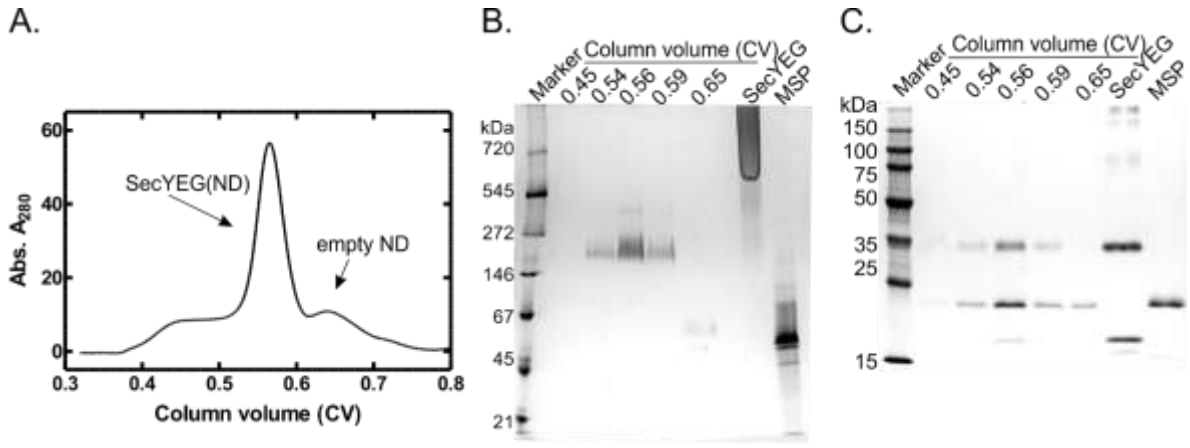

Figure 3-2 Purification and analysis of nanodiscs containing SecYEG.

A. To purify the complexes of SecYEG in nanodiscs (SecYEG(ND)) Superdex 200 size-exclusion chromatography was used. In this purification step SecYEG(ND) was separated from the excess lipids and additionally formed empty nanodiscs. **B.** To analyze the homogeneity of SecYEG(ND) the elution peaks were resolved by clear native PAGE. **C.** The presence of SecYEG and MSP in the complexes was verified by SDS-PAGE.

In some preparations, higher molecular weight species were resolved on the CNP from the same chromatographic peak. In order to verify whether these size differences were due to the presence of an extra copy of SecYEG or to differences in lipid content, we analyzed the gel bands by mass spectrometry. The results confirmed that the bands contained MSP and SecYEG. We also quantitated the ratio between SecY and MSP using intensity based absolute quantification (iBAQ) (Smits et al, 2013). In all bands, the SecY:MSP ratio was 1:2. Thus our nanodisc preparations contained monomeric SecYEG (Figure 3-3, panel A.). Initially we also worked with SecYEG embedded in larger nanodiscs, 12 nm in diameter (SecYEG(ND^{E})

(Denisov et al, 2004). We also quantitated the composition of these discs by iBAQ, because their size allows the embedding of two copies of SecYEG. In our preparations of SecYEG(ND^{E}) the translocon was present as monomer and the exhibited higher molecular weight due to the larger amount of lipids (data not shown) compared to the standard 10 nm SecYEG(ND). In addition we verified the homogeneity of the SecYEG(ND) using negative staining electron microscopy (EM). The disc particles appeared relatively small, but regular in size, and no aggregates were observed (Figure 3-3, panel B.) Thus, we concluded that the difference in the molecular weight observed on the CNP of the same chromatographic peak result from small difference in the lipid amount, which change the electrophoretic mobility, but do not affect the overall appearance of the nanodiscs.

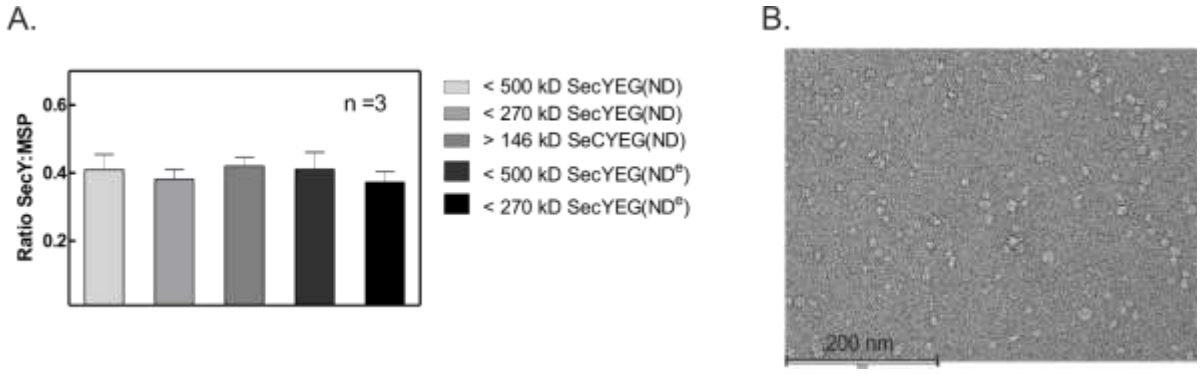

Figure 3-3 Characterization of SecYEG(ND) by iBAQ negative-staining EM

A. Quantification of the number of SecYEG molecules per nanodiscs by subjecting to mass spectrometry gel bands from clean native PAGE and analyzing the results by iBAQ. The analysis was performed by Ilian Atanossov. **B.** Negative stain electron micrograph of SecYEG(ND) which represents nanodiscs of similar shape and size. The imaging was performed by Andruis Krasauskas.

3.2 Binding of FtsY to SecYEG

To monitor the binding of FtsY to SecYEG, we used fluorescence resonance energy transfer (FRET) between SecY labeled at position S111C with MDCC (SecY(111MDCC)EG) and FtsY labeled with an acceptor dye, Bodipy FL at position F196C (FtsY(196Bpy)). The labeling positions and the donor- acceptor pair are the same throughout this work (Figure 3-4, panel B.) unless stated otherwise. We compared the fluorescence change of SecY(111MDCC)EG upon binding to FtsY(196Bpy) under different conditions: (a) SecY(111MDCC)EG in solution

with detergent added, (b) without detergent, and (c) SecY(111MDCC)EG in nanodiscs (SecY(111MDCC)EG(ND). We observed a 30% decrease in the donor fluorescence in the case of SecY(111MDCC)EG(ND), compared to SecY(111MDCC)EG without detergent. In the presence of the detergents Nikkol and/or DDM (Akopian et al, 2013a; Peluso et al, 2001; Shen et al, 2012) no significant change in donor fluorescence was observed Figure 3-4, panel B.). This indicated that FtsY binds to SecY(111MDCC)EG in a similar fashion as to SecY(111MDCC)EG(ND), but the presence of detergents impairs complex formation.

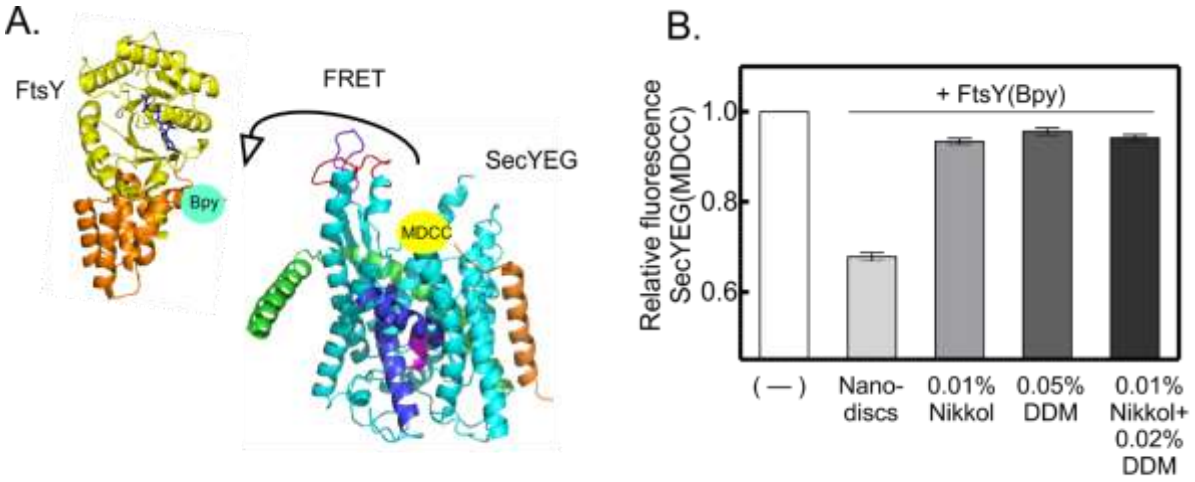

Figure 3-4 FtsY binding to SecYEG in different environments.

A. FRET pair of SecYEG ((Van den Berg et al, 2004) PDB ID 1RHZ) labeled with MDCC and FtsY (structure of FtsY-NG+1 PDB ID 2Q9B) labeled with Bpy. **B.** Comparison of the FRET efficiency of FtsY(196Bpy) binding to SecY(111MDCC)EG embedded in nanodiscs or only in buffer with or without added detergent.

3.2.1 Affinity of FtsY binding to SecYEG

The previous results raised the question whether the presence of lipids has an influence on the binding of FtsY to SecYEG. In order to test this, we measured the affinity of FtsY(196Bpy) to SecY(111MDCC)EG when (a) SecYEG was in solution, (b) embedded in nanodiscs with 10 nm diameter (SecYEG(ND)), or (c) in extended 12 nm nanodiscs (SecYEG(ND^E)), assembled with a longer construct of the MSP protein, which contain more lipids than standard SecYEG(ND). We observed no difference in the affinities dependent on the size of the discs (K_d = 0.18 ± 0.02 µM) and only a 2-fold decrease in the affinity when SecYEG was in solution (K_d = 0.35 ± 0.04

μM) (Figure 3-5).In order to check if the fluorophore labels could have influenced the measurements, we made a comparison with a label-free method – ITC. The affinity of 0.24 μM measured by ITC (J. Jöckel, personal communication) was in the same range as measured by fluorescence. This indicated that the labels did not interfere with the interaction of the two binding partners.

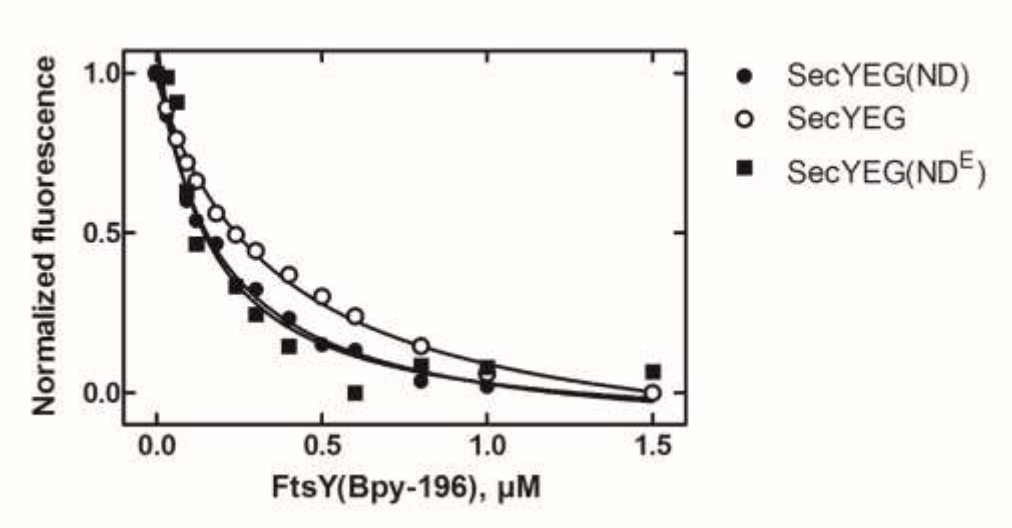

Figure 3-5 Affinity of FtsY binding to SecYEG.

Affinity titration of SecY(111MDCC)EG in solution without detergent, in 10 nm nanodiscs (SecYEG(ND), or in 12 nm nanodiscs (SecYEG(ND^E) with FtsY(196Bpy). K_d values in Table 2 – 1.

Previous work has shown that FtsY binds better to inner-membrane vesicles (INVs) when bound to a non-hydrolyzable GTP analog (GMPPNP) (Angelini et al, 2006). We tested whether FtsY in complex with the different guanine nucleotides has a different affinity to SecY(111MDCC)EG(ND). SecY(111MDCC)EG(ND) was titrated with FtsY(196Bpy) in the presence of GDP, GTP, GMPPNP or in the absence of nucleotide. The affinity of FtsY remained the same independent of the nucleotide (Table 3-1).

In conclusion, we show that FtsY binds to SecYEG with high affinity ($K_d \approx 0.2$ μM). The affinity of the complex is about the same for SecYEG free in solution, or when the translocon is embedded into nanodiscs. Since SecYEG is a membrane protein, the nanodiscs seem to be a suitable environment and ensure that the protein is a monomer.

Table 3-1: Affinity of FtsY binding to SecYEG

FtsY binding to	K_d, µM
SecYEG(ND) + GTP + GDP +GMPPNP No nucleotide	0.18 ± 0.02
SecYEG(ND^E)	0.13 ± 0.02
SecYEG without detergent*	0.35 ± 0.04
SecYEG in detergent**	no binding
SecYEG(ND) ITC data***	0.3

*No detergent present in the reaction buffer
**0.05% DDM, 0.01% Nikkol or a combination of both
*** the ITC measurements were performed by Johannes Jöckel

3.2.2 Interaction of FtsY with empty nanodiscs

Although we have determined the affinity of FtsY to SecYEG(ND), it was still unclear what is the contribution of the lipid binding. Previous work suggested that FtsY has two potential interaction sites at the membrane and each one of them is sufficient for the membrane localization of FtsY. One is a trypsin-sensitive component and the second is the membrane lipids (Millman et al, 2001).

We set out to characterize the interaction of FtsY with lipids using empty nanodiscs (ND). Since the nanodiscs were not labeled, the binding of FtsY to ND was monitored indirectly in a competition experiment with SecYEG(ND). We measured the affinity between SecY(111MDCC)EG(ND) and FtsY(196Bpy) upon addition of increasing concentrations of ND (Figure 3-6, panel A.). The presence of ND did not influence the affinity of FtsY(196Bpy), but

affected only the amplitude of the fluorescence change. This indicated that the ND is a noncompetitive binding partner.

Since, the effect of the ND is to make it appear as if less total FtsY is present by binding to it, then by analyzing the change of the fluorescence amplitude an estimate can be obtained for the apparent affinity ($K_{d_{app}}$) of FtsY to ND. To calculate it the final fluorescence levels were plotted against the ND concentration and fitted to a hyperbolic function: $F_{ND} = \frac{F}{(1+\frac{ND}{K_{d_{app}}})}$ (Segel, 1993), where F_{ND} is the fluorescence level in the presence of ND, *F* is the fluorescence level in the absence of ND and *ND* is the concentration of empty nanodiscs in the titration.

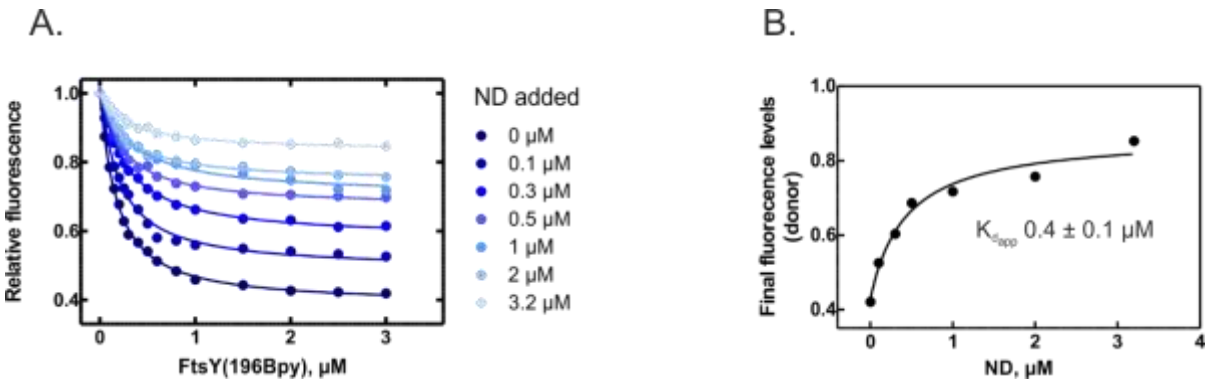

Figure 3-6 FtsY binding to SecYEG(ND) in the presence of ND.

A. SecY(111MDCC)EG(ND) titrated with FtsY(196Bpy) in the presence of increasing concentrations of ND. **B.** Plot of the final fluorescence levels of the titrations versus the ND concentration gives an estimate for the affinity of FtsY to ND.

Therefore, FtsY binds equally well to empty nanodiscs as to SecYEG embedded in nanodiscs. In this sense we could not distinguish whether FtsY binds to SecYEG or the lipids and which interaction is more dominant. This agreed with the previous observation that each of the two interaction sites of FtsY at the membrane are equal in contribution to the localization of FtsY. Furthermore, the noncompetitive character of the binding partners suggested that probably FtsY interacts with SecYEG(ND) and ND in a different conformation (Christopoulos, 2002).

3.2.3 Stability of the FtsY-SecYEG(ND) complex

It has been long disputed in the literature whether FtsY is mostly localized at the membrane or in the cytosol (de Leeuw et al, 1997; de Leeuw et al, 2000; Luirink et al, 1994; Parlitz et al, 2007; Weiche et al, 2008). Importantly, only the membrane bound FtsY is able to induce release of SRP from the signal anchor sequence (SAS) (Valent et al, 1998). Recently, this question has been investigated using *in vivo* GFP-tagged FtsY and fluorescence microscopy (Mircheva et al, 2009). Their results show that FtsY is predominantly localized at the membrane, contrary to 30 - 50% as previously assumed (Luirink et al, 1994; Parlitz et al, 2007). We wanted to test the stability of the complex between FtsY and SecYEG(ND) by using our FRET setup in a stopped-flow apparatus. In the experiment, FtsY(196Bpy) was displaced from SecY(111MDCC)EG(ND) by addition of a 10-fold excess of unlabeled FtsY.

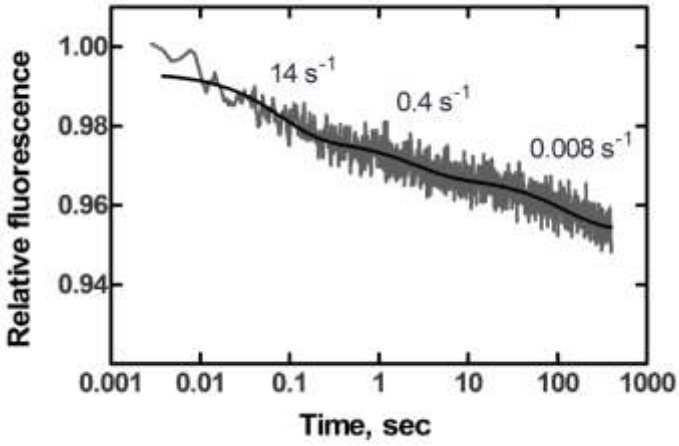

Figure 3-7 Stability of the complex between SecYEG(ND) and FtsY.

The complex of SecY(111MDCC)EG(ND) and FtsY(196Bpy) was pre-formed. Dissociation was induced by rapidly mixing the complexes with a 10-fold excess of unlabeled FtsY, and the change in fluorescence of Bpy was monitored in a stopped-flow apparatus.

The fluorescence trace from the change of the acceptor fluorescence was fitted to a three exponential decay (Figure 3-7). The first two exponents comprised 70% of the main amplitude change. The first phase, a fast dissociation step of 14 s^{-1} was followed by a slower second step of 0.4 s^{-1}. The third phase was too slow to be physiologically relevant (0.008 s^{-1}). Thus, we focused our analysis on the first two steps. The data showed that FtsY dissociates from

SecYEG(ND) in two steps, where the second step is rate-limiting with a half-life time of 1.7 s, indicating a limited stability of the complex. Alternatively, the two-step dissociation could indicate different population of complexes or that there are two binding sites of FtsY on SecYEG(ND). The latter possibility would agree with previous results which suggested that FtsY is associated with the membrane through both protein-lipid and protein-protein contacts (Angelini et al, 2006; Braig et al, 2009; Millman et al, 2001). Further studies have shown that FtsY binds to lipids via its membrane targeting sequence (MTS) located between its A and N domains (Millman & Andrews, 1999; Stjepanovic et al, 2011b) and also is associated with SecY via its A and N domains (Angelini et al, 2005; Kuhn et al, 2011). As to the localization of FtsY in the cell, the limited stability of the FtsY complex with the ND-embedded translocon indicates that part of FtsY may dissociate from the complex during cell extract preparation, explaining the considerable amount of free FtsY observed during cell fractionation (Luirink et al, 1994).

3.2.4 Binding of FtsY NG and A domains to SecYEG(ND)

To further dissect the way FtsY binds to SecYEG(ND), we used four FtsY constructs and compared them to full-length FtsY (Figure 3-8). The first two constructs were well-studied variants of the NG domain: FtsY-NG+1 and FtsY-NG. Both constructs bind GTP and GDP with comparable affinities to FtsY, interact with SRP and stimulate the GTPase function of the complex (Bahari et al, 2007). FtsY-NG comprises amino acids from Ala197 to the end of the C terminus 497. FtsY-NG+1 included also Phe196 at the N-terminus, which completed the MTS that is crucial for lipid association (Parlitz et al, 2007; Stjepanovic et al, 2011b). It has been shown for these two variants that the ΔFtsY phenotype can be rescued by FtsY-NG+1 whereas FtsY-NG cannot (Eitan & Bibi, 2004). The other two constructs were variants of the FtsY A-domain. FtsY-A197 comprised the first 197 N-terminal amino acids and FtsY-A208 the first 208. The main difference between the two variants was that FtsY-A197 included only one amphiphilic sequence at position 1 – 14 and FtsY-A208 included both: 1 – 14 and 195 – 207 – MTS. Previous work has indicated that that both sequences contribute to the lipid binding of FtsY and are important for the membrane localization of FtsY (Braig et al, 2009; Weiche et al, 2008).

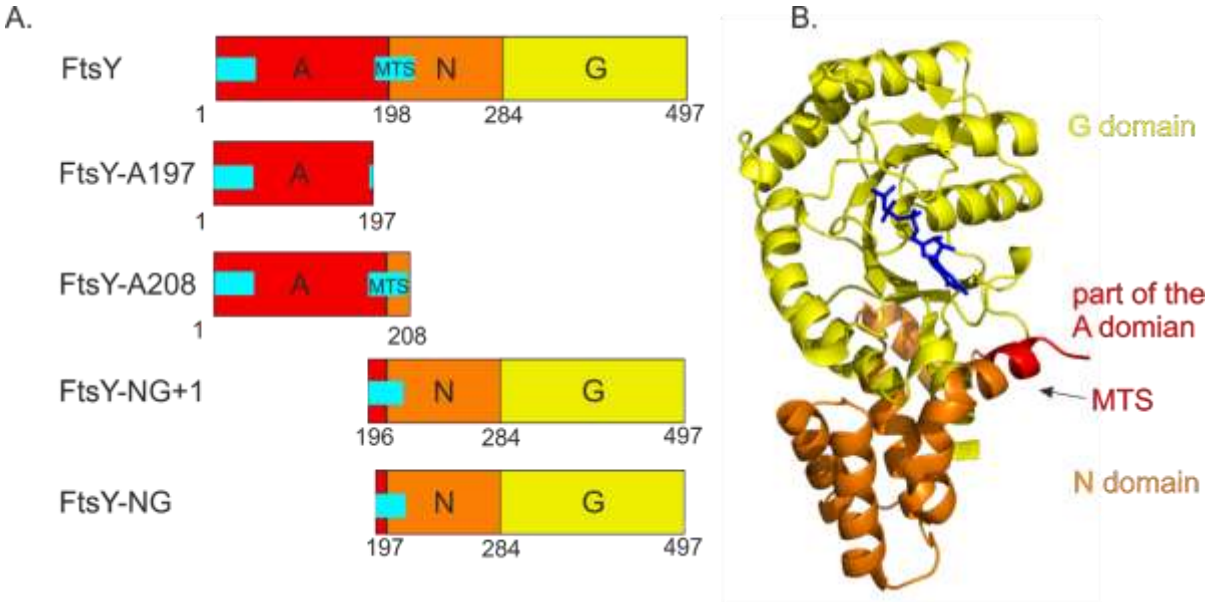

Figure 3-8 FtsY constructs.

A. Schematics of the FtsY constructs used in this work, **B.** Structure of FtsY-NG+1 in complex with GMPPNP (blue) ((Reyes et al, 2007) PDB ID 2Q9B). The A domain is not present in the structure.

To purify the A-domain constructs and to ensure that they are not proteolytically degraded in the cell, we cloned them in a pSUMO vector with an N-terminal His_6-tag and a SUMO-cleavage site between the tag and the first methionine.

First, we examined the binding of all four constructs to SecYEG(ND) and determined their affinity to SecY(111MDCC)EG(ND). Binding was monitored by either the fluorescence change of MDCC induced by FtsY-NG and NG+1, or by FRET between MDCC and Bpy at position 167 in FtsY-A197 and FtsY-A208. All constructs bound with K_d values that were comparable to the binding of full-length FtsY, i.e. around 0.2 µM (Table 3-2). Thus, despite of the substantial truncations the affinities were not affected significantly. These data suggested that the two domains individually bound strongly to SecYEG(ND), but their contribution did not appear as additive when full-length FtsY was bound. This suggested that there was an additional event that consumes part of the binding energy. One possibility is that there is an interaction between the NG and A domains which is disrupted upon binding. In such a scenario, the inter-domain rearrangement will require extra energy. Following, we examine whether the isolated NG and A domains of FtsY form a complex.

Table 3-2: Affinity of FtsY NG and A domains in binding to SecYEG(ND)

FtsY construct	K_d, µM
FtsY	0.18 ± 0.02
FtsY-NG+1	0.15 ± 0.02
FtsY-NG	0.23 ± 0.02
FtsY-A208	0.20 ± 0.01
FtsY-A197	0.30 ± 0.02

3.3 Interaction of the FtsY-NG domain with the FtsY-A domain

3.3.1 Affinity of the FtsY-NG domain binding to the FtsY-A domain

We set out to test whether the NG and A domains of FtsY interact. We inserted fluorescent dyes for FRET measurements into the A domain at position A167C and labeled it with Bodipy FL as donor (FtsY-A197(167Bpy) and FtsY-A208(167Bpy)). FtsY-NG was labeled with the non-fluorescent acceptor dye QSY9 at position V342C (FtsY-NG(342QSY9).

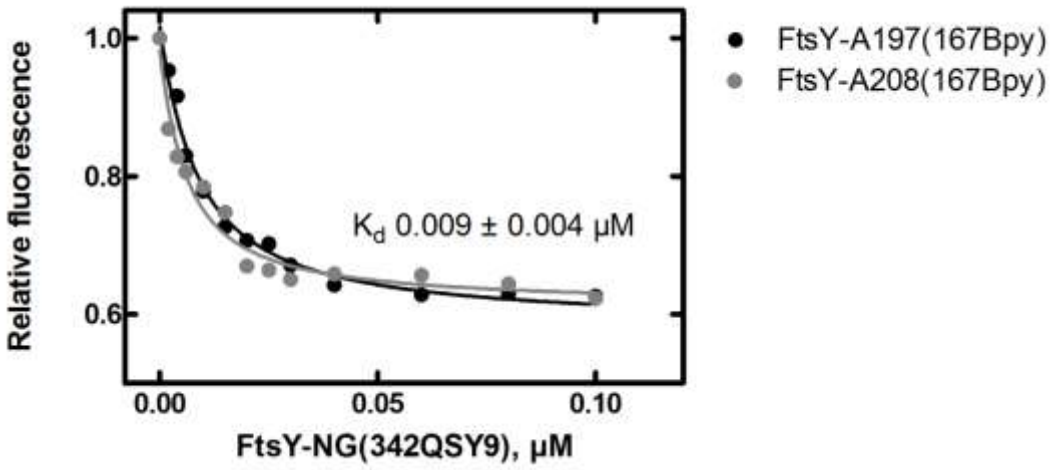

Figure 3-9 Binding of the FtsY-NG and the FtsY-A domain.

Fluorescence titration of 0.02 µM FtsY-A197(167Bpy) or FtsY-A208(167Bpy) with FtsY-NG(342QSY9)

For these measurements, we only used the FtsY-NG construct. It represents the GTPase domain and has the least sequence overlap with the A domain constructs. In fact, as expected, the two domains formed a complex, and the affinity of the complex was very high, K_d = 9 nM. Thus, the interaction between the domains is strong enough to explain the energy loss observed above, although the match was not quantitative.

To clarify if the interaction between the NG and A domain can explain the non-additive effect on the affinity of FtsY and SecYEG(ND), we calculated the free energy of each interaction (ΔG°) using the measured K_d values. The results are summarized in Table 3-3. If the contributions of the NG and A domains for the binding of FtsY were additive, then the ΔG° of the interaction between FtsY and SecYEG(ND) should be the sum of the ΔG° values of the individual interactions, about -15 kcal/mol. The difference between the calculated and the experimentally measured free energy of FtsY binding ($\Delta\Delta G^\circ$) is approximately 8 kcal/mol. This energy is not far from the free energy of the interaction between the two domains, – 9.6 kcal/mol, supporting the model. The discrepancy between the calculated and the measured $\Delta\Delta G^\circ$ may be attributed to a somewhat different behavior of the isolated domains, compared to being connected by a linker, which may also change conformation upon domain separation.

Table 3-3 Free energies of the binding of SecYEG(ND) to FtsY and of the interaction between FtsY NG and A domains

FtsY domain(s)	ΔG° kcal/mol*
FtsY	-7.8
FtsY-NG+1	-7.9
FtsY-NG	-7.7
FtsY-A197	-7.5
FtsY-A208	-7.7
FtsY-NG+FtsY-A	-6.7
FtsY domain interaction	
FtsY-NG:FtsY-A	-9.6

* $\Delta G^\circ = RT\ln K_d$, where R is the universal gas constant (1.98 cal/K mol), T is the absolute temperature in Kelvin and K_d is the dissociation constant in mol/L.

3.3.2 Conformational change of FtsY upon binding to SecYEG(ND)

We measured FRET between FtsY-A(167Bpy) and FtsY-NG(342QSY9) to determine whether the binding to SecYEG(ND) or to ND influences the interaction between the FtsY domains. The titrations of the complexes of FtsY-A197(167Bpy) and FtsY-NG(342QSY), and FtsY-A208(167Bpy) and FtsY-NG(342QSY9) with SecYEG(ND) or ND showed similar affinities (Figure 3-10). The change of FRET accompanying complex formation indicates that the domains of FtsY separate from each other upon binding to SecYEG(ND) or to ND. The analysis of the titrations suggested once more that the affinity of FtsY binding to SecYEG(ND) or to ND is about the same (K_d = 1 ± 0.2 µM).

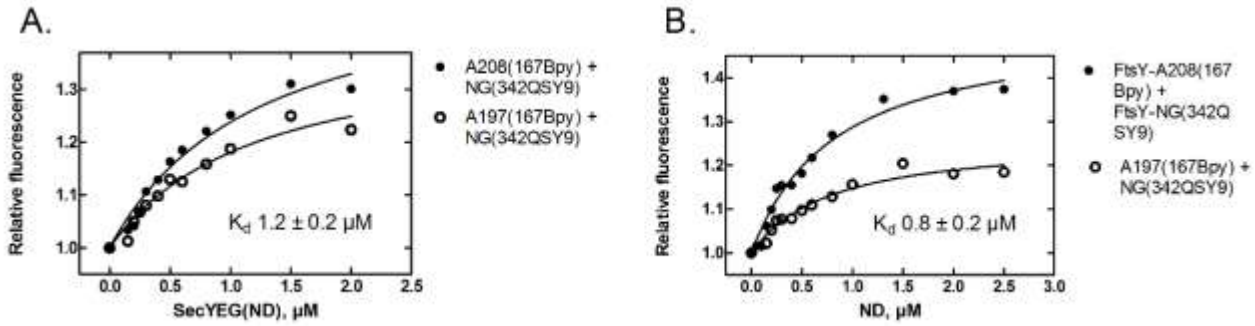

Figure 3-10 Interaction of the complex of FtsY-NG and FtsY-A with SecYEG(ND) or ND.

The 1:1 complex of FtsY-A197(167Bpy) and FtsY-NG(342QSY9) or of FtsY-A208(167Bpy) and FtsY-NG(342Bpy) at 0.05 µM final concentration was titrated with empty ND **(A.)** or with SecYEG(ND) **(B.)**. The increase of Bpy donor fluorescence due to the decrease in FRET was monitored.

We continued the investigation of the conformational change of FtsY upon binding to SecYEG(ND). A a double cysteine mutant of full-length FtsY was constructed for measurements of homoFRET between two identical fluorophores. The same positions were used as in the previous experiments: V342C and A167C, and both positions were labeled with Bodipy FL (FtsY(167Bpy,342Bpy)). Bodipy FL has a small Stokes shift (Figure 3-11, panel A.), high extinction coefficient and the Förster distance for homoFRET is about 57 Å. This makes it suitable for the purpose of our measurements (Buskiewicz et al, 2005; Lakowicz, 2003; Runnels & Scarlata, 1995). In the homoFRET measurements, Bodipy FL is both donor and acceptor, and energy transfer leads to a decreased anisotropy of the fluorescence.

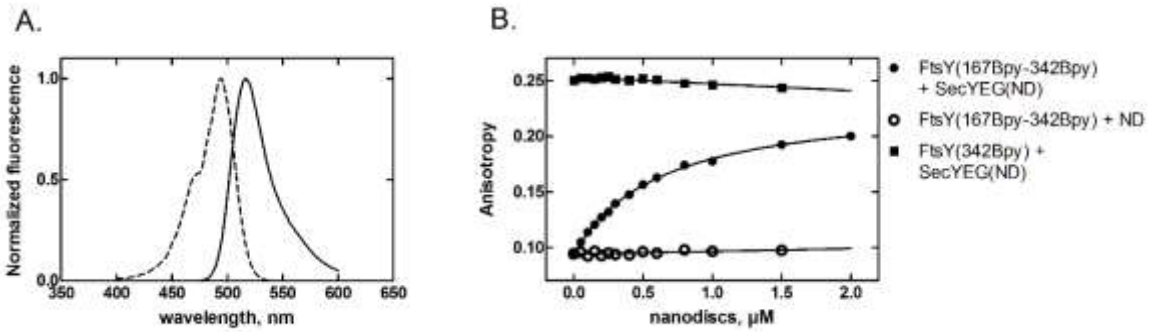

Figure 3-11 FtsY domain rearrangements upon binding toSecYEG(ND) or ND monitored by homoFRET.

A. Bodipy FL (Bpy) excitation (dashe line) and emission (solid line) spectra, showing the small Stokes shift of 20 nm. **B.** Titration of 0.05 µM FtsY, labeled at positions 167 and 342 with Bpy, with SecYEG(ND) or with ND. The increase in anisotrpy was monitored due to the decrease in FRET. As a control we used single-labeled FtsY, at position 342 with Bpy, and titrated it with SecYEG(ND).

We titrated FtsY(167Bpy,342Bpy) with SecYEG(ND) or ND and monitored the change in anisotropy (Figure 3-11, panel B.). In the titration with SecYEG(ND), the anisotropy of FtsY increased from 0.09 to 0.2. The increase in anisotropy indicated that the distance between the two fluorophores increased upon binding, thus the distance between the two FtsY domains also had increased. In the control titration with empty ND, no change of anisotropy was observed, indicating that binding to ND did not cause a change of the domain arrangement of double-labeled FtsY. In the control experiment where we used FtsY labeled only at position 342 with Bodipy FL, the anisotropy remained at an initial value of 0.25. Given the different experimental setups, the K_d of FtsY binding to SecYEG(ND) was comparable with the values obtained in the titrations described above, i.e. 0.2 ± 0.01µM for FtsY(196Bpy) binding to SecY(111MDCC)EG(ND) or 1.2 ± 0.2 µM the binding of the complex of the two domains FtsY-NG(342QSY9) and FtsY-A(167Bpy) to SecYEG(ND).

3.3.3 The contribution of the individual domains of FtsY to the binding to SecYEG(ND)

So far, we have shown that the dissociation of FtsY from SecYEG(ND) takes place in two steps. Also the separate domains of FtsY bind independently to SecYEG(ND). This suggested that there are potentially two binding sites for FtsY on SecYEG(ND). To test this possibility, we

examined the four domain variants of FtsY which we used previously: FtsY-A197, FtsY-A208, FtsY-NG and FtsY-NG+1 (Section 3.2.4.), for their ability to compete with full-length FtsY for binding to SecYEG(ND). Thus, we performed a series of competition titrations. In these experiments, we titrated SecY(111MDCC)EG(ND) with FtsY(196Bpy) in the presence of increasing concentrations of the FtsY domains.

The four variants were added in concentrations up to 10 or 15 µM (Figure 3-12). Given affinities around 0.2 µM (Table 3-2), this concentration range should saturate any effect on FtsY binding. We observed that FtsY-NG+1, FtsY-NG and FtsY-A197 did not affect the affinity of full-length FtsY binding to SecYEG(ND). Only FtsY-A208 decreased the affinity. Additionally, FtsY-A208 caused a significant decrease of the fluorescence change of the donor and FtsY-A197 had a minor effect on the fluorescence signal. The two NG domain construct did not influence the fluorescence signal at all. These results indicated that FtsY-NG and FtsY-NG+1 do not influence the binding of full-length FtsY, although they should be bound, given a binding affinity around 0.2 µM. On the other hand, the A-domain variants appear to alter the binding of FtsY(196Bpy). Especially, FtsY-A208 which decreased the fluorescence amplitude and the affinity of the interaction due to complex formation with SecYEG(ND). FtsY-A197 had a similar, somewhat smaller effect on the fluorescence amplitude.

To quantitate the effect of competitors on the binding of FtsY to SecYEG(ND) the apparent K_ds were plotted against the competitor concentration (Figure 3-12, panel F.). The data was analyzed using a linear function describing competitive binding: $K_{d_{app}} = \frac{K_d^F}{K_d^C} * C + K_d^F$, where $K_{d_{app}}$ is the apparent affinity of FtsY and SecYEG(ND) in the presence of competitor, K_d^F is their affinity in the absence of competitor, C is the competitor concentration, K_d^C is the affinity of the competitor to SecYEG(ND) (Segel, 1993). From the analysis of the apparent K_ds the intrinsic K_d of FtsY was calculated to be 0.2 – 0.3 µM, in agreement with the direct measurements; the K_d of FtsY-A208 was estimated to be 0.3 µM, also in agreement with direct measurements. Nevertheless, the effect of FtsY-A208 seemed to be weaker than of FtsY full-length.

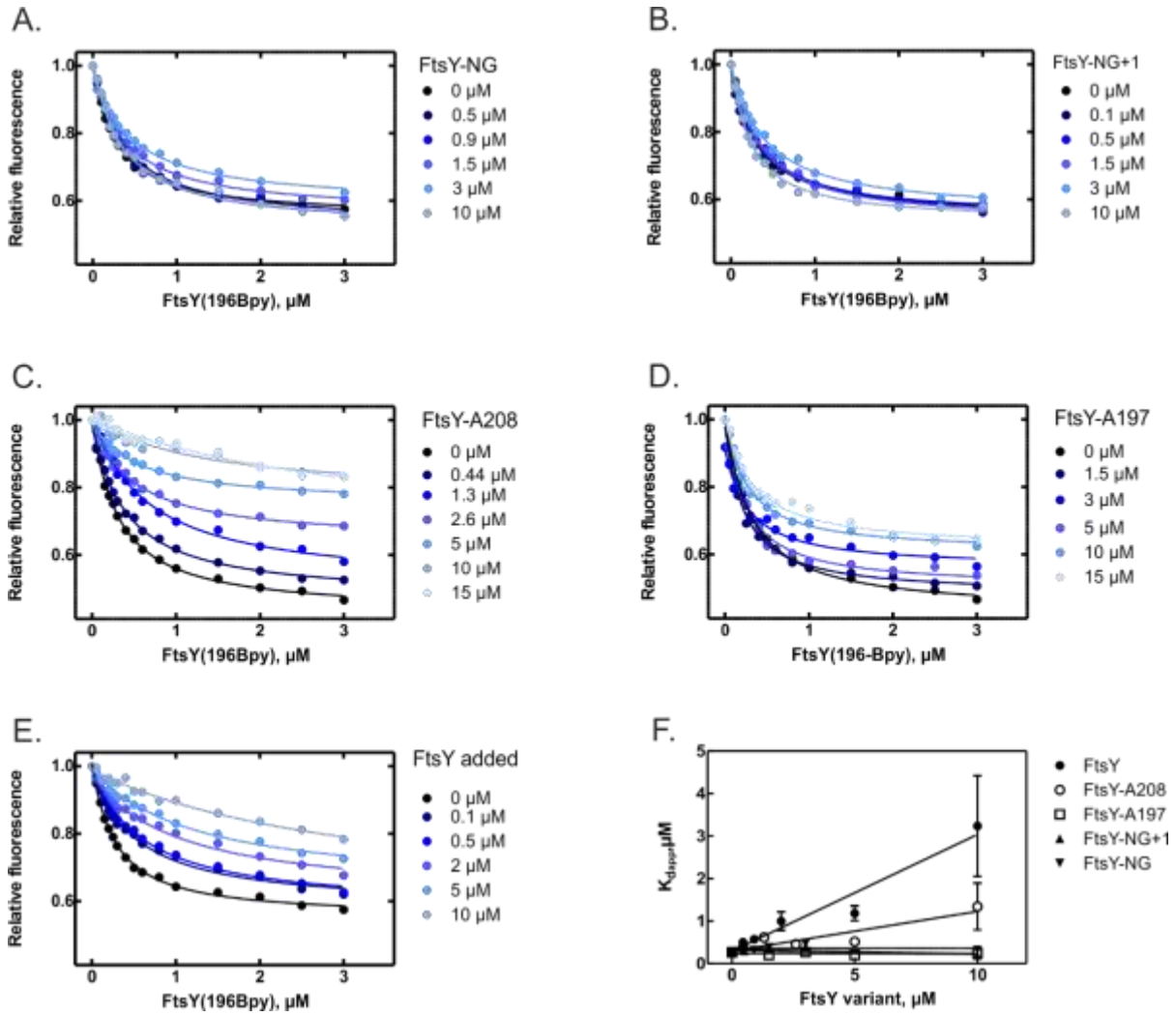

Figure 3-12 Influence of FtsY-NG and A domains on FtsY binding to SecYEG(ND).

SecY(111MDCC)EG(ND) was titrated with FtsY(196Bpy) in the presence of increasing concentrations of competitor: **A.** FtsY-NG, **B.** FtsY-NG+1, **C.** FtsY-A208, **D.** FtsY-A197 or **E.** FtsY. **F.** Plot of the apparent affinities of FtsY(196Bpy) versus the concentration of competitor construct.

3.4 Interaction of the ribosome with SecYEG(ND)

In general the interaction between the Sec translocon and the ribosome has been well characterized. There are numerous structural studies (Becker et al, 2009; Beckmann et al, 1997; Frauenfeld et al, 2011; Gogala et al, 2014; Menetret et al, 2007) which were aiming at capturing different states of the translocon during protein translocation. In addition there are also biochemical data from floatation assays, surface plasmon resonance (SPR) and fluorescence

correlation spectroscopy (FCS), that describe the interaction in thermodynamic terms (Behrens et al, 2013; Prinz et al, 2000; Wu et al, 2012). The later all converge to the same conclusion it is a high affinity interaction in the nanomolar range. Little is known on the interaction of the ribosome with SecYEG in the presence of FtsY. We wanted to investigate the interaction between SecYEG(ND) and the ribosome in the context of the other interaction partner FtsY.

3.4.1 Affinity of the ribosome to SecYEG(ND)

First we established a reporting system for the interaction between the ribosome and SecYEG(ND). We used a FRET reporter pair between the donor MDCC and the acceptor Alexa488 (Alx488). The ribosomal protein L23 protein was labeled with the donor fluorophore at position S21C (70S(L23MDCC)) and SecY was labeled with the acceptor at position S111C (SecY(111Alx488)EG(ND) (Holtkamp et al, 2012b). Based on cryo-EM structure we expected that the two labels will not interfere with each other and will be in a sufficient FRET distance (Figure 3-13, panel A.) (Frauenfeld et al, 2011).

In equilibrium experiments we measured the affinity between the ribosome and SecYEG(ND). We used either vacant ribosomes (70S) or Lep75-RNC or Lep94-RNC (Figure 3-13, panel B). In the presence of the nascent chain the affinity of the ribosome to SecYEG(ND) increased 5 – 7-fold, from 0.05 ± 0.02 μM to 0.010 ± 0.002 for Lep75-RNC and to 0.008 ± 0.003 μM for Lep94-RNC. Our findings were in line with the published data that the interaction with RNC is enhanced compared to the interaction with vacant ribosomes.

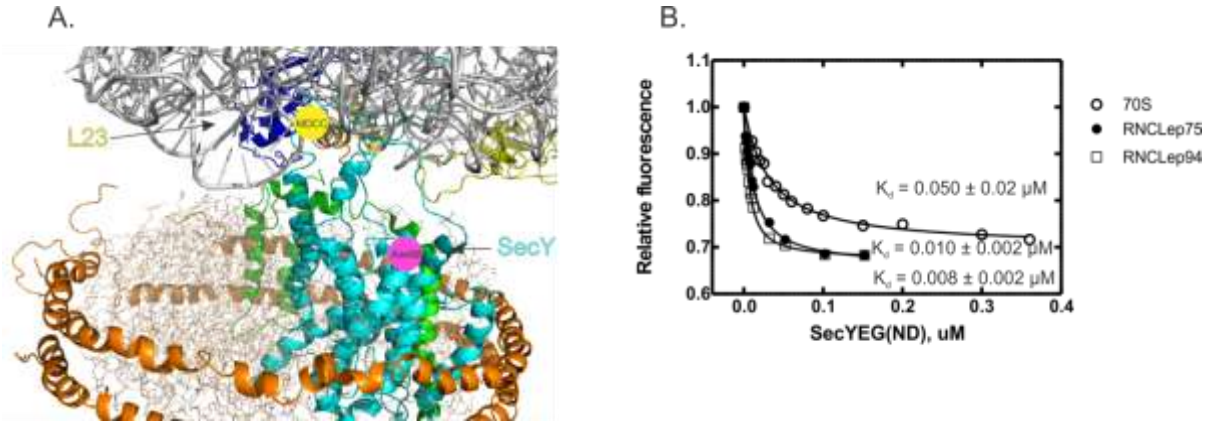

Figure 3-13 Affinity of SecYEG(ND) binding to the ribosome.

A. Reporter positions on the 70S at protein L23 labeled at position S21C with MDCC (yellow) and SecY labeled at position S111C with Alexa 488 (pink) ((Frauenfeld et al, 2011) PDB ID 3J00 and 3J01) **B.** Affinity titration of 70S(MDCC), Lep75-RNC and Lep94-RNC with SecY(111MDCC)EG(ND).

3.4.2 Dynamics of SecYEG(ND) complex formation with the ribosomes

To examine in more detail the effect of the nascent chain on the interaction with SecYEG(ND) we performed a series of kinetic experiments. At first, we probed the complex formation by rapidly mixing MDCC-labeled 70S or Lep75-RNC or Lep94-RNC with increasing concentrations of SecY(111Alx488)EG(ND). The experiments we performed under pseudo-first-order conditions with 0.016 µM ribosomes and an excess of SecYEG(ND) (0.09 to 0.2 µM). All stopped-flow traces could be fitted to a double exponential function (Figure 3-14, panels A – C.). The apparent rate constants of the first step (k_{app1}) increased linearly with the SecYEG(ND) concentrations with a slope corresponding to the $k_1 = 110 \pm 10\ \mu M^{-1}s^{-1}$ and y-intercept corresponding to $k_{-1} = 4 \pm 1\ s^{-1}$ (Figure 3-14, panel D.). The second step (k_{app2}) did not change systematically. (Figure 3-14, panel E.). In the concentration range used the k_{app2} appears to be already saturated at 0.1 µM. Taking into consideration k_{-2} (measured later in this section to be 0.08 s^{-1}) and the $k_{app2} \approx 1.5\ s^{-1}$, the calculated $k_2 \approx 1.4\ s^{-1}$.

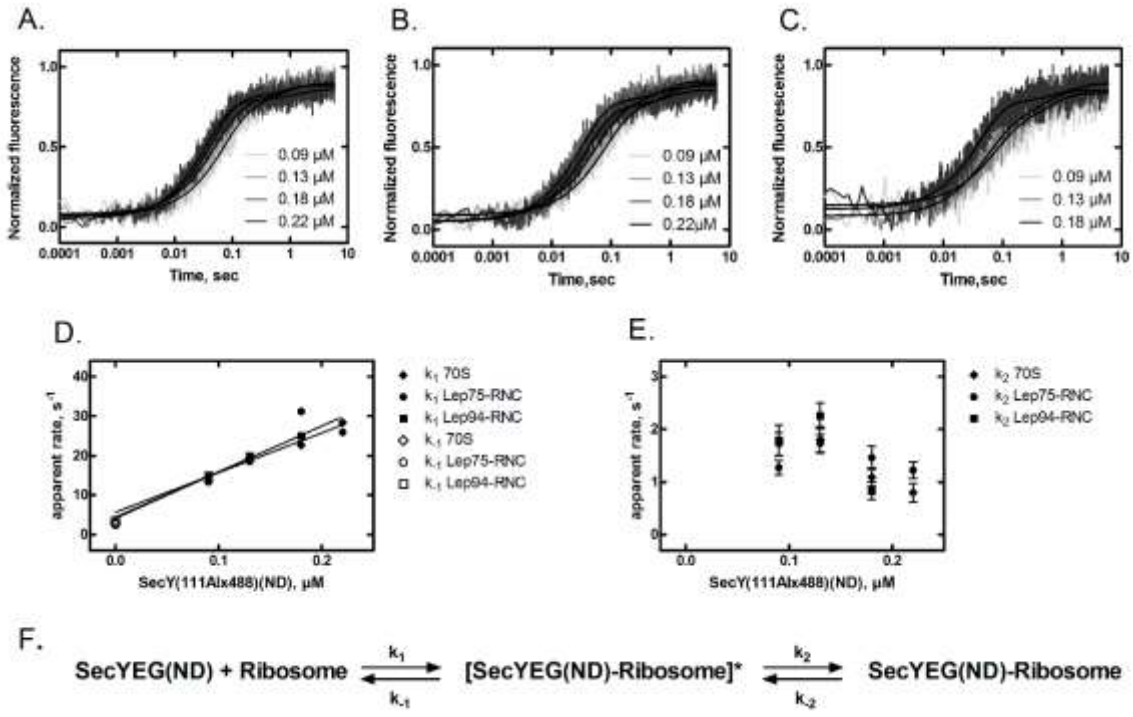

Figure 3-14 Rapid kinetics of SecYEG(ND) complex formation with the ribosomes.

SecYEG(ND) complex formation with **A.** 70S, **B.** Lep75-RNC and **C.** Lep94-RNC. MDCC-labeled 70S or RNC (0.016 µM final concentration) were titrated with Alx488- labeled SecYEG(ND). Complex formation was monitored by the increasing Alx488 fluorescence due to FRET. **D.** Concentration dependence of k_{app1}. **E.** Concentration dependence of k_{app2}. **F.** Two-step scheme of the interaction of SecYEG(ND) and the ribosome.

These results indicated a two-step binding mechanism with a rapid first step, which is close to diffusion controlled and a second slow step. The calculated K_d of 0.03 ± 0.01 µM is similar to the K_d measured at equilibrium.

Next we asked whether the nascent chain on the ribosome could have a stabilization effect on the complex with SecYEG(ND). We performed dissociation experiments where we pre-formed the complex of 0.016 µM 70S(L23MDCC) or Lep75-RNC/Lep94(L23MDCC) and 0.16 µM SecY(111Alx488)EG(ND) and rapidly mixed it with a 10-fold excess of vacant ribosomes (1.6 µM). The stopped-flow traces were again fitted to a double exponential function (Figure 3-15). The rate of the first step (k_{-1}) was similar for vacant ribosome and RNC, 3 ± 1 s^{-1}. The second step (k_{-2}) was also similar in all three cases, 0.08 ± 0.01 s^{-1}. In contrast to the equilibrium

measurements, where the nascent chain enhanced the binding of the ribosome and SecYEG(ND), the kinetic measurements did not show any differences between the complexes. A possible explanation is that the affinity increase of 5 to 7-fold is too small to be seen in the kinetic experiments.

We concluded that the complex between SecYEG(ND) and the ribosome forms rapidly with a k_1 in the same range as the targeting of the ribosome by SRP, but also is a short-lived complex with a half-life of 0.2 s. In comparison to the complex of FtsY and SecYEG(ND) it is 10-times less stable.

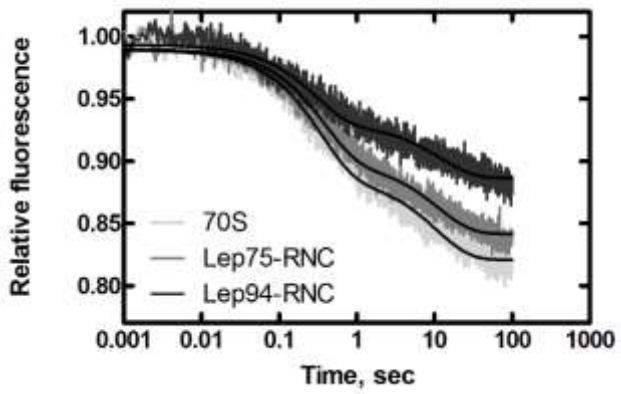

Figure 3-15 Dissociation kinetics of the complex of SecYEG(ND) with the ribosomes.

Complexes of SecY(111Alx488)EG(ND) and 70S(L23MDCC), Lep75-RNC(L23MDCC) or Lep94-RNC(L23MDCC) were pre-formed. Dissociation was induced by rapidly mixing the complexes with 10-fold excess of unlabeled 70S and the change in fluorescence of Alx488 was monitored.

3.5 Interplay of FtsY and the ribosome

In the course of targeting the translating ribosome, carrying a signal anchor sequence, is transferred from SRP to the SecYEG. Previous studies show that SRP and SecY have overlapping binding sites on the ribosome near protein L23 (Frauenfeld et al, 2011; Halic et al, 2006b; Menetret et al, 2007) and the binding to SecY would interfere with the binding to SRP. Recently, it was has shown by using *in vivo* crosslinking techniques that FtsY and the ribosome also bind at similar sites on SecY (Kuhn et al, 2011). This raises the question whether FtsY remains attached to SecYEG after the RNC has been transferred.

To answer this question we used a fluorescence approach in combination with equilibrium and rapid kinetic techniques. First we performed a competition experiment between FtsY and the 70S. The complex of SecY(111MDCC)EG(ND) and FtsY(196Bpy) was pre-formed and the labeled FtsY was displaced with a 10-fold excess of non-labeled competitor, 70S or FtsY, as a control. In both cases the shape of the dissociation traces was similar and we fitted them to exponential decay function (Figure 3-16). The apparent rate constants of both fits were in the same range (k_{app-1} = 12 – 23 s^{-1}, k_{app-2} = 0.4 – 0.7 s^{-1}, k_{app-3} = 0.006 – 0.008 s^{-1}). Thus, we confirmed the previous observations that the ribosome and FtsY can compete for binding to SecY.

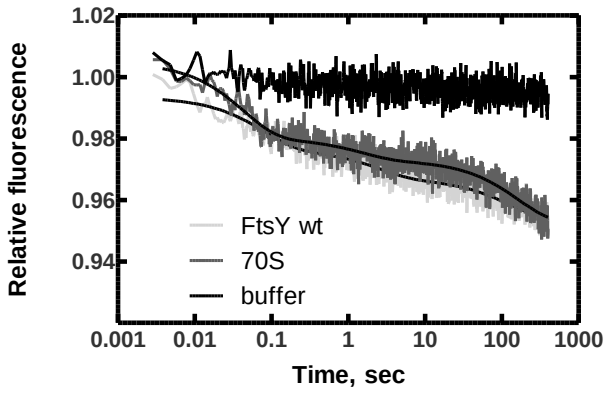

Figure 3-16 Dissociation of FtsY from SecYEG(ND) in competition with vacant ribosomes

Complexes of SecY(111MDCC)EG(ND) and FtsY(196Bpy) were pre-formed. Dissociation was induced by rapidly mixing the complexes with a 10-fold excess of 70S or unlabeled FtsY and the change in fluorescence of Bpy was monitored. In black is the control trace showing that the complex is stable upon mixing with buffer.

These experiments were performed in conditions where we add a large excess of competitor. In the cell, however processes are at steady-state and the concentration of FtsY is only 2 – 3-fold lower than of the ribosomes (Drew et al, 2003). Moreover not more than one third (20 – 30 % of all proteins are extracytosolic) of all ribosomes could be engaged in the synthesis of membrane proteins. In order to gain better understanding of the process, we performed competition experiments at equilibrium conditions. We titrated SecY(111MDCC)EG(ND) with FtsY(196Bpy) in the presence of increasing amounts of vacant ribosomes or RNCs carrying

LepB signal anchor sequence at position 4 – 22 (Figure 3-17). The Lep-RNC were prepared by *in vitro* translation of 3'-truncated Lep-mRNA (Bornemann et al, 2008). We chose RNCs with nascent chains of 75 and 94 amino acids. As 75 amino acids of Lep, of which about 40 are exposed outside the peptide exit tunnel, are sufficient to enter the SecY channel and 95 amino acids should be sufficient for the TM segment to be inserted into the lipid bilayer, forming a rather stable interaction (Ismail et al, 2012).

In the presence of ribosomes or RNCs, FtsY binds to SecYEG(ND) with the same affinity ($K_d \approx$ 0.2 μM) as in the control experiments where no ribosomes are present, but decreased the fluorescence amplitude. Such behavior is typical for noncompetitive binding, where the two ligands occupy different binding sites that do not influence each other, at least not in a way that would change the affinities. This result suggested that a ternary complex of FtsY, SecYEG and the ribosome can be formed.

In the titrations the fluorescence change is dependent also on the concentration of ribosomes. By plotting the final fluorescence levels against the concentration of ribosomes we can obtain an apparent affinity of the ribosomes to SecYEG(ND) in the presence of FtsY (Figure 3-17, panel D.). The data was analyzed by fitting to a hyperbolic function: $F_R = \frac{F}{(1+\frac{R}{K_{d_{app}}})}$, where F is the fluorescence level in the absence of ribosomes, F_R is the fluorescence level in the presence of ribosomes, R is the concentration of the ribosomes in the titration, and $K_{d_{app}}$ is the apparent K_d. The affinities obtained by this analysis were in line with the previous direct measurement of the interaction (Section 3.4.1).

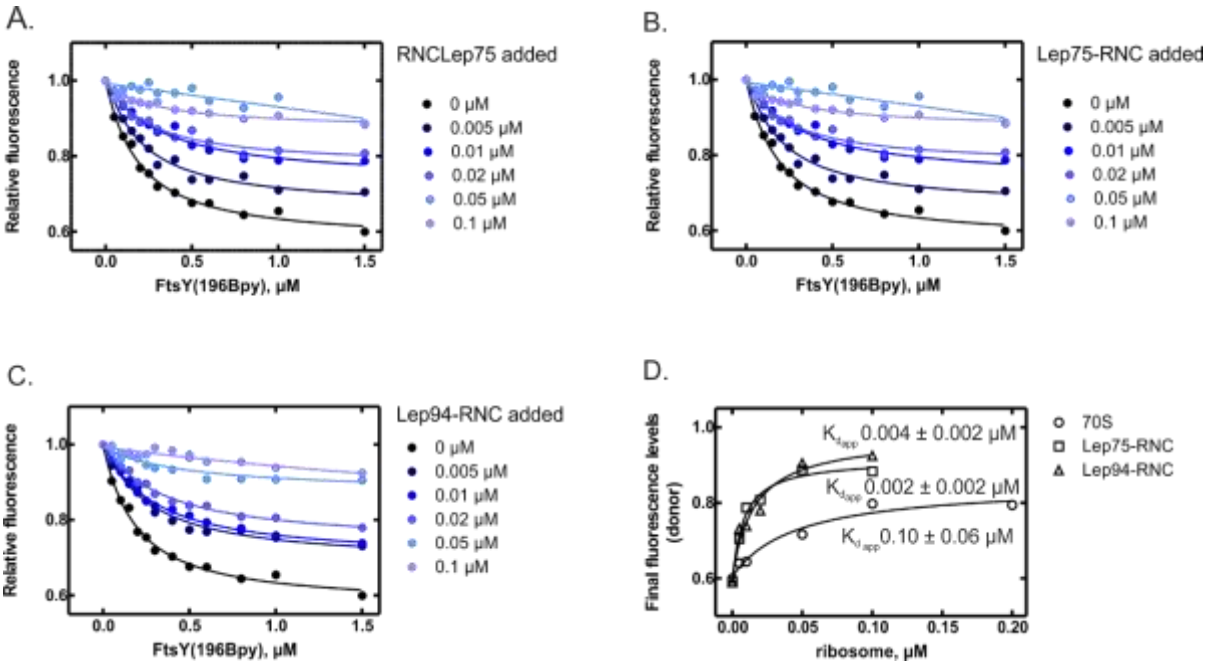

Figure 3-17 Titration of SecY(111MDCC)EG(ND) with FtsY(196Bpy) in the presence of increasing amounts of ribosomes or RNCs.

0.05 µM SecY(111MDCC)EG(ND)was titrated with FtsY(196Bpy) in the presence of **A.** vacant ribosomes, or RNCs carrying different length of the signal anchor sequence of LepB: **B.** Lep75-RNC and **C.** Lep94-RNC. **D.** Plot of the final fluorescence levels change due to the presence of ribosomes against the ribosome concentration.

3.6 The role of the FtsY A domain in the ternary complex with SecYEG(ND) and the ribosome

So far we have demonstrated that FtsY and the ribosome can form a ternary complex with SecYEG(ND) (Section 3.5). Also we have shown that both NG and A domains of FtsY interact with SecYEG(ND). The A domain (FtsY-A208) appears to contribute to the stabilization of FtsY on SecYEG(ND) (Section 3.2). Next, we asked which domain of FtsY is important for formation of the ternary complex. Thus, we performed a series of equilibrium titrations of 70S(L23MDCC) and SecY(111Alx488)EG(ND) in the presence of increasing concentrations of the different FtsY variants (Figure 3-18).

In all titrations the presence of FtsY did not influence the affinity of the complex between the 70S and SecYEG(ND), the K_ds remained in the range between 0.06 and 0.2 µM. Only the

fluorescence amplitude decreased in the presence of FtsY, FtsY-A208 and partly by FtsY-NG+1 (Figure 3-18, panels A., B. and D.). The other two constructs, FtsY-A197 and FtsY-NG (Figure 3-18, panels C. and E.), had very little influence on the interaction. These results are in line with our previous observation that the ribosome and FtsY can interact simultaneously with SecYEG(ND) and do not influence each other's binding affinities. Furthermore, the FtsY variants which affected the signal amplitude encompassed the critical MTS, which would indicate that it takes part in the stabilization of FtsY on SecYEG(ND) also in the presence of the ribosome.

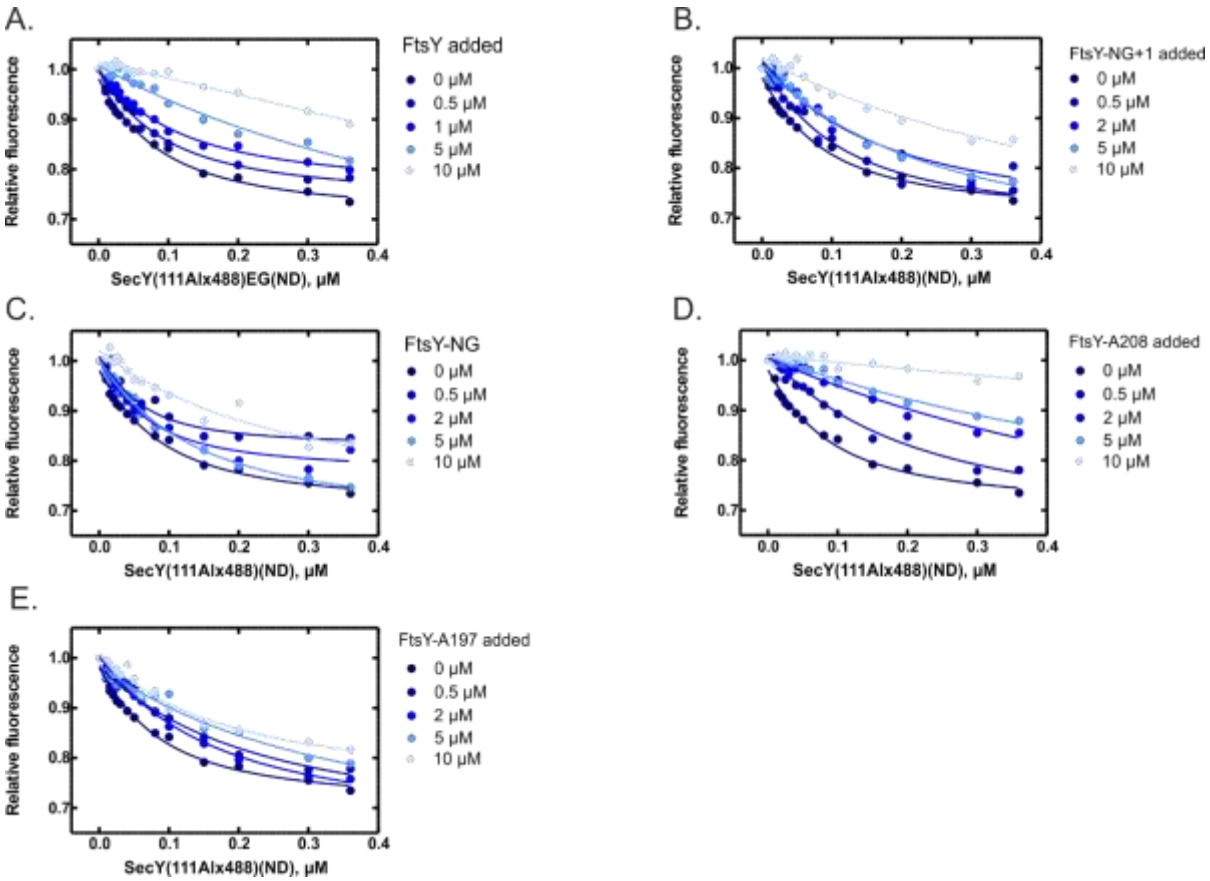

Figure 3-18 FtsY effect on ribosome-SecYEG(ND) complex formation.

Titration of 70S(MDCC) ribosome with SecY(111Alx488)EG(ND) in the presence of increasing concentrations of **A.** FtsY, **B.** FtsY-NG+1, **C.** FtsY-NG, **D.** FtsY-A208 and **E.** FtsY-A197.

3.7 The contribution of the FtsY-A domain to the GTPase activation of FtsY and SRP

Previous work of the GTPase activation of FtsY and SRP has shown that lipid vesicles containing anionic phospholipids increase the intrinsic activity of FtsY and also stimulate the activation of the SRP-FtsY complex (de Leeuw et al, 2000; Lam et al, 2010; Stjepanovic et al, 2011b). So far, there has been no clear evidence on the effect of SecYEG on the GTPase activation of FtsY and the SRP-FtsY complex. We continued our investigation on the function of FtsY A domain, by testing its role in the GTPase activation of the complex between SRP, FtsY and SecYEG(ND). We compared FtsY to FtsY-NG and FtsY-NG+1 in three different approaches: (a) intrinsic GTPase activity; (b) activation of the SRP-FtsY complex; (c) activation of the SRP-FtsY complex in the presence of FtsY interaction partners SecYEG(ND) or ND.

3.7.1 The intrinsic GTPase activity of FtsY

First, we measured the intrinsic GTPase activity of FtsY, FtsY-NG and FtsY-NG+1. FtsY-NG and FtsY-NG+1 showed a 10 – 15 – fold lower catalytic activity (0.002 min^{-1}) compared to the full-length protein (0.03 min^{-1}) (Figure 3-19, panel A.). This suggested that the A domain is involved in the activity of FtsY. To test this possibility, we titrated the NG domain of FtsY with the A domain and compared the activity to the full-length protein (Figure 3-19, panel B.). We observed that at an equimolar ratio of FtsY-A208 to FtsY-NG the hydrolysis activity was stimulated to about 50% of the level of full-length FtsY. The stimulatory effect was not observed with the shorter A domain construct FtsY-A197. These results indicated that the A domain of FtsY and especially the MTS has a function in the intrinsic GTPase activity of FtsY, and is in keeping with the observation that the two domains associate in a high affinity complex (Section 3.3.1).

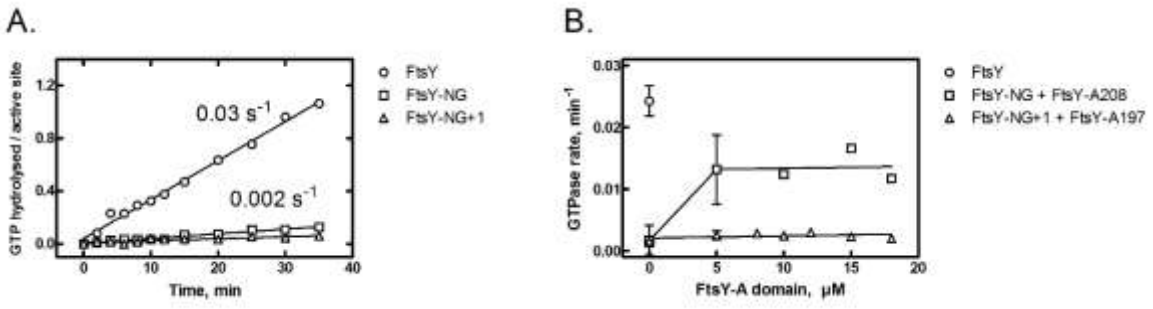

Figure 3-19 Intrinsic GTPase activity of FtsY.

We have measured GTP hydrolysis by FtsY, FtsY-NG+1 and FtsY-NG, **A.** NG domains. **B.** NG domains plus A domains.

3.7.2 Activation of the GTP hydrolysis of the SRP-FtsY complex

In order to characterize the GTPase activity of the activated complex of FtsY and SRP in the presence of SecYEG(ND) or ND we needed to make sure that GTP is present in saturating concentration. First, we measured the K_m for GTP of the separate proteins and in complex (Figure 3-20).

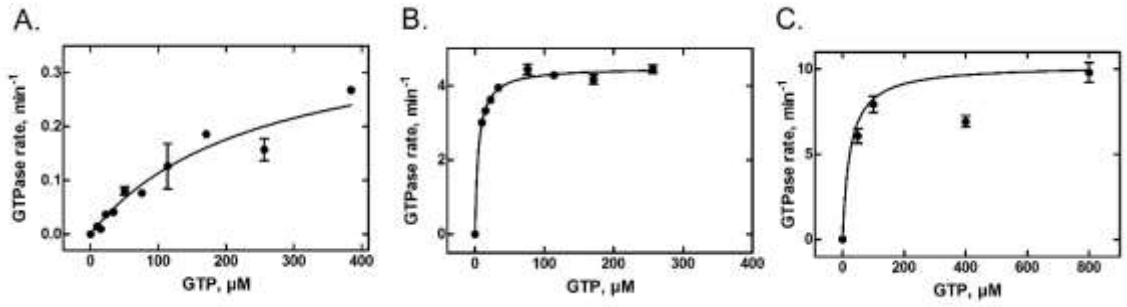

Figure 3-20 Titration of FtsY, SRP and the SRP-FtsY complex with GTP.

Titration of **A.** 5 µM FtsY, **B.** 1 µM SRP. **C.** the complex of SRP and FtsY with increasing concentrations of GTP.

FtsY alone showed a K_m of 250 ± 100 µM, which is rather high in comparison to the physiological concentrations of GTP (200 – 500µM; (Traut, 1994)). Also its catalytic efficiency (k_{cat}/K_m = 0.0005 $\mu M^{-1}*min^{-1}$) was much lower than that of SRP (k_{cat}/K_m = 0.9 $\mu M^{-1}*min^{-1}$).

Accordingly, in complex with SRP the catalytic efficiency increased 1000 fold and also the K_m increased 10 fold to 20 ± 15 µM (Table 3-4). This suggests that in the complex GTP is bound more strongly and that SRP appears to be an activator of FtsY. This is in line with previous crystallographic studies which indicate that SRP - FtsY complex forms a composite active site where the nucleotides are aligned and that a catalytic G (G83) nucleotide from the SRP RNA inserts into that active site to stimulate the hydrolysis (Ataide et al, 2011; Egea et al, 2004; Focia et al, 2004; Spanggord et al, 2005; Voigts-Hoffmann et al, 2013).

In order to fulfill the requirement of multiple turnover hydrolysis based on the K_m of 20 µM, in the following experiments we used a saturating concentration of 100 µM GTP.

Table 3-4: Steady-state GTPase of FtsY, SRP, and FtsY/SRP

GTPase	K_m, µM	k_{cat}, min^{-1}	k_{cat}/K_m, $\mu M^{-1}*min^{-1}$
FtsY	250 ± 100	0.13 ± 0.03	0.0005
SRP	5.1 ± 0.5	4.5 ± 0.1	0.9
SRP:FtsY	20 ± 15	10 ± 2	0.5

To examine the effect of SecYEG(ND) and ND on the GTPase activity of the SRP:FtsY complex, we determined the K_m of the binary complex of FtsY and SecYEG(ND) or ND. We used 5 µM FtsY and titrated SecYEG(ND) and ND from 0 to 22 µM. The Km for both SecYEG(ND) and ND was 6 ± 1 µM and the rate of the GTPase activity of FtsY increased to 2 – 3-fold (Figure 3-21).

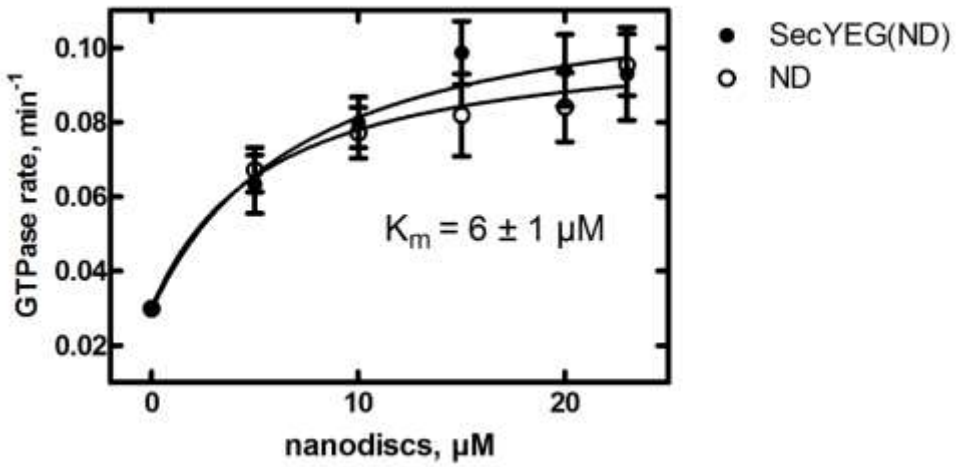

Figure 3-21 GTPase activity of FtsY bound to SecYEG(ND) or ND

To examine whether the A domain of FtsY has an impact on the GTPase activation of the SRP – FtsY complex, 0.5 µM SRP was titrated with FtsY, FtsY-NG and FtsY-NG+1 with or without the addition of 12 µM SecYEG(ND) or ND (Figure 2 – 22). We compared the rate constants of the different complexes (

Table 3-5) and found there was no significant difference in the GTPase activation between SRP in complex with FtsY, FtsY-NG+1 and FtsY-NG. Thus, the NG domain of FtsY appears to be sufficient to form the activated complex with SRP. In addition, the presence of SecYEG(ND) or ND did not have any effect on the K_m or k_{cat} of the complex of SRP and FtsY and its variants.

Table 3-5 GTPase rate constants of the SRP complex with FtsY-NG domain variants in the presence of SecYEG(ND) and ND

SRP in complex with	K_m, µM	k_{cat}, min^{-1}	k_{cat}/K_m, $µM^{-1}*min^{-1}$
FtsY	8 ± 1	17 ± 1	2.1
FtsY + ND	11 ± 3	24 ± 4	2.2
FtsY + SecYEG(ND)	9 ± 3	19 ± 3	2.1
FtsY-NG+1	9 ± 2	16 ± 1	1.8
FtsY-NG+1 + ND	5 ± 1	17 ± 2	3.4
FtsY-NG+1 + SecYEG(ND)	4 ± 1	12 ± 1	3.0
FtsY-NG	18 ± 7	21 ± 5	1.2
FtsY-NG + ND	11 ± 3	24 ± 4	2.2
FtsY-NG + SecYEG(ND)	5 ± 1	11 ± 1	2.2

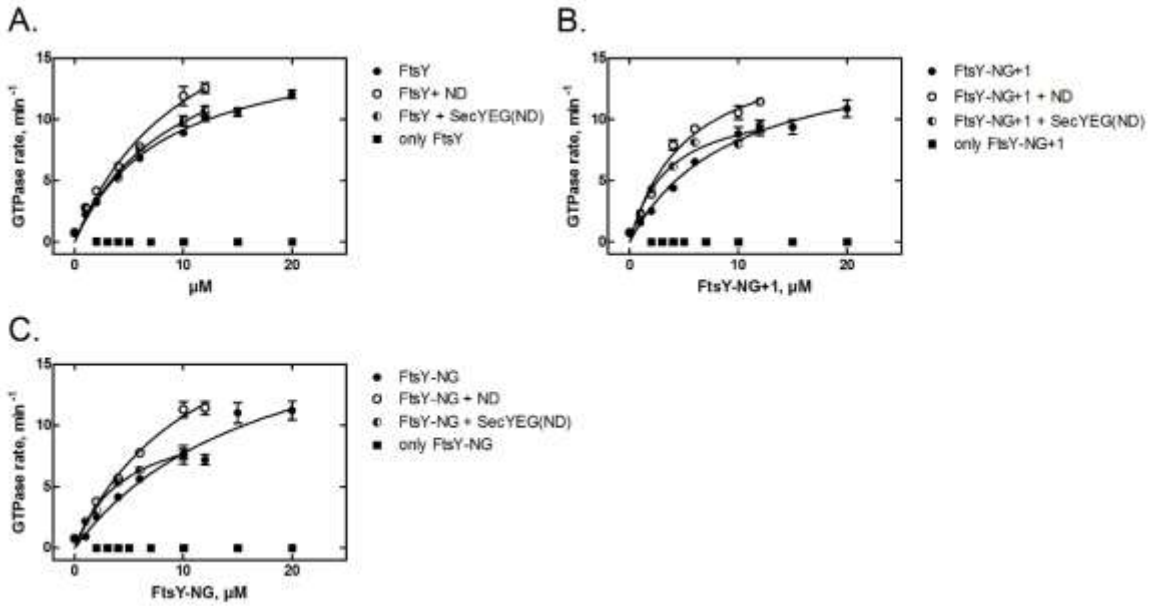

Figure 3-22 GTPase activity of the SRP complex with FtsY or FtsY-NG domain variants in the presence of SecYEG(ND) or ND.

SRP (0.5 μM) in the presence of 100 μM GTP was titrated with increasing concentrations **A.**FtsY, **B.** FtsY-NG+1 and **C.** FtsY-NG in the absence or presence of 12 μM ND or SecYEG(ND).

4. Discussion

4.1 The interaction between FtsY and SecYEG

According to the current understanding of SRP-dependent protein targeting, the translating ribosome is transferred to the SecYEG translocon assisted by SRP and its receptor, FtsY. The accuracy and timing of the process are achieved mainly via the early recognition of the N-terminal SAS by SRP, followed by GTP-controlled interaction of SRP with FtsY, which also reflects the presence of proper SAS (Holtkamp et al, 2012b; von Loeffelholz et al, 2013). As accepted that the scanning and targeting of the ribosome occur in the cytoplasm, it is still speculated whether FtsY resides at the membrane or it shuttles between the membrane and the cytoplasm (Lam et al, 2010; Luirink et al, 1994; Mircheva et al, 2009; Parlitz et al, 2007). Recent results *in vivo* suggest that FtsY is largely present at the membrane, presumably bound to the SecYEG translocon (Mircheva et al, 2009). The present analysis *in vitro* confirms this observation. By performing equilibrium titration, monitored by FRET, we observe that FtsY binds to SecYEG inserted into nanodiscs (SecYEG(ND)) with 0.2 μM affinity. We have also verified the affinity using a label-free method, ITC. The kinetic stability of the complex assessed by dissociation kinetics revealed an overall half-life time of the complex of 1.7 s, which suggests a relatively stable complex. The finding is in agreement with previous observations that it is required for FtsY to be initially associated with the membrane, in order to guide the SRP-RNC complex to SecYEG and also to release SRP from the RNC (Mircheva et al, 2009). In our system the binding affinity of FtsY was independent of the presence of GTP or GTP analogs, whereas the binding of FtsY to inverted vesicles appeared to be enhanced in the presence of GTP (Angelini et al, 2006). Nevertheless, in the cell FtsY is more likely to be in complex with GTP, due to the fast nucleotide exchange rate and the high cellular concentration of GTP (Jagath et al, 1998; Traut, 1994). We did not observe complex formation of FtsY and SecYEG when SecYEG was solubilized in detergent. This observation may explain some controversies in the literature regarding the localization of FtsY and the role of SecYEG as GTPase activator (Akopian et al, 2013a; Shen et al, 2012).

We have also examined the relative contribution of FtsY interaction with SecYEG and lipids to the overall complex stabilization, as it has been reported that FtsY is tethered to the membrane by two interactions, which are equal in contribution. One is with the membrane

phospholipids and the other with a proteinaceous factor, which later has been shown to be SecYEG (Angelini et al, 2005; Millman et al, 2001). Our results confirmed that FtsY binds equally well to SecYEG(ND) and to empty ND. Considering the cellular concentration of FtsY of about 17 μM and the affinity to SecYEG and lipids of 0.2 – 0.4 μM, then FtsY appears to be primarily membrane associated, either in complex with lipids or with the translocon (Kudva et al, 2013).

Previous studies of the cellular localization of FtsY have reported that both the N-terminal A domain and the NG domain can associate with the membrane, suggesting two binding sites for FtsY (de Leeuw et al, 1997; Millman et al, 2001). In our dissociation kinetics we also observed a two-step dissociation of FtsY, which would be consistent with two binding sites. We tested this possibility using four domain variants of FtsY, two of the NG domain and two of the A domain. The two NG variants either encompassed the critical membrane targeting sequence (MTS), or not. The two A domain variants either encompassed two amphiphilic sequences, the N-terminal lipid binding sequence and the MTS, or only the N-terminal lipid binding sequence. Despite the substantial truncations and the ability or disability to bind lipids, all four constructs exhibited similar affinity to SecYEG(ND) as the full-length protein. Further, our analysis focused on the contribution of the separate domains to the membrane localization of FtsY. Interestingly only the A domain which encompasses both lipid-binding sequences was able to compete with FtsY, though to lesser extent than the full-length protein. From our data we could not exclude a partial competition model, where FtsY still could bind to SecYEG(ND) in the presence of the isolated A domain. This would mean that the full-length protein still could bind SecYEG (ND) via the NG domain, thus explaining the decrease of the final fluorescence, observed in our experiments. Even though the affinities to SecYEG(ND) were similar, the NG domain variants were not able to compete with the full-length protein for SecYEG(ND) binding. One possibility is that the NG domain in the full-length protein is more flexible and binds differently to SecYEG(ND) than the isolated NG domain. These results once more pointed out the important role of the MTS, this time for binding to SecYEG. Previous reports have shown that the MTS promotes lipid-binding of the NG domain (Bahari et al, 2007; Parlitz et al, 2007; Stjepanovic et al, 2011a). Whereas here we have demonstrated that as part of the A domain the MTS appears to stabilize FtsY on SecYEG(ND). In a complex where the A-domain contact is predominant, the NG domain would be available for the

interaction with the NG domain of SRP, while FtsY is bound to SecYEG, which would be consistent with the kinetic analysis (Holtkamp et al, 2012b).

The observation that the separate FtsY domains each bind to SecYEG(ND) with similar affinities as the full-length FtsY posed an interesting question. A simple model in which the two domains make separate, equally strong contacts would predict that the full-length protein binds with the added affinities of the individual domains. However, this is not observed. One possibility to explain this behavior would be that in unbound form of FtsY there are binding interactions between the two domains which have to be disrupted in order to allow the binding to SecYEG. A similar model was reported previously for the M and NG domains of Ffh in SRP where domains form strong interactions which have to be disrupted upon SRP binding to the ribosome (Buskiewicz et al, 2005). In fact, when we examined whether there is complex formation between A and NG domains of FtsY we observed a complex of extremely high affinity, K_d = 9 nM. To examine whether the FtsY domains move apart upon binding to SecYEG(ND) we applied a homoFRET approach, using the same fluorophore, Bodipy FL, in the two domains. Our results revealed that the NG and the A domain are in close proximity in unbound FtsY in solution, but the binding to SecYEG(ND) is accompanied by a conformational rearrangement which increases the distance between the domains. The binding to empty ND did not result in any rearrangements.

These results can be summarized in a model where the SRP receptor FtsY is mainly localized at the membrane, contacting both phospholipids and SecYEG. The conformation of FtsY is 'closed' when FtsY interacts only with the lipids. In the case when FtsY binds to SecYEG the NG and A domain undergo a rearrangement and the two domains move apart, forming an 'open' conformation. In this way the A domain may facilitate the stabilization at the SecYEG translocon and the NG domain is available for binding to SRP (Figure 3 – 1). Such a model would also explain previous reports where FtsY with truncated A domain is still functional in SRP binding and GTPase activation, but only partially rescues a ΔFtsY phenotype, probably since it is not bound stably enough at the SecYEG (Bahari et al, 2007; Eitan & Bibi, 2004). Furthermore, a closed conformation of FtsY, which is impaired in binding to SRP and needs to be activated for complex formation by binding to SecYEG, could also explain how FtsY, present in the cell in much higher amounts that SRP, does not trap all SRP.

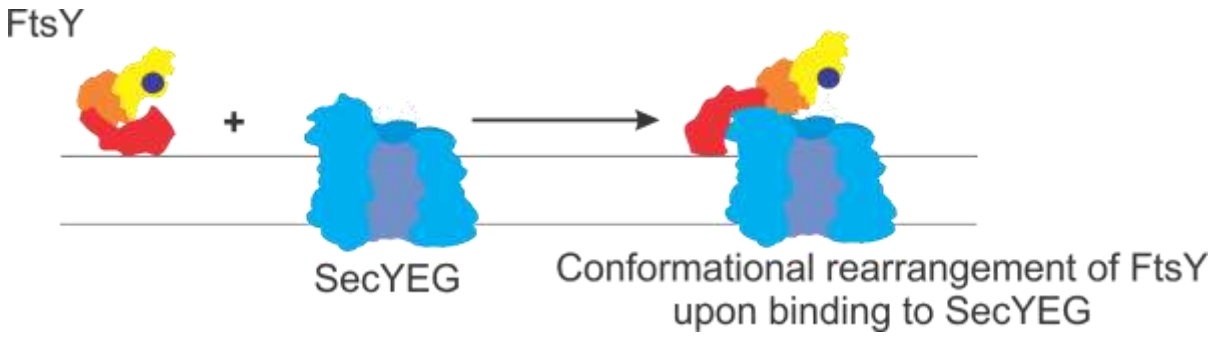

Figure 4-1 Model of FtsY binding to SecYEG

FtsY in complex with the cytoplasmic membrane in closed conformation, where the NG domain (yellow-orange) and the A domain (red) are in close proximity. The main interaction sites are at the A domain: (1) the N-terminal lipid-binding sequence (amino acids 1 – 14), and (2) the membrane targeting sequence (MTS) at the interface between the A domain and the N domain (orange). Upon interaction with SecYEG (blue) FtsY undergoes domain rearrangements, where the N terminal amphiphilic sequence remains in complex with the lipids, the MTS and the NG domain interact with SecYEG. Thus, the A and NG domain move apart and FtsY adopts an open conformation.

4.2 Interplay between FtsY and the ribosome at the SecYEG translocon

In the course of ribosome targeting to the SecYEG translocon, after the transfer of the RNC to the translocon is completed, it remains unclear whether FtsY remains bound to the translocon or leaves the complex. Previous crosslinking studies have shown that FtsY interacts with the cytosolic loops C4 and C5 of SecY, which are the main binding partners for the ribosome as well. This implies that FtsY and the ribosome compete for binding to the translocon (Kuhn et al, 2011). Initially we probed whether the ribosome can induce dissociation of FtsY from SecYEG(ND) and confirmed that they could compete. Nevertheless, our previous data showed that FtsY binds to SecYEG(ND) at two sites via the NG and the A domains. Also that the A domain stabilizes FtsY on SecYEG(ND). Thus, there is the possibility that FtsY remains bound to SecYEG(ND), though in a different conformation, when the ribosome is bound. We tested this hypothesis and observed that FtsY and the ribosome can bind simultaneously to SecYEG(ND) in a noncompetitive manner. Thus, confirming that FtsY participates in the ternary complex with SecYEG(ND) and the ribosome, but in somewhat different conformation.

Our further analysis showed that the NG domain or the A domain, both encompassing the MTS, were able to participate in the ternary complex. These data would explain the *in vivo* observation that the isolated NG domain which includes the MTS is able to rescue the ΔFtsY phenotype, at least partially. Provided that, the critical MTS is responsible for the localization and the isolated NG domain interacts with SRP to promote its release from the RNC (Eitan & Bibi, 2004; Parlitz et al, 2007; Spanggord et al, 2005). Nevertheless, the A domain appeared to bind more firmly than the NG domain. Thus, confirming our previous observation that the two lipid-binding sequence assure the membrane localization and the interaction with SecYEG(ND).

Previously, the ribosome-SecYEG interaction was quantified by surface plasmon resonance (SPR) which has shown that the complex is of high affinity and that the nascent chain further strengthens the interaction (Wu et al, 2012). By performing equilibrium titrations, monitored by FRET, we obtained similar affinities for SecYEG(ND) binding to 70S ribosomes of 50 ± 20 nM and to Lep-RNC of 9 ± 1 nM. The kinetic analysis showed that the ribosome and SecYEG(ND) associate in a two-step mechanism, with a fast diffusion-controlled binding step, followed by a slower rearrangement step. The overall stability of the complex appeared to be low, with half-life time of the complex of 0.2 s. A stabilization of the complex in the presence of the signal sequence we did not observe in the kinetics. Most probably a difference in K_d of 5 – 7-fold is too small to be detected by kinetic measurements.

So far our data have shown that the A domain of FtsY is essential for the stabilization of FtsY on SecYEG. This effect is achieved via two sequences located at the N and the C terminus of the A domain (Braig et al, 2009). There is evidence suggesting that lipid-association stimulates the intrinsic GTPase activity of FtsY (de Leeuw et al, 2000; Lam et al, 2010). However, it is unclear how SecYEG influences the GTPase activation of FtsY and the SRP-FtsY complex. The studies that had investigated this process either used SecYEG solubilized in detergent (DDM) or only liposomes (Akopian et al, 2013b; Lam et al, 2010; Shen et al, 2012). Especially the use of DDM appears problematic, as our results show that FtsY does not interact with SecYEG in the presence of DDM. The GTPase activation of FtsY by liposomes is rather high, more than 100-fold, albeit at very high liposome concentration in the millimolar range (Lam et al, 2010(Lam et al, 2010). Considering the large available surface of the liposomes it is expected that FtsY, used

in 2 – 5 μM concentration, would be saturated also at micromollar concentration of liposomes. Perhaps the use of the detergent (Nikkol) in the reactions could have perturbed the system. In our hands, FtsY is activated 2-fold both by SecYEG(ND) and ND at much lower, micromolar, yet saturating concentrations, which are also in line with the measured affinities. We further analyzed the effect on the GTPase activation of the SRP-FtsY complex by the FtsY binding partners SecYEG(ND) or ND. The GTP hydrolysis rate of the SRP-FtsY complex remained unaffected by SecYEG(ND) or ND. Also the complex of SRP with only the NG domain of FtsY exhibited the same catalytic activity as the SRP-FtsY complex. These results were in agreement with previous observations that the NG domains of SRP and FtsY are sufficient for GTPase activation of the complex (Bahari et al, 2007; Egea et al, 2004; Eitan & Bibi, 2004; Focia et al, 2004). Taken together the data presented on the function of the N-terminal A domain of FtsY converges to the conclusion that this domain mainly stabilizes FtsY on the SecYEG, while the NG domain can bind SRP and hydrolyze GTP.

The present investigation allow for a refinement of the model of the SRP targeting pathway, by providing details of the interaction between SecYEG and FtsY and elucidating the function of the NG and A domains of FtsY (Figure 4-2). According to the current understanding of the targeting process, SRP rapidly scans the ribosomes until it is stably bound to one that has the exit tunnel filled (about 35 amino acids). As in the bacterial system there is no SRP-induced elongation arrest, continued translation may lead to the emergence of a non-signal sequence, resulting in SRP rejection (Bornemann et al, 2008; Holtkamp et al, 2012b). Alternatively, the appearance of a signal-anchor sequence (SAS) leads to a rearrangement of SRP that exposes the NG domain and strongly stabilizes the complex. This way the SRP-RNC complex is ready to be targeted to the membrane. FtsY on the other hand is localized at the membrane in the vicinity of SecYEG. There it can bind to SRP via its NG domain, which is exposed in the FtsY-translocon complex, while it remains associated to the SecYEG via the A-domain contacts. There is evidence that following FtsY binding to SRP, the NG-NG complex translocates to the distal end of the 4.5S RNA, which is possible due to the long linker between NG and M domains of Ffh (Shen et al, 2012).

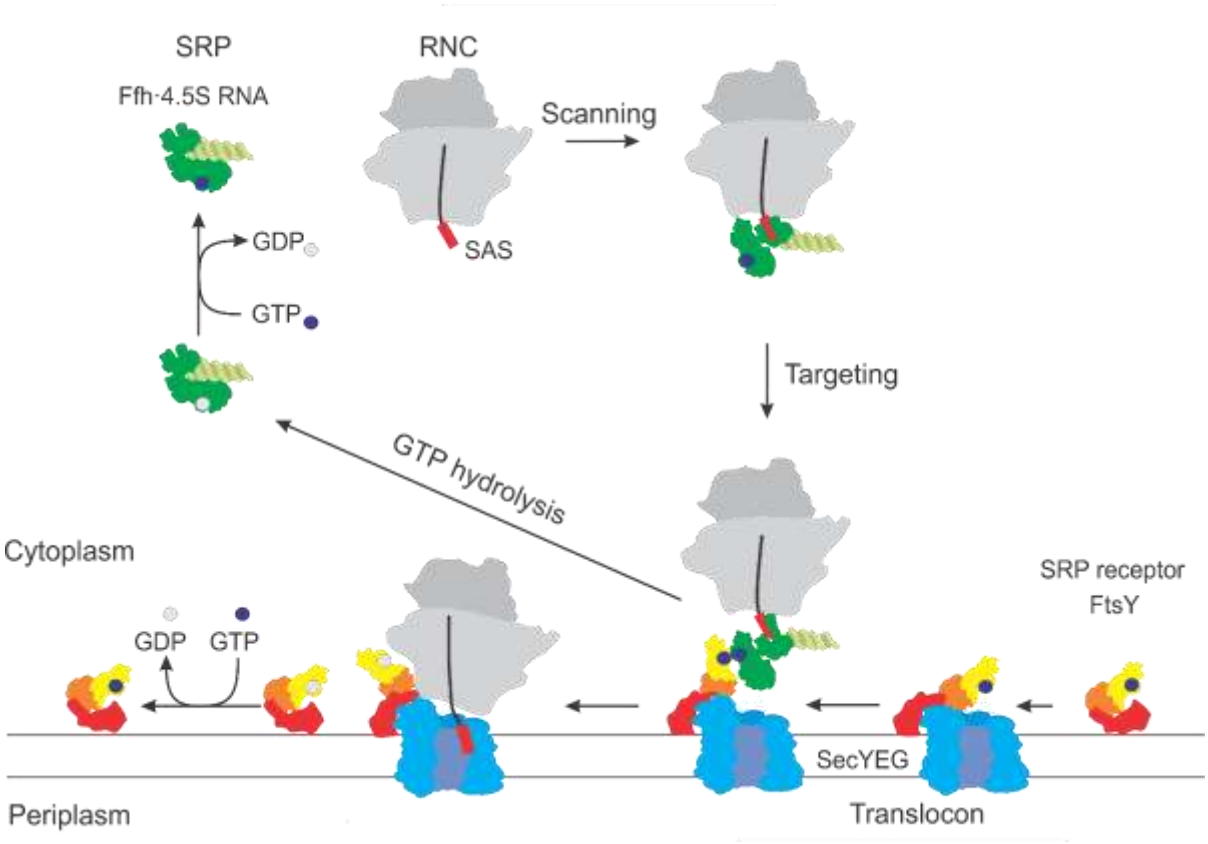

Figure 4-2 Model of SRP targeting pathway

SRP scans the translating ribosomes (RNC) for an emerging nascent chain. In case that the nascent chain exposes a N-terminal signal anchor sequence (SAS) of a membrane protein, SRP rearranges and binds both the ribosome and the SAS. Like that the RNC-SRP complex is ready for targeting to the membrane. FtsY is localized at the membrane in the vicinity of the SecYEG translocon. Upon interaction with SecYEG, FtsY adopts an open conformation, which allows the NG domain (yellow-orange) to interact with the NG domain of SRP (green). Due to the high affinity between the RNC and SecYEG and the increased affinity of SRP and FtsY, the complex of RNC-SRP is targeted to the SecYEG-FtsY complex to the membrane. There in a GTP-dependent manner FtsY and SRP form a complex via their NG domains. The RNC is transferred to SecYEG and SRP is released from the quaternary complex after GTP hydrolysis. FtsY remains bound to SecYEG, though in a different conformation.

Thus, upon initial targeting a quaternary complex is formed, and we speculate that this complex is transient, because the high affinity between RNC and SecYEG will probably lead to RNC transfer to the translocon, and competition between translocon and SRP for binding to overlapping sites at the peptide exit of the ribosome. Concomitantly with the rearrangement, the GTPase activity of the complex is stimulated and the SRP – FtsY complex is released, while

SRP also releases the SAS. During the nascent chain translocation FtsY remains bound to SecYEG via the A domain while the NG domain remains in conformation that does not interfere with the ribosomal binding. In this state FtsY awaits the next round of targeting.

5. Materials and Methods

5.1 Equipment

Table 5-1 List of equipment

Device	Manufacturer
Benchtop centrifuge 5415R and 5810R	Eppendorf
Centrifuge Avanti J-26 XP	Beckmann Coulter
Ultracentrifuge Optima L-100 XP	Beckmann Coulter
Ultracentrifuge Max-XP	Beckmann Coulter
Galaxy mini star centrifuge	VWR
Vortex Genie 2	Scientific Industries
PCR thermocycler Peqstar	Peqlab Biotechnologie
Mini gel electrophoresis chamber	Peqlab Biotechnologie
Electrophoresis power supply EV261	Peqlab Biotechnologie
Semi-dry blotter	Peqlab Biotechnologie
Water bath RE104 and E100	Lauda
Nanodrop 2000C	Peqlab Biotechnologie
Milli-Q Advantage A10	Millipore
Plates incubator INE600	Memmert
Incubator shaker series Innova44	New Brunswick
Fermenter – Biostat B Plus	Sartorius Stedium Biotech
ÄKTA FPLC	GE Healthcare
ÄKTA Explorer	GE Healthcare
Emulsiflex C-3 homogenizer	Avestin
Fluorolog spectrofluorometer	Horiba Jobin Yvon
FluoroMax-4	Horiba Jobin Yvon
Fluorescence cuvette QS 750 µl	Hellma Analytics
FLA-7000 biomolecular imager	Fuji
Bio-vision imaging system	Peqlab Biotechnologie
Stopped-flow SX20D spectrometer	Applied photophysics
Fluorescence cut-off filters	Schott AG
Micro calorimeter iTC200	MicroCal
Liquid scintillation counter	PerkinElmer
pH meter	inoLAB
pH electrode	Sentix81

5.2 Software

Table 5-2 List of software

Software	Provider
MultiGauge 2.0	Fujifilm
FluorEssence 3.5	Horiba Scientific
Pro-Data software suit	Applied Photophysics
Pymol 1.3	Schrödinger
GraphPad Prism 5.0	GraphPad software
Origin 7.0	OriginLab
TableCurve 2D	Systat Software
MaxQuant 1.4.1.2	MaxQuant (Cox & Mann, 2008)

5.3 Chemicals and consumables

Chemicals were purchased from Sigma, Merck or Roth (Germany), unless stated otherwise. The chemicals for electrophoresis: agarose, acrylamide, SDS, were purchased from Serva; DTT and L(+)-Rhamnose monohydrate – Applichem; Complete protease inhibitor – Roche; GMPPNP, GTP and GDP – Jena Bioscience; yeast extract and tryptone – BD; kits for DNA preparation and TLC plates (Polygram PEI 300) – Macherey-Nagel; protein concentrators, nitrocellulose filters, sterile filters – Sartorius; Bio-Beads SM2 Adsorbent – Biorad; DNA oligonucleotides for mutagenesis – IBA Life Sciences, or Eurofins MWG Operon; Phusion DNA polymerase kit – New England Biolabs; FPLC columns and chromatographic resins – GE Healthcare; Ni-IDA resin – IBA Life Sciences; precision cells (Quartz SUPRASIL®) – Hellma Analytics; fluorescent dyes – Molecular Probes, Life Technologies; scintillation liquid IRGA-SAFE Plus – PerkinElmer, Quickszint 361 – Zinsser Analytics; radioactive compounds – Perkin Elmer; [γ-^{32}P]-GTP – Hartmann Analytic.

5.4 Plasmids and strains

Table 5-3: List of plasmids

Plasmid name	Product	Promotor	Tag	Resistance	Source
pTRC99aSecYEG	SecYEG	*trc*	SecE-N term His_6	Ampicillin	C. Schaffitzel
pET9a-FtsY	FtsY wt	*T7*	C term His_6	Kanamycin	J. Luirink
pT-NG+1	FtsY-NG+1	*T7*	C term His_6	Ampicillin	E. Bibi
pT-NG	FtsY-NG	*T7*	C tern His_6	Ampicillin	E. Bibi
pSUMO-FtsY	FtsY	*T7*	N term His_6	Kanamycin	this work
pSUMO-FtsY197	FtsY-A197	*T7*	N term His_6	Kanamycin	this work
pSUMO-FtsY208	FtsY-A208	*T7*	N term His_6	Kanamycin	this work
pET24-Ffh	Ffh wt	*T7*	C term His_6	Kanamycin	J. Jagath
pMSP1D1	MSP1D1	*T7*	N term His_7	Kanamycin	Addgene
pMSPE1D1	MSPE1D1	*T7*	N term His_7	Kanamycin	Addgene
pT7-4.5S	4.5S RNA	*T7*		Ampicillin	G. Lentzen

Table 5-4: List of bacterial strains

Strain	Genotype	Application	Source
DH5α	*F^- endA1 glnV44 thi-1 recA1 relA1 gyrA96 deoR nupG Φ80dlacZΔM15 Δ(lacZYA-argF)U169, hsdR17(r_K^- m_K^+), λ^-*	Plasmid amplification	In house
BL21(DE3)	*F^- ompT gal dcm lon $hsdS_B$(r_B^- m_B^-) λ(DE3 [lacI lacUV5-T7 gene 1 ind1 sam7 nin5])*	MSP expression	In house
BL21(DE3)pLys	*F^- ompT gal dcm lon $hsdS_B$(r_B^- m_B^-) λ(DE3) pLysS(cm^R)*	FtsY and Ffh expression	In house
Lemo21(DE3)	*fhuA2 [lon] ompT gal (λ DE3) [dcm] ΔhsdS/ pLemo(Cam^R) λ DE3 = λ sBamHIo ΔEcoRI-B int::(lacI::PlacUV5::T7 gene1) i21 Δnin5 pLemo = pACYC184-PrhaBAD-lysY*	SecYEG expression	New England Biolabs

Table 5-5 List of primers

Primer	Sequence 5' – 3'
4.5S RNA	sense GGGTGGGGGCCCTGCCAGCTAC
	anti-sense CTTTATGCTTCCGGCTCGTATGTTGTGTGG
SecY(S111C)	sense TAAGAAAGAAGGGGAGTGCGGTCGTCGTAAG
	anti-sense CTTACGACGACCGCACTCCCCTTCTTTCTTA
FtsY(F196C)	sense CAAAGAAGGTTTTTGTGCGCGCCTGAAAC
	anti-sense GTTTCAGGCGCGCACAAAAACCTTCTTTG
FtsY(A167C)	sense GCGGCAGAAGAGTGTGTGATGGTGGTTCC
	anti-sense GGAACCACCATCACACACTCTTCTGCCGC
FtsY(V342C)	sense CGGTTGAACAGCTTCAGTGTTGGGGTCAGCGC
	anti- sense GCGCTGACCCCAACACTGAAGCTGTTCAACCG
pSUMO amplification	sense GATCCGGCTGCTAACAAAGCCCGAAAG
	anti-sense ACCACCAATCTGTTCTCTGTGAGCCTCAATAATATC
FtsY cloning in pSUMO	sense GAACAGATTGGTGGTATGGCGAAAGAAAAAAAACG
	anti-sense GTTAGCAGCCGGATCTTAATCCTCTCGGGC
FtsY-A197	sense CAAAGAAGGTTTTTTCTAACGCCTGAAACGC
	anti- sense GCGTTTCAGGCGTTAGAAAAAACCTTCTTTG
FtsY-A208	sense CGCAGCCTGTTAAAAACCAAATAATAGCTCGGTTC
	anti-sense GAACCGAGCTATTATTTGGTTTTTAACAGGCTGCG

5.5 Site-directed mutagenesis

Site-directed mutagenesis was performed with Phusion polymerase. Each reaction was performed in high fidelity buffer at final volume of 50 µl: 30 ng DNA template, 15 pmol from each primer, 15 nmol from each dNTP and 2 units Phusion polymerase. A typical PCR program starts with 3 min 95°C denaturation, followed by 25 cycles of 1 min 95°C denaturation, 35 sec. annealing at usually 55°C, followed by 30sec/kb elongation step at 72°C. In the last step after all products were elongated for 5 min at 72°C and finally stored at 4°C. Afterwards the template DNA was digested with DpnI restriction enzyme (New England Biolabs) for 1 h at 37 °C with 1 U/µg template DNA and later transformed to DH5α cells.

5.6 Transformation

For plasmid transformations $CaCl_2$ chemically competent cells we used. To 50 µl of competent cells 60 ng of purified plasmid was transformed or 5 µl of PCR reaction. The cells were incubated for 15 min on ice and transformation was induced by 40 sec heat shock at 42°C, followed by 2 min incubation on ice. The cells were recovered for 1 h in 700 µl LB at 37°C. Afterwards the cells were collected by 2 min centrifugation at 5000 rpm in a benchtop centrifuge, resuspended in 200 µl LB and plated on LB-agar plates supplemented with the corresponding resistance antibiotic.

5.7 4.5S RNA preparation

The linearized DNA template for 4.5S RNA transcription was amplified in 1 ml PCR reaction volume. pT7-4.5S plasmid was used as template in combination with 4.5S RNA primers. The PCR had 40 cycles of amplification with an annealing temperature of 57°C. The resulting product was transcribed for 3 h at 37°C in 30 ml transcription buffer supplemented with 10 mM DTT, 3 mM NTP-mix, 5 mM GMP, 150 µM T7 polymerase (home-made) and 3 U inorganic pyrophosphatese (IPP). The RNA was purified using a 5 ml HiTrap Q column with washing buffer RNA-BA and was eluted with a 20 CV gradient of buffer RNA-BB. The fractions of the RNA peak were collected and the RNA was ethanol precipitated by addition of 1:10 volumes 20 % w/v potassium acetate and 2 volumes 100% ethanol. The precipitation was carried out over night at -20°C, followed by 1 h centrifugation at at 4°C, 4 rpm in a benchtop centrifuge. The resulting pellet was washed with 70 % ethanol and centrifuged for 30 min at 4°C, dried and resuspended in water. The concentration of the RNA was measured by absorption in water at λ= 260 nm and the concentration was calculated using the equation: $C = \frac{A_{260} * dilition}{extinction\ coef.}$, using 4.5S RNA extinction coefficient = 1.0821 $M^{-1}cm^{-1}$.

5.8 Protein expression and purification

5.8.1 SecYEG

SecYEG was overexpressed in *E.coli* strain Lemo21(DE3) (see Table 1 and 2 for details on plasmids and strains). Test expression yield positive clones that were kept as 40% glycerol stocks at -80° C. A large scale overexpression culture (6 L of LB) was inoculated with 200 ml overnight culture, supplemented with 100 µg/ml ampicillin, 30 µg/ml chloramphenicol and 800

µM L-rhamnose and 3 drops of Antifoam 204™. The cells were grown at 37° C and induced at OD_{600} ~ 0.6 – 0.7 with 400 µM IPTG for 4 hours. Afterwards the cells were collected for 20 min at 5000 rpm in a Beckmann JLA.8.1000 rotor, washed once with buffer SecRB and shock frozen in liquid nitrogen. The usual pellet weight was 12 g.

All further purification steps were carried out at 4° C. The pellet was thawed on ice and 30 ml opening buffer was added supplemented with 1 tablet of EDTA Free Complete protease inhibitor, lysozyme and one crystal of DNase. The cells were opened in one cycle in the EmusiFlex-C3 at 1.5 bar applied pressure and 1000 bar effective pressure. The debris was decanted for 20 min at 30000 x g in a JA 25.50 Beckmann rotor. The membranes were separated from the supernatant for 2 hours at 150000 x g in a Ti 50.2 Beckmann rotor. The collected membranes were resuspended in a 7 ml mortar and solubilized in 100 ml SecSB + 1 % DDM for 1 hour at 4°C with gentle agitation. The non-solubilized fraction was decanted for 30 min at 75000 x g in a Ti 50.2 Beckmann rotor. The resulting supernatant was loaded onto a 5 ml HisTrap column equilibrated with 5 CV buffer SecNiA.

To avoid overloading of the HisTrap column the sample was loaded in two equal portions. After each loading a complete purification protocol was applied: 5 CV wash with SecNiA and eluted with 5 CV of buffer SecNiB.

The two elution peaks were collected, concentrated to 2 ml in a 20 ml Vivaspin™ (Sartorius) with 10 kDa cutoff. The concentrated sample was rebuffered in SecSPA on a PD-10 (G25) column (GE Healthcare). Both samples were pooled and loaded on a 5 ml QTrap™ (GE Healthcare), equilibrated with 5 ml SecSPA. The column was washed with 5 CV SecSPA. SecYEG was eluted with a 8 CV linear gradient from 0 – 100 % SecSPB with a 2 CV gradient delay. The peak at 60 % was collected, concentrated and rebuffered to BufferA + 0.03 % DDM on a PD-10 (G25) column. Samples were collected from all purification steps and analyzed on a 15 % SDS PAGE and Western blot.

Protein concentration was calculated from the absorbance measured at 205 nm in H_20 using the following equation, where MW of SecYEG is 75 kDa:

$$C\ [\mu M] = \frac{A_{205} * dilution}{31 * MW} * 10^6$$

5.8.2 FtsY

FtsY was previously cloned in a pET9a vector and overexpressed in BL21 (DE3) pLys cells. A 200 ml overnight culture (previously tested for overexpression) was used to inoculate 6 L of LB supplemented with 30 µg/ml kanamycin and 30 µg/ml chloramphenicol. At OD_{600} 0.7 -0.8 the bacteria were induced with 1 mM IPTG for 2 hours. The cells were collected for 20 min at 5000 rpm in a Beckmann JLA 8.1000 rotor, washed with FtsY-QSA and shock-frozen in liquid nitrogen.

In the first purification step the cleared lysate of FtsY is loaded on 42 ml Q-Sepharose column. Typically 15 to 20 g of cell pellet were resuspended in 50 ml FtsY-QSA buffer supplemented with 2 pills of EDTA Free Complete protease inhibitor (Roche), lysozyme (Sigma) and one crystal of DNase. The cells were opened in one cycle in the EmusiFlex at 1.5 bar applied pressure and 1000 bar effective pressure. The debris was decanted for 45 min at 25000 rpm in a JA 25.50 Beckmann rotor. Then the cleared lysate was loaded on the Q-Sepharose column, equilibrated with FtsY-QSA. The unspecifically bound proteins were washed off with FtsY-QSA, and FtsY was eluted with a linear gradient of 20 CV from 0-100 % FtsY-QSB. The peak containing FtsY was collected and loaded on 10 ml NiNTA (Qiagen) gravity flow column, equilibrated with FtsY-NiA. The resin was washed with 5 bed volumes (BV) FtsY-NiA, then with 5 BV FtsY-NiB, 3 BV FtsY-NiA and FtsY was eluted with 3 BV NiC. The elution was collected and dialyzed against 4 x 500 ml FtsY-QTA. Afterwards the sample was loaded on 5 ml HiTrap-Q column, equilibrated with FtsY-QTA. The unspecifically bound proteins were washed off with 5 CV FtsY-QTA and FtsY was eluted with a 20 CV linear gradient from 0 – 100 % FtsY-QTB. The peak containing FtsY was collected concentrated to 3 ml in Vivaspin™ with cutoff 30 kDa and dialyzed against 2 x 500 ml BufferA.

FtsY-NG+1 and FtsY-NG were expressed and purified in the same way as full-length FtsY, with minor amendments. The cells were resuspended in 20 ml FtsY-NiA supplemented with 1 pill of EDTA Free Complete protease inhibitor (Roche), lysozyme (Sigma) and one crystal of DNase. The cells were opened in one cycle in the EmusiFlex at 1.5 bar applied pressure and 1000 bar effective pressure. The debris was decanted for 45 min at 25000 rpm in a JA 25.50 Beckmann rotor. Then the cleared lysate was loaded on 5 ml HisTrap column, washed with 5 CV FtsY-NiB buffer supplemented with 0.01 % Nikkol. Then 5 CV FtsY-NiA buffer and finally

eluted with 5 CV FtsY-NiC buffer. The elution was collected and dialyzed against 4 x 500 ml Ffh-QTA. Afterwards the sample was loaded on 5 ml HiTrap-SP column, equilibrated with Ffh-QTA. The unspecifically bound proteins were washed off with 5 CV Ffh-QTA and FtsY was eluted with a 20 CV linear gradient from 0 – 100 % Ffh-QTB. The peak containing FtsY was collected concentrated to 3 ml in Vivaspin™ with cutoff 10 kDa and dialyzed against 2 x 500 ml BufferA.

FtsY-A197 and FtsY-A208 were expressed and purified in the same way as full-length FtsY, with minor amendments. The cell pellet was resuspended in 20 ml FtsY-NiA supplemented with 1 pill of EDTA Free Complete protease inhibitor (Roche), lysozyme (Sigma) and one crystal of DNase. The cells were opened in one cycle in the EmusiFlex at 1.5 bar applied pressure and 1000 bar effective pressure. The debris was decanted for 45 min at 25000 rpm in a JA 25.50 Beckmann rotor. Then the cleared lysate was loaded on 5 ml HisTrap column, washed with 5 CV FtsY-NiB buffer supplemented with 0.01 % Nikkol. Then 5 CV FtsY-NiA buffer and finally eluted with 5 CV FtsY-NiC buffer. The elution was collected and dialyzed against 4 x 500 ml FtsY-QTA. Then the protein was concentrated to 100 µM in a Vivaspin with a cutoff of 10 kDa and incubated overnight at 4°C with Ulp1 SUMO-protease 1:100 ratio of protease:FtsY-A. Afterwards the sample was loaded on 5 ml HiTrap-Q column, equilibrated with FtsY-QTA. The unspecifically bound proteins were washed off with 5 CV FtsY-QTA and FtsY was eluted with a 20 CV linear gradient from 0 – 100 % FtsY-QTB. The peak containing FtsY was collected and incubated for 15 min with 4 ml of NiNTA equilibrated with BufferA. The flowthrough was collected and concentrated to 3 ml in Vivaspin™ with cutoff 10 kDa and dialyzed against 2 x 500 ml BufferA.

The concentration of FtsY was calculated by from the absorbance measured at 205 nm in water by the same equation as in section 4.8.1, where the molecular weight of FtsY is 50 kDa, FtsY-NG+1 and NG – 33 kDa, FtsY-A208 – 23 kDa and FtsY-A197 – 22 kDa. .

5.8.3 Ffh

pET24-Ffh vector was used to overexpress Ffh in *E.coli* BL21(DE3) pLys. A 200 ml overnight culture (previously tested for overexpression) was used to inoculate 6 L of LB supplemented

with 1 % glucose, 30 µg/ml kanamycin and 30 µg/ml chloramphenicol. At OD_{600} 0.7 -0.8 the bacteria were induced with 5 mM IPTG for 2 hours. The cells were collected for 20 min at 5000 rpm in a Beckmann JLA 8.1000 rotor, washed with Ffh-NiA and shock-frozen in liquid nitrogen. The usual pellet weight was 10 – 12 g.

For the first step of purification the cell pellet was resuspended in 20 ml FfhNiA supplemented with 1 pill EDTA Free Complete protease inhibitor (Roche), lysozyme (Sigma) and one crystal of DNase. The cells were opened in one cycle in the EmusiFlex-C3 at 1.5 bar applied pressure and 1000 bar effective pressure. The debris was decanted for 45 min at 25000 rpm in a JA 25.50 Beckmann rotor. The cleared lysate was loaded on a 5 ml HisTrap column, equilibrated with FfhNiA. The unbound sample was washed off with 10 CV FfhNiA and Ffh was eluted with 4 CV FfhNiB. The 20 ml eluate was diluted 10 times with buffer FfhSPA and loaded on HiTrap SP HP 5 ml column. The unbound sample was washed off with 10 CV FfhSPA and Ffh was eluted withlinear gradient of 20 CV from 0 – 100 % FfhSPB. The peak containing Ffh was collected concentrated to 3 ml in a Vivaspin™ with cutoff 30 kDa and dialyzed two times against 500 ml BufferA.

The concentration of Ffh was calculated by from the absorbance measured at 205 nm in water by the same equation as in section 4.8.1, where the MW of Ffh is 54 kDa.

5.8.4 MSP

MSP1D1 and MSPE1D1 were overexpressed in BL21(DE3) cells in a fermenter with LB media supplemented with 30 µg/ml kanamycin and induced at OD_{600} 0.6 with 1 mM IPTG for 2 h.

For the purification 7 -10 g of cells were resuspended in 20 ml MSP-B1 buffer supplemented with 2 pills of EDTA Free Complete protease inhibitor (Roche), lysozyme, one crystal of DNase. The cells were opened in one cycle in the EmusiFlex-C3 at 1.5 bar applied pressure and 1000 bar effective pressure. The volume was brought to 80 ml with MSP-B1 and the debris was decanted in Beckmann Avanti centrifuge for 30 min 30000 rpm, 4°C in JA25.30 rotor. The cleared lysate was adjusted to 0.5 M NaCl and loaded on a 7 ml self-packed Ni-IDA column equilibrated with buffer MSP-B2. The column was washed with 4 CV MSP-B2, followed by 6 CV MSP-B3, 6 CV MSP-B4, 3 CV 5% MSP-B5 and finally the protein was eluted with 100 %

MSP-B5. The purity of the protein was verified by 15 % SDS-PAGE to be > 95%. The peak of MSP was collected concentrated to 5 ml in a Vivaspin with a cutoff of 10 kDa and dialyzed three times against 500 ml BufferA.

The concentration of FtsY was calculated by from the absorbance measured at 205 nm in water by the same equation as in section 4.8.1, where the MW of MSP1D1 is 22 kDa and MSPE1D1 is 24 kDa.

5.8.5 Fluorescence labeling of proteins

All proteins were labeled according to the Invitrogen© recommendations for maleimide-thiol coupling reactions. The labeling buffer is described in Table 4 - 6 with slight modifications depending on the protein: for Ffh the buffer contained 300 mM KCl; for SecYEG the buffer contained 0.03 % DDM. The dyes were dissolved in DMSO to concentration of 20 mM. The protein and the dye were mixed in 1:5 ratios and incubated at room temperature for 2 hours with gentle agitation. The reaction was quenched with 10 mM DDT, diluted to 2.5 ml with BufferA and applied on a PD-10 (G25) desalting column. The 3.5 ml eluate was concentrated and the concentration of protein was measured at A_{205} and the concentration of the dye was measured at the respective absorption wavelength and calculated according to the extinction coefficient. The ration of the dye:protein concentration was taken as the efficiency of the labeling procedure. In case of residual dye the protein was dialyzed overnight in BufferA.

5.9 Gel electrophoresis and blotting

5.9.1 Soldium dodecyl sulfate polyacrylamide gel electrophoresis (SDS-PAGE)

To analyse the proteins, SDS-polyacrylamide gels were used. The usual acrylamide concentration was 12 or 15 % (acrylamide/Bis solution29:1). Gels were prepared and ran vertically in SDS-PAGE running buffer. SDS-PAGE was basically performed as described previously (Laemmli, 1970; Weber et al, 1972).

5.9.2 Clear native polyacrylamide gel electrophoresis (CN-PAGE)

To analyze nanodisc complexes clear native polyacrylamide gel electrophoresis was performed. We used pre-casted gradient gels (4-20% acrylamide), according to the manufacturer's instruction – Serva Electophoresis. In brief the samples were prepared in 2 X clear native PAGE

samples buffer and loaded on the gel. The electrophoresis was performed in two step 15 min 50V, followed by 2h at 200 V and the chamber was cooled to 10°C using a water bath.

5.9.3 Native polyacrylamide gel electrophoresis

SRP and SRP-FtsY complex formation was monitored on nondenaturating 7% polyacrylamide gel electrophoresis (acrylamide/Bis solution 19:1) (Jagath et al, 2000). The 4.5S RNA, Ffh and FtsY were incubated in BufferA + 25% glycerol in the presence of 0.2 mM GMPPNP for 5 min at 25°C before loading on the gel. The electrophoresis was performed in 1x gel-shift running buffer, supplemented with 5 µM GMPPNP, for 3 h at 80 V, at 10°C (the chamber was cooled by a waterbath).

5.9.4 Denaturating polyacrylamide gel electrophoresis

To check the quality of the RNA preparation, denaturating urea PAGE with 12 % polyacrylamide (19:1) was used. 10 ml of urea PAGE solution was polymerized by adding 100 µM APS and 10 µM TEMED. The gel was pre-ran for 15 min at 20 Watts. The samples were prepared with formamide loading dye. The gel was ran in 0.5 x TBE buffer, on a water bath at 50°C at 20 Volts until the dye reached the end of the gel. The gel was fixed for 10 min in 10 % v/v acetic acid and stained with methylene blue. Destaining was performed in water for 30 min.

5.9.5 Western blot

To visualize the expression of SecYEG we used western blot against the His_6-tag of SecE. The blotting procedure was performed in a semi-dry chamber according to the manufacturer's instructions – PeqLab. The blotted membrane was immobilized with 20 % skim milk solution in 1x PBST buffer overnight at 4°C. Afterwards the membrane was washed 3 – 4x with PBST and incubated with for 2 h at room temperature with the primary anti-body (Anti-6x-His Epitope tag purchased from Thermo Fischer) diluted 1:1000 in 5 % skim milk in 1x PBST. To prepare the blot for the secondary anti-body the membrane was washed 3 – 4 x with PBST. It was then incubated for another 2 h with the secondary anti-body (Peroxidase-conjugated anti-rabbit IgG, purchased from Dianova), horseradish peroxidase conjugated anti-body (1:10000 dilution in 5% skim milk in PBST). Finally the membrane was thoroughly washed with PBST and incubated with the chemiluminescent substrate (Thermo Fisher) for several minutes before exposing on a chemiluminiscence film and developed it.

5.10 Nanodisc preparation

5.10.1 Lipids preparation

In a round-bottom glass vessel 1 ml total E.*coli* lipid extract was pipetted. The chlorophorm solvent was evaporated under a nitrogen stream and the lipids were carefully layered on the walls of the vessel. Next, the dried lipids were placed in desiccator overnight. Then, the lipids were resuspended in 800 ml of H_2O at 37° C for 2 hours with gentle agitation. Afterwards the lipids solution was collected and solubilized by addition of 10 % DDM. When the solution turned permanently clear at room temperature it was buffered with 0.5 M Hepes pH 7.5. The lipids were aliquoted and kept at -20° C.

5.10.2 Nanodiscs assembly and purification

The nanodiscs were formed overnight. For SecYEG in nanodiscs ratio of 1:2:30, SecYEG:MSP:lipids was used. For empty nanodiscs a ratio of 1:100 MSP:lipids was used. The samples were brought to total volume of the reaction of 400 µl by BufferA. After the components were mixed together the reaction was incubated on ice for 1 hour. In the meantime the BioBeads™ were soaked and equilibrated in BufferA. Firstly, approximately 0.5 ml of beads were added in an 1.5 ml eppendorf tube and washed 3 times with 1 ml 100 % Methanol, followed by 3 x 1 ml H_2O and 3 x 1 ml BufferA. The beads were drained from the excess buffer and the equivalent of 50 µl was added to each nanodiscs reaction. These were incubated overnight at 4° C with gentle agitation. Next, the beads were decanted and the reactions were transferred into new tubes, centrifuged for 5 min at 16 000 rpm in a bench top centrifuge and loaded on a self-packed Superdex 200 column (170 ml CV). The peaks containing nanodiscs were collected and concentrated in Vivaspin™ with cut-off 100 kDa for SecYEG(ND) or 30 kDa for ND.

5.11 Mass spectrometry sample preparation

Nanodisc samples were resolved on a clear native PAGE (in triplicates) and the bands of interest were excised. After in-gel trypsin digest the peptides extracted as previously described (Shevchenko et al, 1996). The tryptic fragments were analyzed in a LC-coupled ESI Q-ToF (QToF Ultima) and/or in an orbitrap (LTQ-Orbitrap XL) mass spectrometer under standard conditions. Raw data were processed by MaxQuant for peptide/protein identification and

intensity base absolute quantification (iBAQ) (Smits et al, 2013). The sample digest and mass-spectrometry analysis were performed by Monika Raabe and the data analysis by Ilian Atanassov at the group of Prof. Hening Urlaub, Bioanalytical Mass Spectroscopy, Max Planck Institute of Biophysical Chemistry, Göttingen.

5.12 Negative staining for electron microscopy

Serial dilutions of SecYEG(ND) were prepared in the range 2 – 0.02 µM in BufferA. The sample particles were absorbed on a mica carbon film, which afterwards was adhered on a copper grid, leaving the adsorbed particles on the solvent exposed side. The particles were stained for 1 min in uranyl formate solution and visualized on a CM200 electron microscope, Philips. The negative-stain EM was performed by Andruis Krasauskas at the group of Prof. Holger Stark, 3D Electron Cryo-Microscopy, Max Planck Institute of Biophysical Chemistry, Göttingen.

5.13 Ribosomal nascent chain complexes preparation

Ribosomes from *E.coli* MRE600, initiation factors (IF1,IF2 and IF3), EF-TU, EG-G, f[^{3}H]Met-tRNA^{fMet} and totat tRNA were prepared as described (Rodnina & Wintermeyer, 1995). RNCs were prepared by *in vitro* transcription of mRNAs with truncated coding sequence, as described previously (Bornemann et al, 2008; Rodnina & Wintermeyer, 1995). About 80-90% of the ribosomes in the RNC preparations carried the respective peptide chain. The RNCs for this project were prepared by our technical assistant Anna Bursy.

5.14 Fluorescence measurements

5.14.1 Fluorescence and FRET measurements

All fluorescence measurements performed at equilibrium were done at 25ºC in a 750 µl quartz cuvette coated with lipids dissolved in chloroform (1:1000 v/v dilution). The titrations were performed by sequential addition of titrant and incubation for 1 – 2 min before each the measurement. To monitor the fluorescence of MDCC, the dye was excited at 420 nm and the emission was measured at 460 nm, the width of the slits was adjusted so that the counts per seconds (CPS) would be around 100000. The data was fitted to the quadratic equation: $F = F_0 + (F_{max} - F_0)\frac{(P_t+L_t+K_d)-\sqrt{(P_t+L_t+K_d)^2-4*P_t*L_t}}{2}$, where F is the fluorescence change, F_0 the

initial fluorescence, F_{max} the final fluorescence level, P_t the total protein concentration, L_t added titrant concentration and K_d is the dissociation constant of the complex of P and L.

5.14.2 Fluorescence anisotropy measurements

The equilibrium measurements of fluorescence anisotropy were performed using the standard conditions provided by the software FluorEssence. The slit width was adjusted so that the fluorescence would be around 100000 CPS. The experimental conditions were the same as for the fluorescence measurements. The data was analyzed by fitting to the quadratic equation (explained above).

5.15 Rapid kinetics (Stopped-flow)

Stopped-flow measurements were performed in a stopped-flow apparatus SX-20 MV. Equal volumes (~ 55 µl) from the sample syringes were rapidly mixed in 10 mm path length cell and the change of fluorescent signal was recorded. This allowed monitoring of reaction kinetics in the time scale from 3 msec to several minutes. The fluorescence donor MDCC was excited at 420 nm and the acceptor (BodipyFL or Alexa488) emission was measured after passing cut-off filter KV530. The reactions between SecYEG(ND) and FtsY, SecYEG(ND) and the ribosome were carried out at pseudo-first order conditions in BufferA at 25^0C. In general, five to six traces were averaged and evaluated by fitting to exponential function, $F = F_\infty + A * e^{-k_{app}*t}$, with time constant ($k_{app}$), the amplitude of the signal change (A), the final signal (F_∞) and fluorescence signal at time $t(F)$. If necessary, additional exponential terms were included.

5.16 GTP hydrolysis

GTP hydrolysis was measured in multiple turnover conditions with excess of substrate over enzyme. The experiments were performed at 25^0C in BufferA. The reactions were initiated by adding of GTP doped with [γ^{32}P]-GTP. Aliquots were taken at specific time points and the reaction was stopped by the addiing 50 % formic acid. At such acidic conditions spontaneous hydrolysis of GTP is unlikely to occur (Rodnina et al, 1999). To remove any precipitation the samples were centrifuged for 10 min at 13000 x g, at 4^0C and 1 µl of the supernatant was loaded on PEI 300 Polygram® plates. Inorganic phosphate and GTP were separated by thin layer chromatography for 20 min in 0.5M KH_2PO_4 pH 3.5 as mobile phase. The plates were developed on a FLA-7000 image reader and quantified using the densitometry software by

MultiGauge. The amount of hydrolyzed GTP was calculated from the ration between the product, P_i and the total amount of GTP. The velocity of the reactions was measured the early stages of the reaction and the rates were calculated by fitting to a linear function, $GTP_{hydr.} = a + k_{obs} * t$, with apparent rate constant (k_{obs}), offset (a) and GTP hydrolyzed at time (t). The observed rates were plotted against the substrate concentration and fitted to a hyperbolic function, $k_{obs} = \frac{E*k_{cat}*S}{K_m+S}$, with the total concentration of active sites (E), and the concentration of substrate (S)

5.17 Buffers and Media

Table 5-6 List of buffers and media

Buffer	Component
Luria broth (LB)	10 g/l NaCl, 10 g/l tryptone, 5 g/l yeast extract; autoclave 20 min at 15 psi
Luria broth agar	10 g/l NaCl, 10 g/l tryptone, 5 g/l yeast extract, 15 g/l agar; autoclave 20 min at 15 psi
BufferA	20 mM HEPES pH 7.5, 70 mM NH_4Cl, 30 mM KCl, 7 mM $MgCl_2$, 10 % (w/v) glycerol
Western blot Buffer A	25 mM Tris-HCl pH 9.4, 40 mM 6-aminocarpoic acid, 20 % (v/v) methanol
Western blot Buffer B	25 mM Tris-HCl pH 10.4, 20 % (v/v) methanol
Western blot Buffer C	300 mM Tris-HCl pH 10.4
10x PBS	80 g/l NaCl, 2 g/l KCl, 14.4 g Na_2PO_4, 2.4 g/l KH_2HPO_4
Native PAGE 10x cathode buffer	500 mM Tricine, 150 mM bis-Tris
Native PAGE 10x anode buffer	500 mM bis-Tris-HCl pH7.0
Clear native PAGE 2x sample buffer	4 mM 6-aminocarpoic acid, 100 mM NaCl, 100 mM imidazole, 2 mM EDTA, 0.02 % (w/v) Ponceau, 20 % (w/v) glycerol
4x Tris-Glycine SDS-PAGE stacking buffer	0.5M Tris-HCl pH 6.8, 0.4 % (w/v) SDS
4 x Tris-Glycine SDS-PAGE separating buffer	1.5 M Tris-HCl pH 8.8, 0.8 % (w/v) SDS

5x SDS running buffer	125 mM Tris, 960 mM glycine, 0.5 % (w/v) SDS
6x SDS loading buffer	100 mM Tris-HCl pH 6.5, 20 mM BME, 6% SDS, 60% (w/v) glycerol, 0.2 % (w/v) bromphenol blue
10x Gel-shift gel buffer	500 mM Tris pH 6.5, 750 mM ammonium acetate, 10 mM magnesium acetate
1 x Gel-shift running buffer	50 mM Tris pH 6.5, 75 mM ammonium acetate, 1 mM EDTA, 1 mM DTT
Colloidal Coomassie	10 % (w/v) ammonium sulphate, 0.1 % (w/v) Coomassie G-250, 3 % (v/v) ortho-phosphoric acid, 20 % (v/v) ethanol
SecRB	20 mM HEPES pH 7.5, 200 mM NaCl, 5 mM $MgCl_2$
SecSB	20 mM HEPES pH 7.5, 1 M NaCl, 5 mM $MgCl_2$, 20 mM imidazole pH 8.0, 10 % w/v glycerol, 1 % w/v DDM
SecNiA	20 mM HEPES pH 7.5, 200 M NaCl, 5 mM $MgCl_2$, 20 mM imidazole pH 8.0, 10 % w/v glycerol, 0.03 % w/v DDM
SecNiB	20 mM HEPES pH 7.5, 200 M NaCl, 5 mM $MgCl_2$, 200 mM imidazole pH 8.0, 10 % w/v glycerol, 0.03 % w/v DDM
SecSPA	50 mM HEPES pH 8.0, 50 mM NaCl, 1 mM DTT, 10 % w/v glycerol, 0.03 % DDM
SecSPB	50 mM HEPES pH 8.0, 600 mM NaCl, 1 mM DTT 10 % w/v glycerol, 0.03 % DDM
Labeling buffer	20 mM HEPES pH 7.0, 150 mM KCl, 10 % w/v glycerol
FY-QSA	20 mM HEPES pH 7.5, 150 mM KCl, 2 mM EDTA pH 8.0, 2 mM DTT, 0.01 % v/v Nikkol
FY-QSB	20 mM HEPES pH 7.5, 500 mM KCl, 2 mM EDTA pH 8.0, 2 mM DTT, 0.01 % v/v Nikkol
FY-NiA	20 mM HEPES pH 7.5, 150 mM KCl, 10 % w/v glycerol
FY-NiB	20 mM HEPES pH 7.5, 1000 mM KCl, 10 mM imidazole pH 8.0, 10 % w/v glycerol

FY-NiC	20 mM HEPES pH 7.5, 150 mM KCl, 200 mM imidazole pH 8.0, 10 % w/v glycerol
FY-QTA	20 mM HEPES pH 7.5, 150 mM KCl + 10 % w/v glycerol
FY-QTB	20 mM HEPES pH 7.5, 500 mM KCl + 10 % w/v glycerol
Ffh-NiA	20 mM HEPES pH 7.5, 60 mM NH_4Cl, 150 mM KCl, 7 mM $MgCl_2$, 20 mM imidazole pH 8.0
Ffh-NiB	20 mM HEPES pH 7.5, 60 mM NH_4Cl, 500 mM KCl, 7 mM $MgCl_2$, 20 mM imidazole pH 8.0
Ffh-NiC	20 mM HEPES pH 7.5, 60 mM NH_4Cl, 500 mM KCl, 7 mM $MgCl_2$, 250 mM imidazole pH 8.0
Ffh-SPA	20 mM HEPES pH 7.5, 60 mM NH_4Cl, 50 mM KCl, 7 mM $MgCl_2$ + 10 % glycerol + 10 mM BME
Ffh-SPB	20 mM HEPES pH 7.5, 60 mM NH_4Cl, 1.0 M KCl, 7 mM $MgCl_2$ + 10 % glycerol + 10 mM BME
MSP-B1	20 mM Tris pH 7.5, 1 % v/v Triton X-100, 0.01 % v/v Nikkol
MSP-B2	10 mM Tris pH 8.0, 500 mM NaCl, 1 % v/v Triton X, 10 % w/v glycerol
MSP-B3	10 mM Tris pH 8.0, 500 mM NaCl, 50 mM Na-cholate, 10 % w/v glycerol
MSP-B4	10 mM Tris pH 8.0, 500 mM NaCl, 10 % w/v glycerol
MSP-B5	10 mM Tris pH 8.0, 500 mM NaCl, 200 mM imidazole pH 8.0, 10 % w/v glycerol
5x transcription buffer	200mM Tris pH 7.5, 75 mM $MgCl_2$, 10 mM Spermidin, 50 mM NaCl
RNA-BA	30 mM bis-Tris – Hcl pH 6.0, 1 mM EDTA, 300 mM KCl
RNA-BB	30 mM bis-Tris – HCl pH 6.0, 1 mM EDTA, 1.5 M KCl
10x TBE	107.8 g/L Tris-base, 55.03 g/L boric acid, 40 ml 0.5 M EDTA pH 8.0
RNA formamide loading dye	80% v/v formamide, 1x TBE, 0.1 % w/v Bromphenol

	blue, 0.1 % w/v Xylencyanol FF
UREA PAGE	1x TBE, 12% v/v Acrylamide (19:1), 8 M Urea
Methylene blue staining	80 mM NaOAc pH 5.0, 0.016 % w/v Methylene blue
50x TAE buffer	242 g/L Tris-base, 57.1 ml/L glacial acetic acid, 100 ml/L 0.5 M EDTA pH 8.0
6x DNA loading dye	0.25 % w/v Bromphenol blue, 0.25 % w/v xylene cyanol FF, 30 % v/v glycerol

References

Akopian D, Dalal K, Shen K, Duong F, Shan SO (2013a) SecYEG activates GTPases to drive the completion of cotranslational protein targeting. *J Cell Biol* **200:** 397-405

Akopian D, Shen K, Zhang X, Shan SO (2013b) Signal recognition particle: an essential protein-targeting machine. *Annu Rev Biochem* **82:** 693-721

Alami M, Dalal K, Lelj-Garolla B, Sligar SG, Duong F (2007) Nanodiscs unravel the interaction between the SecYEG channel and its cytosolic partner SecA. *EMBO J* **26:** 1995-2004

Angelini S, Boy D, Schiltz E, Koch HG (2006) Membrane binding of the bacterial signal recognition particle receptor involves two distinct binding sites. *J Cell Biol* **174:** 715-724

Angelini S, Deitermann S, Koch HG (2005) FtsY, the bacterial signal-recognition particle receptor, interacts functionally and physically with the SecYEG translocon. *EMBO Rep* **6:** 476-481

Ariosa AR, Duncan SS, Saraogi I, Lu X, Brown A, Phillips GJ, Shan SO (2013) Fingerloop activates cargo delivery and unloading during cotranslational protein targeting. *Mol Biol Cell* **24:** 63-73

Ataide SF, Schmitz N, Shen K, Ke A, Shan SO, Doudna JA, Ban N (2011) The crystal structure of the signal recognition particle in complex with its receptor. *Science* **331:** 881-886

Bahari L, Parlitz R, Eitan A, Stjepanovic G, Bochkareva ES, Sinning I, Bibi E (2007) Membrane targeting of ribosomes and their release require distinct and separable functions of FtsY. *J Biol Chem* **282:** 32168-32175

Bassford P, Beckwith J (1979) Escherichia coli mutants accumulating the precursor of a secreted protein in the cytoplasm. *Nature* **277:** 538-541

Batey RT, Rambo RP, Lucast L, Rha B, Doudna JA (2000) Crystal structure of the ribonucleoprotein core of the signal recognition particle. *Science* **287:** 1232-1239

Batey RT, Sagar MB, Doudna JA (2001) Structural and energetic analysis of RNA recognition by a universally conserved protein from the signal recognition particle. *J Mol Biol* **307:** 229-246

Beck K, Eisner G, Trescher D, Dalbey RE, Brunner J, Muller M (2001) YidC, an assembly site for polytopic Escherichia coli membrane proteins located in immediate proximity to the SecYE translocon and lipids. *EMBO Rep* **2:** 709-714

Becker T, Bhushan S, Jarasch A, Armache JP, Funes S, Jossinet F, Gumbart J, Mielke T, Berninghausen O, Schulten K, Westhof E, Gilmore R, Mandon EC, Beckmann R (2009) Structure of monomeric yeast and mammalian Sec61 complexes interacting with the translating ribosome. *Science* **326:** 1369-1373

Beckmann R, Bubeck D, Grassucci R, Penczek P, Verschoor A, Blobel G, Frank J (1997) Alignment of conduits for the nascent polypeptide chain in the ribosome-Sec61 complex. *Science* **278:** 2123-2126

Beckwith J (2013) The Sec-dependent pathway. *Res Microbiol* **164:** 497-504

Behrens C, Hartmann E, Kalies KU (2013) Single rRNA helices bind independently to the protein-conducting channel SecYEG. *Traffic* **14:** 274-281

Berks BC, Sargent F, Palmer T (2000) The Tat protein export pathway. *Mol Microbiol* **35:** 260-274

Bernstein HD, Poritz MA, Strub K, Hoben PJ, Brenner S, Walter P (1989) Model for signal sequence recognition from amino-acid sequence of 54K subunit of signal recognition particle. *Nature* **340:** 482-486

Bernstein HD, Zopf D, Freymann DM, Walter P (1993) Functional substitution of the signal recognition particle 54-kDa subunit by its Escherichia coli homolog. *Proc Natl Acad Sci U S A* **90:** 5229-5233

Bessonneau P, Besson V, Collinson I, Duong F (2002) The SecYEG preprotein translocation channel is a conformationally dynamic and dimeric structure. *EMBO J* **21:** 995-1003

Blobel G, Dobberstein B (1975) Transfer of proteins across membranes. I. Presence of proteolytically processed and unprocessed nascent immunoglobulin light chains on membrane-bound ribosomes of murine myeloma. *J Cell Biol* **67:** 835-851

Bonardi F, London G, Nouwen N, Feringa BL, Driessen AJ (2010) Light-induced control of protein translocation by the SecYEG complex. *Angew Chem Int Ed Engl* **49:** 7234-7238

Bornemann T, Joeckel J, Rodnina MV, Wintermeyer W (2008) Signal sequence-independent membrane targeting of ribosomes containing short nascent peptides within the exit tunnel. *Nat Struct Mol Biol* **15:** 494-499

Boy D, Koch HG (2009) Visualization of distinct entities of the SecYEG translocon during translocation and integration of bacterial proteins. *Mol Biol Cell* **20:** 1804-1815

Braig D, Bar C, Thumfart JO, Koch HG (2009) Two cooperating helices constitute the lipid-binding domain of the bacterial SRP receptor. *J Mol Biol* **390:** 401-413

Breyton C, Haase W, Rapoport TA, Kuhlbrandt W, Collinson I (2002) Three-dimensional structure of the bacterial protein-translocation complex SecYEG. *Nature* **418:** 662-665

Brown S, Fournier MJ (1984) The 4.5 S RNA gene of Escherichia coli is essential for cell growth. *J Mol Biol* **178:** 533-550

Buskiewicz I, Kubarenko A, Peske F, Rodnina MV, Wintermeyer W (2005) Domain rearrangement of SRP protein Ffh upon binding 4.5S RNA and the SRP receptor FtsY. *RNA* **11:** 947-957

Cannon KS, Or E, Clemons WM, Jr., Shibata Y, Rapoport TA (2005) Disulfide bridge formation between SecY and a translocating polypeptide localizes the translocation pore to the center of SecY. *J Cell Biol* **169:** 219-225

Cheng Z, Jiang Y, Mandon EC, Gilmore R (2005) Identification of cytoplasmic residues of Sec61p involved in ribosome binding and cotranslational translocation. *J Cell Biol* **168:** 67-77

Chiba K, Mori H, Ito K (2002) Roles of the C-terminal end of SecY in protein translocation and viability of Escherichia coli. *J Bacteriol* **184:** 2243-2250

Christopoulos A (2002) Allosteric binding sites on cell-surface receptors: novel targets for drug discovery. *Nat Rev Drug Discov* **1:** 198-210

Cox J, Mann M (2008) MaxQuant enables high peptide identification rates, individualized p.p.b.-range mass accuracies and proteome-wide protein quantification. *Nat Biotechnol* **26:** 1367-1372

Dalal K, Duong F (2010) Reconstitution of the SecY Translocon in Nanodiscs. In *Protein Secretion*, Economou A (ed), Vol. 619, 9, pp 145-156. Humana Press

Dalbey RE, Wang P, Kuhn A (2011) Assembly of bacterial inner membrane proteins. *Annu Rev Biochem* **80:** 161-187

de Gier JW, Luirink J (2001) Biogenesis of inner membrane proteins in Escherichia coli. *Mol Microbiol* **40:** 314-322

de Leeuw E, Poland D, Mol O, Sinning I, ten Hagen-Jongman CM, Oudega B, Luirink J (1997) Membrane association of FtsY, the E. coli SRP receptor. *FEBS Lett* **416:** 225-229

de Leeuw E, te Kaat K, Moser C, Menestrina G, Demel R, de Kruijff B, Oudega B, Luirink J, Sinning I (2000) Anionic phospholipids are involved in membrane association of FtsY and stimulate its GTPase activity. *EMBO J* **19:** 531-541

Denisov IG, Grinkova YV, Lazarides AA, Sligar SG (2004) Directed self-assembly of monodisperse phospholipid bilayer Nanodiscs with controlled size. *J Am Chem Soc* **126:** 3477-3487

Deville K, Gold VA, Robson A, Whitehouse S, Sessions RB, Baldwin SA, Radford SE, Collinson I (2011) The oligomeric state and arrangement of the active bacterial translocon. *J Biol Chem* **286:** 4659-4669

Drew D, Froderberg L, Baars L, de Gier JW (2003) Assembly and overexpression of membrane proteins in Escherichia coli. *Biochim Biophys Acta* **1610:** 3-10

Egea PF, Shan SO, Napetschnig J, Savage DF, Walter P, Stroud RM (2004) Substrate twinning activates the signal recognition particle and its receptor. *Nature* **427:** 215-221

Eitan A, Bibi E (2004) The core Escherichia coli signal recognition particle receptor contains only the N and G domains of FtsY. *J Bacteriol* **186:** 2492-2494

Flanagan JJ, Chen JC, Miao Y, Shao Y, Lin J, Bock PE, Johnson AE (2003) Signal recognition particle binds to ribosome-bound signal sequences with fluorescence-detected subnanomolar affinity that does not diminish as the nascent chain lengthens. *J Biol Chem* **278:** 18628-18637

Focia PJ, Shepotinovskaya IV, Seidler JA, Freymann DM (2004) Heterodimeric GTPase core of the SRP targeting complex. *Science* **303:** 373-377

Frauenfeld J, Gumbart J, Sluis EO, Funes S, Gartmann M, Beatrix B, Mielke T, Berninghausen O, Becker T, Schulten K, Beckmann R (2011) Cryo-EM structure of the ribosome-SecYE complex in the membrane environment. *Nat Struct Mol Biol* **18:** 614-621

Funes S, Kauff F, van der Sluis EO, Ott M, Herrmann JM (2011) Evolution of YidC/Oxa1/Alb3 insertases: three independent gene duplications followed by functional specialization in bacteria, mitochondria and chloroplasts. *Biol Chem* **392:** 13-19

Gogala M, Becker T, Beatrix B, Armache JP, Barrio-Garcia C, Berninghausen O, Beckmann R (2014) Structures of the Sec61 complex engaged in nascent peptide translocation or membrane insertion. *Nature* **506:** 107-110

Gu SQ, Peske F, Wieden HJ, Rodnina MV, Wintermeyer W (2003) The signal recognition particle binds to protein L23 at the peptide exit of the *Escherichia coli* ribosome. *RNA* **9:** 566-573

Gumbart J, Chipot C, Schulten K (2011a) Free-energy cost for translocon-assisted insertion of membrane proteins. *Proc Natl Acad Sci U S A* **108:** 3596-3601

Gumbart J, Chipot C, Schulten K (2011b) Free energy of nascent-chain folding in the translocon. *J Am Chem Soc* **133:** 7602-7607

Gumbart JC, Teo I, Roux B, Schulten K (2013) Reconciling the roles of kinetic and thermodynamic factors in membrane-protein insertion. *J Am Chem Soc* **135:** 2291-2297

Hainzl T, Huang S, Merilainen G, Brannstrom K, Sauer-Eriksson AE (2011) Structural basis of signal-sequence recognition by the signal recognition particle. *Nat Struct Mol Biol* **18:** 389-391

Hainzl T, Huang S, Sauer-Eriksson AE (2007) Interaction of signal-recognition particle 54 GTPase domain and signal-recognition particle RNA in the free signal-recognition particle. *Proc Natl Acad Sci U S A* **104:** 14911-14916

Halic M, Blau M, Becker T, Mielke T, Pool MR, Wild K, Sinning I, Beckmann R (2006a) Following the signal sequence from ribosomal tunnel exit to signal recognition particle. *Nature* **444:** 507-511

Halic M, Gartmann M, Schlenker O, Mielke T, Pool MR, Sinning I, Beckmann R (2006b) Signal recognition particle receptor exposes the ribosomal translocon binding site. *Science* **312:** 745-747

Hanada M, Nishiyama K, Tokuda H (1996) SecG plays a critical role in protein translocation in the absence of the proton motive force as well as at low temperature. *FEBS Lett* **381:** 25-28

Hanein D, Matlack KE, Jungnickel B, Plath K, Kalies KU, Miller KR, Rapoport TA, Akey CW (1996) Oligomeric rings of the Sec61p complex induced by ligands required for protein translocation. *Cell* **87:** 721-732

Hegde RS, Bernstein HD (2006) The surprising complexity of signal sequences. *Trends Biochem Sci* **31:** 563-571

Higy M, Gander S, Spiess M (2005) Probing the environment of signal-anchor sequences during topogenesis in the endoplasmic reticulum. *Biochemistry* **44:** 2039-2047

Holland IB (2010) The extraordinary diversity of bacterial protein secretion mechanisms. *Methods Mol Biol* **619:** 1-20

Holtkamp W, Lee S, Bornemann T, Senyushkina T, Rodnina MV, Wintermeyer W (2012a) Dynamic switch of the signal recognition particle from scanning to targeting. *Nat Struct Mol Biol***:** doi: 10.1038/nsmb.2421

Holtkamp W, Lee S, Bornemann T, Senyushkina T, Rodnina MV, Wintermeyer W (2012b) Dynamic switch of the signal recognition particle from scanning to targeting. *Nat Struct Mol Biol* **19:** 1332-1337

Hsu LM, Zagorski J, Fournier MJ (1984) Cloning and sequence analysis of the Escherichia coli 4.5 S RNA gene. *J Mol Biol* **178:** 509-531

Ismail N, Hedman R, Schiller N, von Heijne G (2012) A biphasic pulling force acts on transmembrane helices during translocon-mediated membrane integration. *Nat Struct Mol Biol* **19:** 1018-1022

Jagath JR, Matassova NB, de Leeuw E, Warnecke JM, Lentzen G, Rodnina MV, Luirink J, Wintermeyer W (2001) Important role of the tetraloop region of 4.5S RNA in SRP binding to its receptor FtsY. *RNA* **7:** 293-301

Jagath JR, Rodnina MV, Lentzen G, Wintermeyer W (1998) Interaction of guanine nucleotides with the signal recognition particle from *Escherichia coli*. *Biochemistry* **37:** 15408-15413

Jagath JR, Rodnina MV, Wintermeyer W (2000) Conformational changes in the bacterial SRP receptor FtsY upon binding of guanine nucleotides and SRP. *J Mol Biol* **295:** 745-753

Janda CY, Li J, Oubridge C, Hernandez H, Robinson CV, Nagai K (2010) Recognition of a signal peptide by the signal recognition particle. *Nature* **465:** 507-510

Junne T, Kocik L, Spiess M (2010) The hydrophobic core of the Sec61 translocon defines the hydrophobicity threshold for membrane integration. *Mol Biol Cell* **21:** 1662-1670

Kedrov A, Kusters I, Krasnikov VV, Driessen AJ (2011) A single copy of SecYEG is sufficient for preprotein translocation. *EMBO J* **30:** 4387-4397

Keenan RJ, Freymann DM, Walter P, Stroud RM (1998) Crystal structure of the signal sequence binding subunit of the signal recognition particle. *Cell* **94:** 181-191

Kihara A, Akiyama Y, Ito K (1995) FtsH is required for proteolytic elimination of uncomplexed forms of SecY, an essential protein translocase subunit. *Proc Natl Acad Sci U S A* **92:** 4532-4536

Krieg UC, Walter P, Johnson AE (1986) Photocrosslinking of the signal sequence of nascent preprolactin to the 54-kilodalton polypeptide of the signal recognition particle. *Proc Natl Acad Sci U S A* **83:** 8604-8608

Kudva R, Denks K, Kuhn P, Vogt A, Muller M, Koch HG (2013) Protein translocation across the inner membrane of Gram-negative bacteria: the Sec and Tat dependent protein transport pathways. *Res Microbiol* **164:** 505-534

Kuhn P, Weiche B, Sturm L, Sommer E, Drepper F, Warscheid B, Sourjik V, Koch HG (2011) The bacterial SRP receptor, SecA and the ribosome use overlapping binding sites on the SecY translocon. *Traffic* **12:** 563-578

Laemmli UK (1970) Cleavage of structural proteins during the assembly of the head of bacteriophage T4. *Nature* **227:** 680-685

Lakowicz JR (2003) *Principles of fluorescence spectroscopy, 3rd Edition*: Springer.

Lam VQ, Akopian D, Rome M, Henningsen D, Shan SO (2010) Lipid activation of the signal recognition particle receptor provides spatial coordination of protein targeting. *J Cell Biol* **190:** 623-635

Leipe DD, Wolf YI, Koonin EV, Aravind L (2002) Classification and evolution of P-loop GTPases and related ATPases. *J Mol Biol* **317:** 41-72

Luirink J, ten Hagen-Jongman CM, van der Weijden CC, Oudega B, High S, Dobberstein B, Kusters R (1994) An alternative protein targeting pathway in Escherichia coli: studies on the role of FtsY. *EMBO J* **13:** 2289-2296

Lycklama ANJA, Driessen AJ (2012) The bacterial Sec-translocase: structure and mechanism. *Philos Trans R Soc Lond B Biol Sci* **367:** 1016-1028

Maillard AP, Lalani S, Silva F, Belin D, Duong F (2007) Deregulation of the SecYEG translocation channel upon removal of the plug domain. *J Biol Chem* **282:** 1281-1287

Martoglio B, Hofmann MW, Brunner J, Dobberstein B (1995) The protein-conducting channel in the membrane of the endoplasmic reticulum is open laterally toward the lipid bilayer. *Cell* **81:** 207-214

Menetret JF, Schaletzky J, Clemons WM, Jr., Osborne AR, Skanland SS, Denison C, Gygi SP, Kirkpatrick DS, Park E, Ludtke SJ, Rapoport TA, Akey CW (2007) Ribosome binding of a single copy of the SecY complex: implications for protein translocation. *Mol Cell* **28:** 1083-1092

Millman JS, Andrews DW (1999) A site-specific, membrane-dependent cleavage event defines the membrane binding domain of FtsY. *J Biol Chem* **274:** 33227-33234

Millman JS, Qi HY, Vulcu F, Bernstein HD, Andrews DW (2001) FtsY binds to the Escherichia coli inner membrane via interactions with phosphatidylethanolamine and membrane proteins. *J Biol Chem* **276:** 25982-25989

Milstein C, Brownlee GG, Harrison TM, Mathews MB (1972) A possible precursor of immunoglobulin light chains. *Nat New Biol* **239:** 117-120

Mircheva M, Boy D, Weiche B, Hucke F, Graumann P, Koch HG (2009) Predominant membrane localization is an essential feature of the bacterial signal recognition particle receptor. *BMC Biol* **7:** 76

Mitra K, Schaffitzel C, Shaikh T, Tama F, Jenni S, Brooks CL, 3rd, Ban N, Frank J (2005) Structure of the E. coli protein-conducting channel bound to a translating ribosome. *Nature* **438:** 318-324

Mori H, Ito K (2006) Different modes of SecY-SecA interactions revealed by site-directed in vivo photo-cross-linking. *Proc Natl Acad Sci U S A* **103:** 16159-16164

Murphy CK, Beckwith J (1994) Residues essential for the function of SecE, a membrane component of the Escherichia coli secretion apparatus, are located in a conserved cytoplasmic region. *Proc Natl Acad Sci U S A* **91:** 2557-2561

Nagamori S, Smirnova IN, Kaback HR (2004) Role of YidC in folding of polytopic membrane proteins. *J Cell Biol* **165:** 53-62

Nishiyama K, Suzuki T, Tokuda H (1996) Inversion of the membrane topology of SecG coupled with SecA-dependent preprotein translocation. *Cell* **85:** 71-81

Papanikou E, Karamanou S, Economou A (2007) Bacterial protein secretion through the translocase nanomachine. *Nat Rev Microbiol* **5:** 839-851

Park E, Rapoport TA (2012) Mechanisms of Sec61/SecY-mediated protein translocation across membranes. *Annu Rev Biophys* **41:** 21-40

Parlitz R, Eitan A, Stjepanovic G, Bahari L, Bange G, Bibi E, Sinning I (2007) Escherichia coli signal recognition particle receptor FtsY contains an essential and autonomous membrane-binding amphipathic helix. *J Biol Chem* **282:** 32176-32184

Peluso P, Shan SO, Nock S, Herschlag D, Walter P (2001) Role of SRP RNA in the GTPase cycles of Ffh and FtsY. *Biochemistry* **40:** 15224-15233

Pogliano JA, Beckwith J (1994) SecD and SecF facilitate protein export in Escherichia coli. *EMBO J* **13:** 554-561

Pollastri G, Przybylski D, Rost B, Baldi P (2002) Improving the prediction of protein secondary structure in three and eight classes using recurrent neural networks and profiles. *Proteins* **47:** 228-235

Pool MR, Stumm J, Fulga TA, Sinning I, Dobberstein B (2002) Distinct modes of signal recognition particle interaction with the ribosome. *Science* **297:** 1345-1348

Powers T, Walter P (1997) Co-translational protein targeting catalyzed by the Escherichia coli signal recognition particle and its receptor. *EMBO J* **16:** 4880-4886

Prinz A, Behrens C, Rapoport TA, Hartmann E, Kalies KU (2000) Evolutionarily conserved binding of ribosomes to the translocation channel via the large ribosomal RNA. *EMBO J* **19:** 1900-1906

Pugsley AP (1993) The complete general secretory pathway in gram-negative bacteria. *Microbiol Rev* **57:** 50-108

Raden D, Song W, Gilmore R (2000) Role of the cytoplasmic segments of Sec61alpha in the ribosome-binding and translocation-promoting activities of the Sec61 complex. *J Cell Biol* **150:** 53-64

Reinau ME, Thogersen IB, Enghild JJ, Nielsen KL, Otzen DE (2010) The diversity of FtsY-lipid interactions. *Biopolymers* **93:** 595-606

Reyes CL, Rutenber E, Walter P, Stroud RM (2007) X-ray structures of the signal recognition particle receptor reveal targeting cycle intermediates. *PLoS One* **2:** e607

Rodnina MV, Savelsbergh A, Matassova NB, Katunin VI, Semenkov YP, Wintermeyer W (1999) Thiostrepton inhibits the turnover but not the GTPase of elongation factor G on the ribosome. *Proc Natl Acad Sci U S A* **96:** 9586-9590

Rodnina MV, Wintermeyer W (1995) GTP consumption of elongation factor Tu during translation of heteropolymeric mRNAs. *Proc Natl Acad Sci U S A* **92:** 1945-1949

Romisch K, Webb J, Herz J, Prehn S, Frank R, Vingron M, Dobberstein B (1989) Homology of 54K protein of signal-recognition particle, docking protein and two E. coli proteins with putative GTP-binding domains. *Nature* **340:** 478-482

Rosendal KR, Wild K, Montoya G, Sinning I (2003) Crystal structure of the complete core of archaeal signal recognition particle and implications for interdomain communication. *Proc Natl Acad Sci U S A* **100:** 14701-14706

Runnels LW, Scarlata SF (1995) Theory and application of fluorescence homotransfer to melittin oligomerization. *Biophys J* **69:** 1569-1583

Sachelaru I, Petriman NA, Kudva R, Kuhn P, Welte T, Knapp B, Drepper F, Warscheid B, Koch HG (2013) YidC occupies the lateral gate of the SecYEG translocon and is sequentially displaced by a nascent membrane protein. *J Biol Chem* **288:** 16295-16307

Saparov SM, Erlandson K, Cannon K, Schaletzky J, Schulman S, Rapoport TA, Pohl P (2007) Determining the conductance of the SecY protein translocation channel for small molecules. *Mol Cell* **26:** 501-509

Satoh Y, Matsumoto G, Mori H, Ito K (2003) Nearest neighbor analysis of the SecYEG complex. 1. Identification of a SecY-SecG interface. *Biochemistry* **42:** 7434-7441

Scheuring J, Braun N, Nothdurft L, Stumpf M, Veenendaal AK, Kol S, van der Does C, Driessen AJ, Weinkauf S (2005) The oligomeric distribution of SecYEG is altered by SecA and translocation ligands. *J Mol Biol* **354:** 258-271

Scotti PA, Urbanus ML, Brunner J, de Gier JW, von Heijne G, van der Does C, Driessen AJ, Oudega B, Luirink J (2000) YidC, the Escherichia coli homologue of mitochondrial Oxa1p, is a component of the Sec translocase. *EMBO J* **19:** 542-549

Segel IH (1993) *Enzyme Kinetics: Behavior and Analysis of Rapid Equilibrium and Steady-State Enzyme Systems*: Wiley.

Shen K, Arslan S, Akopian D, Ha T, Shan SO (2012) Activated GTPase movement on an RNA scaffold drives co-translational protein targeting. *Nature* **492:** 271-275

Shen K, Wang Y, Hwang Fu YH, Zhang Q, Feigon J, Shan SO (2013) Molecular mechanism of GTPase activation at the signal recognition particle (SRP) RNA distal end. *J Biol Chem* **288:** 36385-36397

Shevchenko A, Wilm M, Vorm O, Jensen ON, Podtelejnikov AV, Neubauer G, Mortensen P, Mann M (1996) A strategy for identifying gel-separated proteins in sequence databases by MS alone. *Biochem Soc Trans* **24:** 893-896

Siekevitz P, Palade GE (1958) A cyto-chemical study on the pancreas of the guinea pig. III. In vivo incorporation of leucine-1-C14 into the proteins of cell fractions. *J Biophys Biochem Cytol* **4:** 557-566

Smits AH, Jansen PW, Poser I, Hyman AA, Vermeulen M (2013) Stoichiometry of chromatin-associated protein complexes revealed by label-free quantitative mass spectrometry-based proteomics. *Nucleic Acids Res* **41:** e28

Spanggord RJ, Siu F, Ke A, Doudna JA (2005) RNA-mediated interaction between the peptide-binding and GTPase domains of the signal recognition particle. *Nat Struct Mol Biol* **12:** 1116-1122

Stjepanovic G, Kapp K, Bange G, Graf C, Parlitz R, Wild K, Mayer MP, Sinning I (2011a) Lipids trigger a conformational switch that regulates signal recognition particle (SRP)-mediated protein targeting. *J Biol Chem* **286:** 23489-23497

Stjepanovic G, Kapp K, Bange G, Graf C, Parlitz R, Wild K, Mayer MP, Sinning I (2011b) Lipids trigger a conformational switch that regulates signal recognition particle (SRP)-mediated protein targeting. *J Biol Chem* **286:** 23489-23497

Tam PC, Maillard AP, Chan KK, Duong F (2005) Investigating the SecY plug movement at the SecYEG translocation channel. *The EMBO journal* **24:** 3380-3388

Traut TW (1994) Physiological concentrations of purines and pyrimidines. *Mol Cell Biochem* **140:** 1-22

Tsukazaki T, Mori H, Echizen Y, Ishitani R, Fukai S, Tanaka T, Perederina A, Vassylyev DG, Kohno T, Maturana AD, Ito K, Nureki O (2011) Structure and function of a membrane component SecDF that enhances protein export. *Nature* **474:** 235-238

Valent QA, Scotti PA, High S, de Gier JW, von Heijne G, Lentzen G, Wintermeyer W, Oudega B, Luirink J (1998) The Escherichia coli SRP and SecB targeting pathways converge at the translocon. *EMBO J* **17:** 2504-2512

Van den Berg B, Clemons WM, Jr., Collinson I, Modis Y, Hartmann E, Harrison SC, Rapoport TA (2004) X-ray structure of a protein-conducting channel. *Nature* **427:** 36-44

van der Sluis EO, Driessen AJ (2006) Stepwise evolution of the Sec machinery in Proteobacteria. *Trends Microbiol* **14:** 105-108

Veenendaal AK, van der Does C, Driessen AJ (2001) Mapping the sites of interaction between SecY and SecE by cysteine scanning mutagenesis. *J Biol Chem* **276:** 32559-32566

Voigts-Hoffmann F, Schmitz N, Shen K, Shan SO, Ataide SF, Ban N (2013) The structural basis of FtsY recruitment and GTPase activation by SRP RNA. *Mol Cell* **52:** 643-654

von Heijne G, Abrahmsen L (1989) Species-specific variation in signal peptide design. Implications for protein secretion in foreign hosts. *FEBS Lett* **244:** 439-446

von Loeffelholz O, Knoops K, Ariosa A, Zhang X, Karuppasamy M, Huard K, Schoehn G, Berger I, Shan SO, Schaffitzel C (2013) Structural basis of signal sequence surveillance and selection by the SRP-FtsY complex. *Nat Struct Mol Biol* **20:** 604-610

Wagner S, Klepsch MM, Schlegel S, Appel A, Draheim R, Tarry M, Hogbom M, van Wijk KJ, Slotboom DJ, Persson JO, de Gier JW (2008) Tuning Escherichia coli for membrane protein overexpression. *Proc Natl Acad Sci U S A* **105:** 14371-14376

Weber K, Pringle JR, Osborn M (1972) Measurement of molecular weights by electrophoresis on SDS-acrylamide gel. *Methods Enzymol* **26:** 3-27

Weiche B, Burk J, Angelini S, Schiltz E, Thumfart JO, Koch HG (2008) A cleavable N-terminal membrane anchor is involved in membrane binding of the Escherichia coli SRP receptor. *J Mol Biol* **377:** 761-773

White SH, von Heijne G (2008) How translocons select transmembrane helices. *Annu Rev Biophys* **37:** 23-42

Wu ZC, de Keyzer J, Kedrov A, Driessen AJ (2012) Competitive binding of the SecA ATPase and ribosomes to the SecYEG translocon. *J Biol Chem* **287:** 7885-7895

Zhang B, Miller TF, 3rd (2012) Long-timescale dynamics and regulation of Sec-facilitated protein translocation. *Cell Rep* **2:** 927-937

Zhang X, Kung S, Shan SO (2008) Demonstration of a multistep mechanism for assembly of the SRP x SRP receptor complex: implications for the catalytic role of SRP RNA. *J Mol Biol* **381:** 581-593

Zimmer J, Nam Y, Rapoport TA (2008) Structure of a complex of the ATPase SecA and the protein-translocation channel. *Nature* **455:** 936-943

Zopf D, Bernstein HD, Johnson AE, Walter P (1990) The methionine-rich domain of the 54 kd protein subunit of the signal recognition particle contains an RNA binding site and can be crosslinked to a signal sequence. *EMBO J* **9:** 4511-4517

Zwieb C. (2011) SRPDB.

Zwieb C, van Nues RW, Rosenblad MA, Brown JD, Samuelsson T (2005) A nomenclature for all signal recognition particle RNAs. *RNA* **11:** 7-13

Appendix

List of abbreviations

Abbreviation	Description
Alx488	Alexa Fluor 488
APS	Ammonium persulfate
BME	β-mercaptoethanol
Bpy	Bodipy FL
CNP	Clear native PAGE
Cryo-EM	Cryo electron microscopy
CV	Column volume
DDM	n-Dodecyl β-D-Maltopyranoside
dNTP	Deoxyribonucleotide triphosphate
DTT	Dithiothreitol
e.g.	*exempli gratia,* for example
EM	Electron microscopy
ER	Endoplasmic reticulum
et al.	*et alii,* and other
FCS	Fluorescence correlation spectroscopy
FRET	Fluorescence resonance energy transfer
FtsY-A197	FtsY construct 1 – 197 amino acids
FtsY-A208	FtsY construct 1 – 208 amino acids
FtsY-NG	FtsY construct 197 – 497 amino acids
FtsY-NG+1	FtsY construct 196 – 497 amino acids
GAP	GTPase activation factor
GDP	Guanosine diphosphate
GEF	Guanine nucleotide exchange factor
GFP	Green fluorescent protein
GMPPNP	Non-hydrolyzable GTP analog 5'-Guanylyl imidodiphosphate
GTP	Guanosine triphosphate
i.e.	*id est,* that is
iBAQ	Intensity based absolute quantification
INV	Inner membrane vesicles
ITC	Isothermal titration calorimetry

k_{app}	Apparent rate constant
k_{cat}	Catalytic rate constant
K_d	Dissociation constant
K_m	Michaelis-Menten constant
LepB	Leader peptidase
MDCC	7-Diethylamino-3-((((2-Maleimidyl)ethyl)amino)carbonyl)coumarin
MTS	Membrane targeting sequence
MW	Molecular weight
ND	Nanodiscs
Nikkol	Nonaethylene glycol monododecyl ether
PMF	Proton-motive force
QSY9	Fluorescence quencher
RNC	Ribosomal nascent chain complex
SAS	Signal anchor sequence
SDS	Soldiumdodecylsulfate
SDS-PAGE	Soldiumdodecylsulfate polyacrylamide gel electrophoresis
SecYEG(ND)	SecYEG embedded in nanodisc
SPase	Signal peptidase
SPR	Surface plasmon resonance
SRP	Signal recognition particle
SS	Signal sequence
TEMED	Tetramethylethylenediamine
TM	Trans membrane

List of tables

List of figures

Aknowledgements

In the past four years I have walked a long way and a lot of people have contributed to it, I hope I will not forget anyone.

I am very grateful to Marina Rodnina and Wolfgang Wintermeyer for taking me on board and giving me the opportunity to do my doctoral work with them. I would like especially to thank Wolfgang for teaching me about fluorescence and thermodynamics, for his ideas and for the help during writing this thesis. I would like ot thank Marina for all the discussions and advices.

I would like to thank my thesis committee members Marina Bennati and Kai Tittmann for their advices and also my extended examination board members Holger Stark, Manfred Konrad and Peter Rehling. Likewise, I have really appreciated the GGNB program and the whole organizational team.

I would also like to thank everyone at the Ribosome Dynamics group: Thomas Bornemann and Wolf Holtkamp for the day to day discussions, support and for the nice working atmosphere in the lab; Sejeong Lee and Yan Ge for the working side by side, for their friendship and showing me Asian culture and cuisine; Anna Bursy for making my PCR reactions work and making tones of RNCs; Franziska Hummel for always showing me that there is more than one way to do things. Nevertheless, Johannes Jöckel is no longer part of our group, I would like to thank him for the introduction to nanodiscs preparation and for providing us with the ITC data.

Also many thanks to the postdocs at the Physical Biochemistry department, especially to: Pohl Milon for the help with the stopped-flow and sharing his experience on kinetics and protein labeling; Andrey Koneverga for the help with the HPLCs and all the discussions; Ingo Wohlgemuth for sharing his knowledge about GTPases and for idea to use iBAQ; Marcus Jäger for all the talks about FRET and fluorescence; I really learned a lot from all of you. I should not forget Michael Thommen, we are very grateful with Anna for the help with RNC preparation. My appreciation to the people who help me with the iBAQ – Illian Atanassov (and for always lifting my spirit), and negative staining EM – Andrius Krasauskas (and for the funny jokes and comments).

Also I would like to thank technical assistants of the department Manuela Beck-Corell, Anna Bursy, Olaf Geintzer, Franziska Hummel, Sandra Kapller, Christina Kothe, Theresia Uhlendorf, Antony Wiles, Tanja Wiles, Michael Zimmermann, for the excellent technical support.

I would also like to thank everyone in the department for the great atmosphere; PhD/Postdocs get together organization. Speaking about organization I would like to thank our secretary Dimitra Papastavrou, for all the bureaucracy assistance.

But it was not all the time only work, I also met great friends to go skiing, diving, travelling, playing volleyball, mushroom hunting thank you: Liu, Dima, Ka, Lena, Andrey, Sergey, Katya, Michi, Raffa, Riccardo, Inessa, Tales, Tanja (thank you for taking me pony petting). Also learning German was fun with Eve and Rebecca. Bulgarian lunches were great with Plamen, Anastassia, Miro, Irena, Ivan. Andreea, it was a pleasure to be student representative with you, to organize the retreat and to have so many cocktails. My dear friend Miro (Mirsha), thank you so much for patience and support, all your solid logic... And Michi thank you for being there, for the road trip and for trying to teach me to snowboard.

Last but least I would like to give my deepest gratitude to my family and parents (Eli and Joro) and my brother Alex, who despite the distance supported me, advised me and were always there.

Curriculumn vitae

Albena Georgieva Draycheva

Born: 20 Jan 1985, Sofia, Bulgaria

Nationality: Bulgarian

Education:

Georg-August University, Göttingen, Germany **April 2010 – Sept 2014**

Graduate studies at Göttingen Graduate School for Neurosciences, Biophysics, and Molecular Biosciences (GGNB)

Free University, Berlin, Germany **Oct 2008 – March 2010**

Graduate studies at Berlin-Brandenburg School of Regenerative Therapies (BSRT)

Uppsala University, Uppsala, Sweden **Jan 2007 – Aug 2008**

Master studies in biology

Sofia University, Sofia, Bulgaria **Nov 2003 – July 2007**

Bachelor studies in molecular biology

29 SOU Kuzman Shapkarev, Sofia, Bulgaria **Sept 1998 – June 2003**

High school education in humanitarian studies – major subjects: literature and history

151 SOUPI, Sofia, Bulgaria **Sept 1991 – June 1998**

Primary school education

Further information at:

LinkedIn page http://www.linkedin.com/pub/albena-draycheva/2/250/948

ResearchGate page https://www.researchgate.net/profile/Albena_Draycheva/